ISSN : 2717 - 5022

JOURNAL ON GEOINFORMATICS
Nepal

Number: 23 Jestha 2081 (May/June, 2024)

Annual Publication of Survey Department, Government of Nepal

Journal on Geoinformatics
Nepal

Number : 23

Jestha 2081 BS
May/June 2024 AD

Annual publication of Survey Department, Government of Nepal

Published by:
Government of Nepal
Ministry of Land Management, Cooperatives & Poverty Alleviation
Survey Department
Min Bhawan, Kathmandu
Nepal

No. of copies : 500

FOREWORDS

Survey Department, National Mapping Agency of Nepal provides user focused, cost effective, reliable and high quality geospatial data, and information to meet the needs of national security, sustainable national development, and geo information in the field of surveying and mapping activities for innovative market. In addition to the technical responsibility, department also support the academia in sharing and disseminate knowledge and information through its annual publication the 23rd issue of “Journal on Geoinformatics, Nepal”. It gives me great pleasure to congratulate the Editorial Board and express my gratitude to all the contributor for their invaluable assistance in shaping this journal.

Survey Department continuously contributes Land Administration services to the citizens through its district level offices adopting with modern advanced system. Besides this service, department provides the technical support in international boundary, generating geo-information services, strengthening geodetic network control, and conducting pertinent need-based surveying and mapping activities to assist the planners and scientists in the field of land resource management. Department also supports in the field of Surveying, Mapping, Geo-information Science and Earth Observation that is very crucial for the planned development of hitherto under developed areas in the country.

Currently, fifty-five district survey offices have implemented the Nepal Land Information System (NeLIS) and "MeroKitta" as web based modern land administration service system. Based on these systems, Citizens can receive the service of map print, field book print and plot register print after online revenue payment and obtain the digital copy of map/document in hand without visiting the survey office. The system has been implemented with the objective of decentralization concept of the government according to the constitution. The Department is planning to rollout the system in all district level offices in near future. Besides this turning point system, department is also conducting the LiDAR survey which generates a very high-resolution DEM useful for different development activities and disaster mitigation planning. Department is also planning to continue the LiDAR survey to cover the whole country. Updating of the topographical base maps. Establishment of CORS and defining the spatial reference frame are some other major activities that the department is conducting. I believe that this journal has been the platform for sharing the activities and products of Survey Department from history to present status and also from varied research fields.

Further, I like to express my sincere appreciation to the fellow colleagues, the members of Advisory Council and the Editorial Board for their invaluable contribution in this issue. The team deserves special thanks for their tireless efforts in bringing this issue in the stipulated time. More importantly, I extend sincere gratitude to all the authors for their resourceful professional contribution. I like to request for such kind of support and professional contribution in the upcoming issues too.

Enjoy Reading!
Thank you!

Prakash Joshi
Director General
lightjoshiji@gmail.com

EDITORIAL

Survey Department, The National Mapping Organization of Nepal is conducting many different activities in the field of Surveying and Mapping. Besides the technical activities in this field, department is also contributing in academic sector of this field by publishing journal on different research and findings about geoinformatics through "Journal on Geoinformatics, Nepal", the annual publication of the department. Editorial board is happy to share the 23rd issues of this journal. The journal has been a platform for sharing information on geoinformation and its wide range of application for the researchers and professionals working in this field from wide range of community including government, non-government, international organization as well as universities. Editorial board believes that this has also supported in professional development through knowledge sharing in the field of surveying, mapping and geospatial technologies.

Driving from the first issue since 2002 till this 23rd issues, the journal has covered from the history of the surveying and mapping to the latest technologies in this field. The editorial board like to thank sincerely to all those authors who contributed in making the successful publication of the issues and also to the advisor board and the editorial for making this happen. This issue is also the continuous product of the previous efforts. This issue also as in previous one, includes interesting and worth reading papers related to geospatial technologies and its applications and findings.

I am also thankful to Survey Department for providing me the responsibility of the Editor-in-Chief for this 23rd issue of the journal. With the continuous guidance and critical comments from the advisory board have been able to bring this issue of the journal for readers. On behalf of all the members of the Editorial Board, I would like to express sincere thanks to all contributing authors, paper reviewers, members of Advisory Board and all other persons who have contributed for the publication of 23rd issue of the journal.

At last, on the behalf of Editorial Board, let me humbly request all of you to contribute your valuable articles, research papers, review papers for the upcoming issue of this journal.

Karuna K.C.
Editor-in Chief,
Jestha, 2081 (May 2024)

Advisory Council

Editorial Board

Journal on
GEOINFORMATICS
Nepal

Jestha 2081, May 2024
Number 23

Features

Contents

List of Paper Reviewer
Susheel Dangol
Bikash Kumar Karna (Ph. D.)
Ram Kumar Sapkota
Ajit Kuwar
Sudip Shrestha
Prashant Ghimire
Harisharan Nepal
Sanjeeban Shrestha

Cover Concept
Establishment of CORS Station

Articles

Contents

Contents

Assessing the Impact of Urban Expansion on Forest Cover using LULC Maps, NDVI, and NDBI: A Case Study of Kathmandu District.

Arun Kumar Bhomi[1], Rabina Poudyal[1], Suraj Kumar Tolange[1], Susmita Chaudhary[1]
arunbhomi12345@gmail.com, rabinapoudyal815@gmail.com, surajkr.tolange019@gmail.com, susmitachaudhari13@gmail.com
[1]Department of Geomatics Engineering, Kathmandu University

KEYWORDS

NDVI, NDBI, LULC, Urbanization, Deforestation

ABSTRACT

Rapid urbanization poses significant challenges to the delicate balance between urban development and environmental conservation. This study investigates the impact of urban expansion on forest cover in the Kathmandu District, employing a comprehensive approach that integrates Land Use/Land Cover (LULC) maps, Normalized Difference Vegetation Index (NDVI), and Normalized Difference Built-Up Index (NDBI). The aim of the study area is to provide insights into the dynamic interplay between urban growth and its consequences on the region's ecological landscape. LULC maps derived from remote sensing data offer a spatially explicit representation of land-use changes over time, enabling the identification of areas where urbanization has encroached upon forest area. The NDVI, a vegetation health indicator, serves as a quantitative measure of changes in the density and health of vegetation cover, aiding in the assessment of ecological impacts. Complementing this, the NDBI highlights intensity of built-up areas, allowing for a nuanced understanding of the urbanization process. This study employs NDBI and NDVI to dynamically assess urban growth and land use cover change, enhancing analytical accuracy. Findings reveal a substantial 89.9 km² increase in built-up areas between 2013 and 2016, coupled with a minor 18.4 km² increase between 2016 and 2021, reflecting continuous urban expansion driven by population growth and development initiatives. Concurrently, forest area marginally increased by 2.3 km² in 2016, suggesting reforestation and conservation efforts, yet a subsequent 23.5 km² decline by 2021, due to deforestation, urban encroachment, and natural disasters such as wildfires. Notably, vacant land decreased by 92.3 km² in 2016, absorbed by built-up areas and forest expansion, underscoring the urgent need for spatial planning to accommodate the growing population and its evolving needs.

1. INTRODUCTION

Everyday everything around us is changing, it is an inevitable process. Among the different changes, Land Use Land Cover Changes (LULC) is the one that don't just reflect natural features like geology and topography; they're also influenced by social and economic conditions (Rai et al., 1994). Population is the main factor that determines the changes in the environment. The growth in population and economic activities are closely linked to the expansion of urban areas, resulting in growth of urbanization which has the close relation with the LULC changes (Yasin et al., 2022) . Urbanization is the major cause that has resulted in fast evolution in the land use and land cover leading to forest deforestation and transformation of fertile land into other activities and demand for food and land (Krishna, 2021) .Due to improper and unmanaged urbanizations, deforestation is increasing daily which can cause soil erosion, flood, fewer crops, extinction of flora and fauna, the health of humans and wildlife and many more (Chaudhary et al., 2015). Urban heat islands, air pollutant emission, ecological injury, and urban climatic alteration are some other environmental problems related to rapid urbanization. Therefore, an accurate urban data, including NDVI and NDBI, is essential for understanding environmental issues and urbanization. This data offers insights into land changes and vegetation, aiding in effective land management and environmental monitoring. This understanding is important for investigating land use and land cover change that provides vital input in making better decisions on management. Analyzing land use changes over time is key for managing forests sustainably. It helps balance protection, conservation, and production, ensuring resources are utilized sustainably in temperate ecosystems. Understanding evolving land patterns informs informed forest management decisions. Additionally, in urban settings, the relationship between land use and land cover patterns and the resulting thermal characteristics of the environment has gained significant attention. Urbanization influences these dynamics, leading to alterations in the thermodynamics of the air within cities. Studying these spatial dynamics is crucial for comprehending the impact of urban growth on the thermal environment and can guide strategies for urban planning and management to mitigate adverse effects associated with these changes. The study of the changes due to urbanization is essential to study the land use land cover change and for the information for appropriate decision making (Deng et al., 2009).

2. STUDY AREA

The study area for this study is the Kathmandu District situated in the central part of the country. Kathmandu District covers an area of approximately 395 km². It is one of the three districts located in the Kathmandu Valley. It is located from 27°27′E to 27°49′E latitude and from 85°10′N to 85°32′N longitude. It is surrounded by Bhaktapur and Kavrepalanchowk in the east, Dhading and Nuwakot in the west, Nuwakot and Sindhupalchowk in the north, and Lalitpur and Makwanpur in the south. It is the most densely populated district in Nepal, with a population of over 2.04 million residents as of the most recent data available (NSO, 2021). The main reason to choose Kathmandu as the study area is that it is the most developed district among others in Nepal. A huge number of people have migrated from rural to urban areas, and the rapid increase in population has resulted in challenging problems such as crowding and land use conflicts, environment and problems in urban planning and management The district is characterized by rapid urban growth and environmental changes . Hence, this research project is centered in the Kathmandu District, Nepal, with a focus on LULC change detection, urbanization trends, and forest dynamics.

Studying these spatial dynamics is crucial for comprehending the impact of urban growth on the thermal environment and can guide strategies for urban planning and management

to mitigate adverse effects associated with these changes. The study of the changes due to urbanization is essential to study the land use land cover change and for the information for appropriate decision making (Deng et al., 2009).

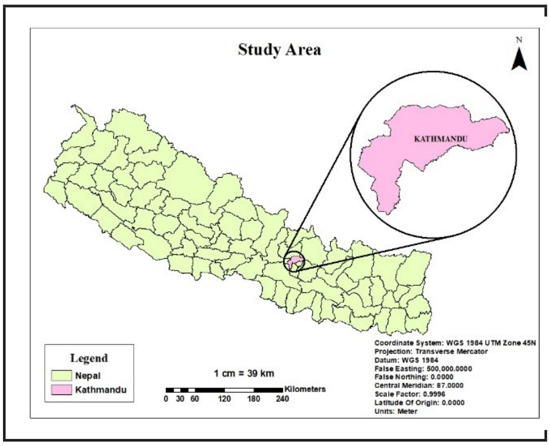

Figure 1: Study Area Map.

3. METHODOLOGY

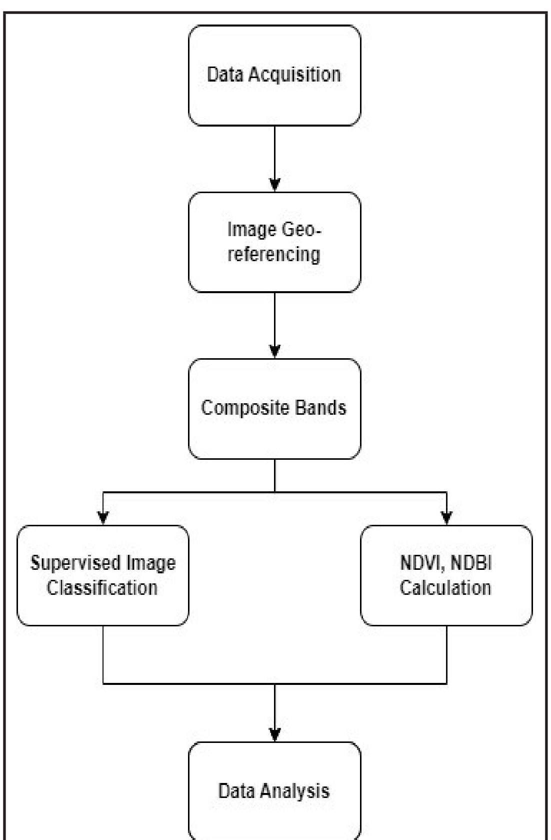

Figure 2: Workflow of Project.

3.1. Data acquisition

Landsat 8 with Operational Land Imager (OLI) sensor was acquired. Satellite image with spatial resolution of 30m was used of the time of 2013, 2016 and 2021. The detail of satellite data is given as:

- Satellite: LandSat 8
- Sensor: Operational Land Imager (OLI)
- Path and Row: 141 and 041
- Date: 2013/11/02, 2016/10/25, 2021/11/08
- Resolution: 30m
- Bands: 1-8

3.2. Image geo-referencing

Satellite information which acquired in raster image format was geo-referenced to WGS-84 datum.

3.3. Composite bands

Landsat 8 images were used to create a composite that consists all the necessary required for this study. Composite Images for 2013, 2016 and 2021 of Kathmandu District was created with the help of GIS Environment Composite Band Toolbar.

3.4. Supervised image classification

Supervised image classification is a fundamental technique used to categorize land cover and land use in remote sensing and GIS applications. In this study, we employed supervised image classification to create LULC maps.

At an initial step, we selected some of the training data. Representative samples of various land cover and land use classes within the study area were identified. These samples were collected based on multi-spectral satellite images. After training data, Maximum Likelihood Classification (MLC) Algorithm was used for categorizing the land cover classes based on the extracted features. The algorithm utilized the spectral information of the training samples to establish decision boundaries in feature space. Once trained, the classifier was applied to the entire study area to classify each pixel into one of the predefined land cover classes. Finally, the LULC maps were generated based on the classification results, with each pixel assigned to a specific land cover or land use category.

3.5. NDVI, NDBI calculation

To quantitatively assess vegetation and built-up areas within the study area, we calculated NDVI and NDBI. These indices are derived from remote sensing data and provide valuable information about land cover and land use. The following steps were taken to compute NDVI and NDBI:

- Band Selection: Since Landsat 8 OLI imagery has been used for this study, Band 4(Red), Band 5(NIR) and Band 6(SWIR) were used for the calculation of NDVI and NDBI. These bands were chosen due to their sensitivity to vegetation and built-up features.
- NDVI Calculation: This index measures the presence, density and health of vegetation, with higher values indicating healthier vegetation cover which is calculated by:

$$NDVI = \frac{NIR - Red}{NIR + Red}$$

- NDBI Calculation: This index is used to assess the distribution of built-up or urban areas, with higher values indicating a greater extent of built-up features which is calculated by:

$$NDBI = \frac{SWIR - NIR}{SWIR + NIR}$$

- Mapping NDVI, NDBI: Hence, the map is prepared from NDBI and NDVI calculations.

3.6. Data analysis

We represented and interpreted all the collected data using bar diagrams in MS Excel 2016 and created maps using a GIS environment.

Numerous efforts have been made to extract information from remotely sensed images, with quantitative analysis being a key approach. Image Classification, a powerful digital technique, is commonly used for information extraction. We have utilized image classification to extract following data:

Table 1: Extracted Data from Digital Interpretation.

Classification Category	2013		2016		2021	
	Area (km²)	Area (%)	Area (km²)	Area (%)	Area (km²)	Area (%)
Built-Up Area	126.7	31	216.6	52	235	57
Forest Area	192.7	47	195	47	171.5	41
Vacant Land	94.2	22	1.9	1	7	2

Table 1 explains the area covered in km² and percentage of each classification categories in different time periods of Kathmandu District.

4. RESULT AND DISCUSSION

Table 1 and the Figure 3, 4, 5 clearly explains that the capital city of Nepal has become increasingly congested, and the city has expanded outwards depleting the forest or vegetation area. From the classification of imagery of 3 different years i.e., 2013, 2016 and 2021, LULC map has been prepared for the following study area.

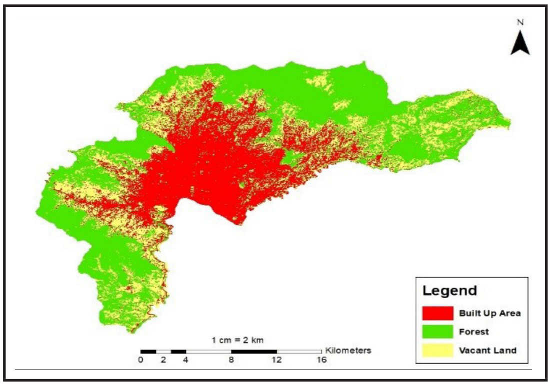

Figure 3: LULC Map of Kathmandu (2013).

Figure 3 shows the LULC map of Kathmandu District for the year 2013 reveals a dynamic distribution of land across various categories. Notably, the built-up area encompasses 126.7 km², constituting 31% of the district's total land. A significant portion of the landscape is dominated by lush forest cover, covering 192.7 km² and representing 47% of the district. Complementing these urban and natural landscapes is the presence of vacant land, accounting for 94.2 km², equivalent to 22% of the total area. This comprehensive breakdown provides valuable insights into the spatial composition of the district, reflecting the interplay between urban development, environmental preservation, and open spaces within the Kathmandu region in 2013.

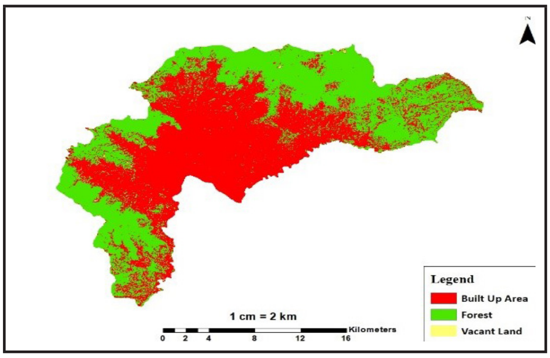

Figure 4: LULC Map of Kathmandu (2016).

Figure 4 shows the LULC map of Kathmandu District for the year 2016 reveals that built-up area has undergone a substantial expansion, surging from 126.7 km² in 2013 to 216.6 km² in 2016. This signifies a remarkable increase of 89.9 km², reflecting a substantial 71% growth over the three-year period, indicative of intensified urban development. In contrast, the forested area has seen a marginal decline, decreasing from 192.7 km² in 2013 to 195 km² in 2016, representing a modest reduction of 2.7 km² or a 1.4% decrement. The most significant transformation is observed in vacant land, which has experienced a drastic reduction from 94.2 km² in 2013 to 1.9 km² in 2016. This translates to a substantial decrement of 92.3 km², highlighting a notable 98% decrease over the three-year span. These shifts underscore the dynamic interplay between urbanization, environmental conservation, and evolving land use patterns within the Kathmandu District during this period.

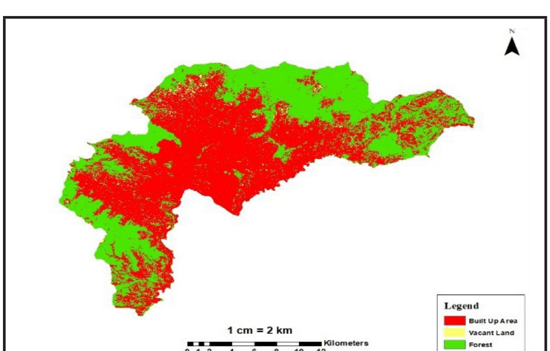

Figure 5: LULC Map of Kathmandu (2021).

Figure 5 shows the LULC map of Kathmandu District for the year 2021. Over the span of five years, from 2016 to 2021, reveals noteworthy shifts in the distribution of land across key categories. The built-up area has demonstrated a consistent expansion, increasing from 216.6 km² in 2016 to 235 km² in 2021, marking an 8.5% growth over this period. Conversely, the forested area has experienced a more pronounced reduction, diminishing from 195 km² in 2016 to 171.5 km² in 2021, representing a 12% decrease. A compelling observation is the notable rise in vacant land, escalating from 1.9 km² in 2016 to 7 km² in 2021, signaling a substantial 268% increase. These trends underscore the ongoing transformation in land use patterns, emphasizing persistent urbanization, a significant decrease in forested areas, and a notable increase in vacant land within Kathmandu District during the five-year period. The intricate dynamics reflect the evolving balance between urban development and environmental conservation in the region.

The overall changes seen over time from 2013 to 2021 is tabulated below:

Table 2: Change Detection in Land Use Land Cover.

Classification Category	2013/2016		2016/2021	
	Change in area (km²)	Change in area (%)	Change in area (km²)	Change in area (%)
Built-Up Area	89.9	21	18.4	5
Forest Area	2.3	1	-23.5	-6
Vacant Land	-92.3	-22	5.1	1

Above tabular data can be visualized in bar chart diagram as follow:

Figure 6: Change in Land Use Distribution.

Table 2 and Figure 6 clearly show that the built-up areas have been increased by around 89.9 km² in between 2013 & 2016 while 18.4 km² in between 2016 & 2021. Similarly, Forest area has been increased by 2.3 km² in 2016 while decreased by 23.5 km² till 2021. Talking about the vacant land, it has been decreased by 92.3 km² in 2016 which was utilized by built-up areas and forest to some extent while increased by 5.1 km² by 2021.

Thus, from 2013 to the end of 2021 the changes seen in built-up areas, forest area and vacant land is increased by 108km², decreased by 21.2km² and decreased by 87.2km² respectively. Similarly, we have calculated the indexes like NDVI and NDBI which resulted the following maps:

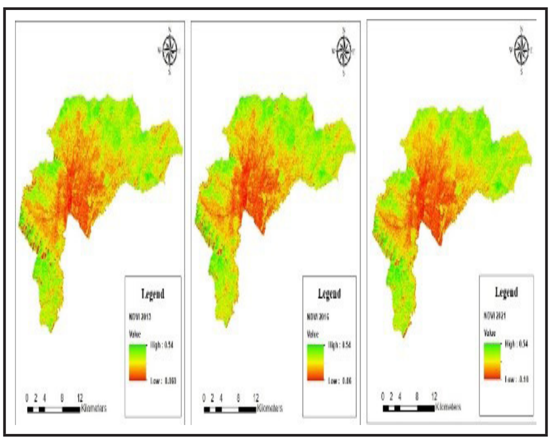

Figure 7: NDVI Map of Kathmandu District.

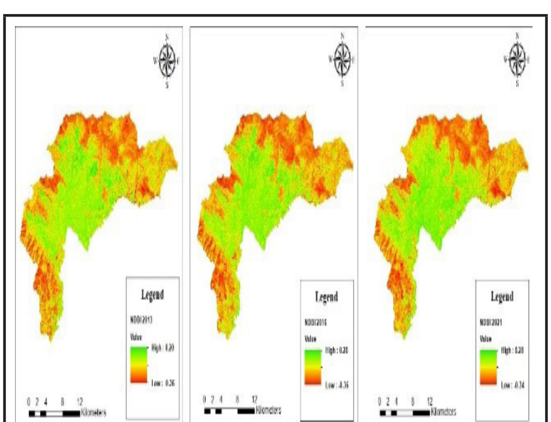

Figure 8: NDBI Map of Kathmandu District.

The above map resulted from NDVI and NDBI shows the increment in the built-up area that has an adverse effect on forest area. This result expected a linear trend as follows:

Table 3: Linear Trend and Future Expectation.

Classification Category	Generated Equation	Estimated Area by 2024
Built-up Area	y = 12.532x - 25079	285.8km²
Forest Area	y = -2.8592x + 5952.4	165.3km²

This estimated trend shows the built-up area to be increased to about 285.8 km² in 2024 while the trend line shows the decrement of forest area to 165.3 km² in 2024 which can be shown through the linear graph.

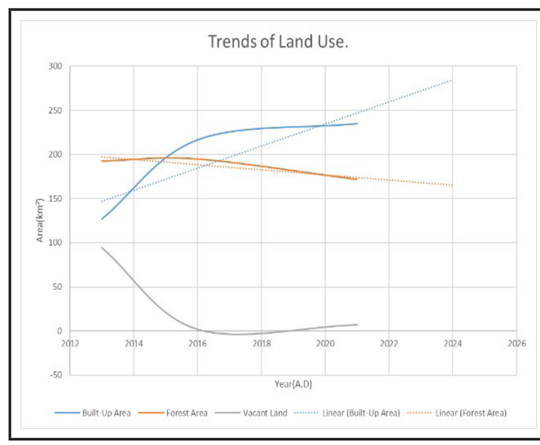

Figure 9: Estimated Linear Trend.

5. CONCLUSION

As a result of this study, it has been revealed that NDBI and NDVI provide a dynamic view of urban growth and may significantly improve the accuracy of analyses of land use cover change due to their dynamic nature. Also, it reveal significant transformations in the Kathmandu District over the study period, with a notable increase in built-up areas at the expense of forested regions and vacant land. The rapid urban expansion observed underscores the urgent need for sustainable land management practices and effective urban planning strategies.

Despite the valuable insights gained from the study, certain limitations were identified, including the spatial resolution of satellite imagery and the focus on a limited number of land use categories. Future research endeavors should address these limitations and incorporate additional factors to provide a more comprehensive understanding of land use dynamics and their implications.

In conclusion, the study contributes to the existing body of knowledge by shedding light on the complex interplay between urbanization, land use changes, and environmental conservation in the Kathmandu District. The findings underscore the need for collaborative efforts among policymakers, land-use planners, and stakeholders to promote sustainable land management practices and safeguard vital ecosystems for future generations.

ACKNOWLEDGEMENT

We extend our heartfelt gratitude to Er. Umesh Bhurtyal, Head of Department of Geomatics Engineering at Western Region Campus (WRC), for providing us with this invaluable opportunity. Special thanks to Er. Ajay Kumar Thapa, Graduate Coordinator of Geomatics Engineering at Kathmandu University, for his unwavering guidance throughout this endeavor.

REFERENCES

Chaudhary, R. P., Uprety, Y., & Rimal, S. K. (2015). *Deforestation in Nepal: Causes, consequences and responses.* ResearchGate.

Deng, J. S., Wang, K., Hong, Y., & Qi, J. G. (2009). Spatio-temporal dynamics and evolution of land use change and landscape pattern in response to rapid urbanization. *Landscape and Urban Planning*, *92*(3–4), 187–198. https://doi.org/10.1016/j.landurbplan.2009.05.001

Krishna, T. V. (2021). Impact of Population growth on Land Use / Land Cover changes and Environment - A case study of Tribal region of Visakhapatnam District. *International Journal of Scientific Development and Research (IJSDR)*, *6*(7).

NSO. (2023). *National population and housing census 2021: National Report.* National Statistics Office, Kathmandu, Nepal.

Rai, S. C., Sharma, E., & Sundriyal, R. C. (1994). Conservation in the Sikkim Himalaya: Traditional Knowledge and Land-use of the Mamlay Watershed. *Environmental Conservation*, *21*(1), 30–34. https://doi.org/10.1017/S0376892900024048

Yasin, M. Y., Abdullah, J., Noor, N. M., Yusoff, M. M., & Noor, N. M. (2022). Landsat observation of urban growth and land use change using NDVI and NDBI analysis. *IOP Conference Series: Earth and Environmental Science*, *1067*(1), 012037. https://doi.org/10.1088/1755-1315/1067/1/012037

Author's Information

Name	:	Rabina Poudyal
Academic Qualification	:	Undergraduate Student of Geomatics Engineering
Organization	:	Department of Geomatics Engineering, Kathmandu University
Current Designation	:	Student

Price of Maps

S.No.	Description	Scale	Coverage	No. of sheets	Price per sheet (NRs)
1.	Topo Maps	1:25 000	Terai and mid mountain region of Nepal	590	150
2.	Topo Maps	1:50 000	HIgh Mountain and Himalayan region of Nepal	116	150
3.	Land Utilization maps	1:50 000	Whole Nepal	266	40
4.	Land Capibility maps	1:50 000	Whole Nepal	266	40
5.	Land System maps	1:50 000	Whole Nepal	266	40
6.	Geological maps	1:125 000	Whole Nepal	81	40
7.	Districts maps Nepali	1:125 000	Whole Nepal	76	50
8.	Zonal maps (Nepali)	1:250 000	Whole Nepal	15	50
9.	Region maps (Nepali)	1:500 000	Whole Nepal	5	50
10.	Nepal (English)	1:500 000	Whole Nepal	3	50
11.	Nepal Map (Nepali)	1:1000 000	Nepal	1	50
12.	Nepal Map (Nepali)	1:2000 000	Nepal	1	15
13.	Nepal Map (English)	1:1000 000	Nepal	1	50
14.	Nepal Map (English)	1:2000 000	Nepal	1	15
15.	Physiographic Map	1:2000 000	Nepal	1	15
16.	Relief Map	1:2000 000	Nepal	1	15
17.	Photo Map			1	150
18.	Wall Map (loosesheet)		Nepal	1 set	50
19	VDC/Municipality Maps (Colour)		Whole Nepal	4181	50
20.	VDC/Municipality Maps A4 Size		Whole Nepal	4181	5
21.	VDC/Municipality Maps A3 Size		Whole Nepal	4181	10
22.	Orthophoto Map		Urban Area (1:5000) and Semi Urban Area (1:10000)	-	1 000
23.	Outlined Administrative Map A4 size		Nepal	1	5

Price of Co-ordinates of Control Points

Type	Control Points	Price per point
Trig.Point	First Order	Rs 3 000.00
Trig. Point	Second Order	Rs 2 500.00
Trig. Point	Third Order	Rs 1 500.00
Trig. Point	Fourth Order	Rs 250.00
Bench Mark	First & Second Order	Rs 1 000.00
Bench Mark	Third Order	Rs 250.00
Gravity Point	-	Rs 1 000.00

Price of CORS Station Data

Type	Price
24 hr CORS Rinex data with 1 sec frequency for post processing	Rs 200
24 hr CORS Rinex data with 15 sec frequency for post processing	Rs 100
1 hr CORS Rinex data with 1 sec frequency for post processing	Rs 10
1 hr CORS Rinex data with 15 sec frequency for post processing	Rs 5
RTK Correction Service Unlimited Subscription 1 month	Rs 10000
RTK Correction Service Unlimited Subscription 3 months	Rs 27000
RTK Correction Service Unlimited Subscription 12 months	Rs 96000
GNSS Post-processing Service per point per hour data	Rs 10

Price of Geoid Data

Type	Price	Remarks
Geoid N-Sepration (per point)	Rs 200	
Geoid Determined Orthometric Height (per point)	Rs 1000	
Geoid Data (per 100 sq. km)	Rs 10000	Minimum 100 sq.km and multiple of 100 sq.km

Cadastre in Nepal: Need for 3D and Way Towards 4D

Pravesh Yagol[1], Susheel Dangol[1], Prakash Joshi[1]
shrpravesh@gmail.com, susheeldangol@gmail.com, lightjoshiji@gmail.com
[1]Survey Department

KEYWORDS

Cadastre, Cadastral System, 3D cadastre, 4D Cadastre

ABSTRACT

Increase in population and its migration towards urban areas are leading to unmanaged urbanization generating pressure on the land. To meet the demand of migrating people, high rise buildings are being developed. Since land is a limited resource, this is a better solution. Rights on vertical strata in the same parcel need to be recorded technically and legally in cadastral data as well as land registers. In Nepali context, despite some limited legal provisions for recording 3D cadastral data, there is still a gap in recording spatial information technically. On the other hand, due to the lack of clear spatial information recording and limited provisions for recording in land registers, land disputes are also arising. However, an increase in land dispute cases is not the only issue; there are a huge number of reasons related to legal and technical provisions in land administration. Therefore, in order to minimize land dispute cases, 4D cadastre can provide a better solution. The paper discusses the legal provisions of 3D cadastre and its need in the context of Nepal, along with the need for 4D cadastre to support in reducing land dispute cases

1. BACKGROUND

Rapid population growth leading to intense pressure on land for urban development ultimately creates limited availability for a growing population, necessitating the development of high-rise apartments and complex building structures above and below the ground. This demand for efficient land administration services to record ownership details of these complex structures (Karki, 2013). Population increase around the world has put more emphasis on land use, and this trend has highlighted the importance of recording changes in the relationship between humans and land clearly and indisputably in a system (Stoter, 2004). Such a system is referred to in various ways, such as cadastral system, cadastral registration, land registry, land registration, land administration, property register, land book etc. In this paper, the system is simply termed cadastre. The paper follows the term cadastre as defined by the International Federation of Surveyors (FIG) in its statement on the cadastre (FIG, 1995): "A Cadastre is normally a parcel based, and up-to-date land information system containing a record of interests in land (e.g., rights, restrictions and responsibilities). It usually includes a geometric description of land parcels linked to other records describing the nature of the interests, the ownership or control of those interests, and often the value of the parcel and its improvements. It may be established for fiscal purposes (e.g., valuation and equitable taxation), legal purposes (conveyancing), to assist in the management of land and land use (e.g., for planning and other administrative purposes), and enables sustainable development and environmental protection."

Cadastral registration in Nepal is a record of the land rights that are registered on land and the information of land registration which is linked to parcels are maintained in two different data structures. Hence cadastral registration in this paper refers to both spatial and attribute data. In Nepal, there are two different institutions working for land administration services. Cadastral survey and first registration are done by Survey Offices (SO) and after that, regular land administration services are provided from Land Revenue Office (LRO). In the land administration service, cadastral subdivision and other technical activities are conducted by the SO.

Cadastral registration was originally introduced in Nepal to assist with land taxation during the implementation of land reform program after the formulation of Land Related Act, 1965. It now also provides detailed information required for land transactions, increasing efficiency in land transactions and tenure security. It also provides relevant cadastral information for the government and private sector for various development activities (Stoter, 2004). However, to meet all of these requirements, the system must provide all relevant information such as legal status, Rights, Restrictions & Responsibilities (RRR), location, size, value, use and more. The basic entity for all of this information is the parcel, which is currently shown in 2-Dimensional (2D) cadastral maps. Even though the parcel is represented in a 2D cadastral map, the owner of the parcel is always entitled to the space above and below that parcel in 3D. If the ownership is restricted to the surface only then the use of property would be impossible (Stoter, 2004). The Bathurst Declaration of FIG concluded that "the most land administration systems today are not adequate to cope with the increasingly complex range of rights, restrictions and responsibilities in relation to land" (FIG, 1999) and there is a need for re-engineering in the present land administration system to handle the increasing complexity of the relationship between personal and parcel (Williamson & Grant, 2002).

2. RESEARCH IN 3D CADASTRE

Accurately measuring and visualizing 3D property units is crucial for implementing 3D cadastre. Precise measurement of all dimensions, including height, is necessary to define the 3D boundaries of a property unit (Stoter, 2004). Recent studies have investigated various techniques for 3D cadastral mapping and data collection, including aerial photogrammetry, terrestrial laser scanning, indoor mobile mapping systems, and utilizing existing 3D datasets like building information models (BIM) (Oldfield *et al.*, 2017).

Research is also focusing on 3D visualization and querying mechanisms through web-based 3D cadastral mapping portals, integration with building models, and virtual/augmented reality solutions (Atazadeh *et al.*, 2017). Conceptual data models such as LADM, IndoorGML, and CityGML have been proposed and studied for standardized 3D digital representation of cadastral objects and property units (Kara *et al.*, 2020). Different studies show that institutional and governance aspects, including legislative reforms, professional capacity building, stakeholder collaboration, and business models, are crucial for the successful implementation of 3D cadastral systems (Dimopoulou & Elia, 2012).

3. INTERNATIONAL PRACTICE IN 3D CADASTRE

Global efforts in 3D cadastre showcase the various strategies employed by different countries. Many countries have made progress towards developing 3D cadastral systems and standards in recent years. For example, the Dutch Cadastre, Land Registry, and Mapping Agency (Kadaster) have been at the forefront of implementing 3D cadastre whose system enables the registration of 3D property units such as apartments, utilities, and complex spatial constructions (Stoter *et. al*., 2017).

In 2004, Sweden implemented a 3D cadastral system that enables the registration of 3D property units called 3D property spaces which can represent buildings, apartments, or other structures with intricate spatial dimensions (Paulsson, 2007). Similarly, the Queensland Government has introduced a 3D cadastral system using "building format plans" to define the spatial boundaries of individual property units within a building. This system enables the registration of 3D property units like apartments and townhouses in multi-level developments (Karki *et. al*., 2010).

Singapore has adopted a 3D cadastral system for registering strata titles, used for owning apartments, office units, and multi-level properties. This system also facilitates the registration of subterranean properties like underground tunnels and utilities (Khoo, 2012).

International practices in 3D cadastre offer valuable insights and solutions. They utilize techniques such as 3D digital cadastral databases, spatial data models, and legal frameworks for 3D property rights (Stoter *et al*., 2017; Karki *et al*., 2010; Paulsson, 2007). The insights from global practices can guide Nepal in developing a successful 3D land administration system that suits its specific socio-economic conditions.

4. NEED OF 3D CADASTRE

Tremendous pressure on land especially in urban areas has led to the development of apartments where ownership of apartments overlaps on a single parcel or multiple parcels (Karki, 2013; Stoter, 2004). The significant pressure on the limited available land to develop infrastructure for a growing population is the main driving force behind the emerging 3D cadastre (Acharya, 2011). Different ownership on different floors or even on the same floor in an apartment is also being registered. In the context of Nepal some basic legal provisions have been made to register the flat system in apartments. However, these legal provisions are not efficiently practiced in reality due to unclear working procedures and database management for 3D registration. Despite the legal provisions, there has always been a challenge in describing and recording 3D information in cadastral registration (Stoter, 2004). In addition to high-rise apartments, there is also an increasing number of underground utilities that need to be mapped in cadastral registration. These above-ground and underground developments have increased the interest in 3D cadastral registration, with reasons including but not limited to the following:

- Addressing the challenges of overlapping ownership in multi-level apartments.
- Efficient management of complex ownership structures in urban areas.
- Facilitating accurate property valuation and taxation.
- Enhancing land administration and management practices.
- Improving spatial data infrastructure for urban planning and development off underground structures and utilities.

Overall, the growing complexities in land ownership and development patterns necessitate the adoption of 3D cadastral registration to ensure efficient and effective land administration in urban areas.

5. EXISTING PROVISION OF 3D CADASTRE IN NEPAL

Besides the provision of surveying and registration of land in 2D context, land related laws and regulations spell out some provision of 3D registration of land.

5.1. Organizational aspect

Two different organizations are involved in land administration services: the Survey Office (SO) and the Land Revenue Office (LRO). The SO conducts cadastral survey and maintains all the spatial data related information such as cadastral maps and field books from the initial survey. Once the cadastral survey and first registration are completed, the SO provides a copy of a register to the LRO. The LRO then maintains all attribute information of land owners including Rights, Restrictions & Responsibilities (RRR) and other information related to person-parcel relationship. All land transactions are handled by the LRO, while the technical aspects of the transactions are handled by the SO.

The Land administration system in Nepal only includes 2D information, with attributes and spatial components limited to two dimensions. Parcels, buildings, roads, canals and other objects on the ground are measured in 2D and their attributes are recorded accordingly. Acharya (2011) identified several shortcomings in the cadastral maps of Nepal including:

- Vertical information is sparse in cadastral maps and does not exist in all subdivision plans, particularly building subdivisions.
- Determination and measurement of dimensions and areas from these maps and plans may not always be as accurate as the clients' aspirations.
- Rights, restrictions and responsibilities cannot be spatially represented in the plans.
- Restrictions and responsibilities are not mentioned in the title.
- Paper-based plans cannot depict the 3D structure and do not support 3D analysis.
- There is no provision for visualizing the third component on the cadastral maps.

5.2. Legal aspect

The 4th amendment of Land (Survey & Measurement) Act in 1978 incorporated the provisions for registering stratified properties, indicating an early recognition of the need for 3D cadastre. However, it was acknowledged that these provisions were insufficient to address all issues related to 3D cadastre. Article 6, sub-article 5(b) of the Land (Survey & Measurement) Act 1963 stipulates that if different floors of the building have different ownership or even if the same floor has different owners, then the ownership should be registered in the name of separate land owners according to the prescribed format provisioned by land (Survey & Measurement) Rules 4 (4). The existing format of the land register and certificate indicate that, in the case of high-rise buildings, such as apartments, the ownership of the land remains with the developer company.

According to the Land Administration Directive" (LAD), directive number 38 clarifies that if the ground floor belongs to one owner and the upper floor has other owners, details of land parcel should be written in the register of the ground floor owner and the description of all the owners of upper floor should be written in its remarks. In the register of the owner of the uppermost floor, the length and breadth of the house and the parcel number of the ground floor are written in its remarks. The LAD does not address the registration of apartments/flats on a floor. The owner of the ground floor can sell a part of his/her property but the directive remains silent about the subdivision of the property in the upper floor.

The Ownership of Joint Residence Related Act 1997 controls and regulates the permission for construction, sale, ownership and transfer of the property. Some relevant legal provisions are listed as follows: -

- An Apartment can be constructed with the permission of concerned legal authority.
- The apartment can be sold, rented or given to use through other means by the legal founder person (having permission to build the apartment) according to the act.
- The apartment owner can transfer the right or sell the apartment with the permission of the founder.

Similarly, the land administration directives provide guidance on recording details of multi-floor properties in land registers, but they do not comprehensively address complex 3D property scenarios, such as shared ownership of a single floor. The legal framework should be enhanced to facilitate proper 3D cadastral registration and documentation of all types of 3D property interests.

5.3. Technical aspect

The technical aspect of 3D cadastre in Nepal encompasses limited regulatory provisions meanwhile insufficient technological infrastructure. According to the Land (Survey and Measurement) Regulation of 2058 B.S., there are provisions for recording the flat system and the related owners' names in the Field Book. Additionally, the Land Records Information Management System (LRIMS), a centralized system operated through intranet and used by LROs, plays a crucial role in ensuring record of apartment and its details. It ensures whether the particular property has an apartment or not, limiting to further transaction of that parcel.

Within LRIMS, there are provisions for recording detailed information about apartments, including apartment number, name, builder's name, block number, flat number, area, height, length, and type. Moreover, LRIMS captures data related to apartment societies, such as society name, district, municipality, ward number, and relevant details.

The integration of LRIMS involves linking the Apartment Table and Apartment Society Table with the main Property Table using Property ID. Additionally, the Apartment Society Table is linked to the Apartment Table using Apartment ID. Furthermore, LRIMS incorporates a Facilities Table, which records information about amenities such as parking, groceries, and shops, linked with the Apartment ID.

Despite these advancements, one notable limitation is the absence of provisions for recording the names of individual flat owners. Also, spatial representation of 3D property is also not included in cadastral data. This gap in data collection represents an area for potential improvement in the technical infrastructure of LRIMS to enhance the comprehensiveness of 3D cadastral information in Nepal.

6. ISSUES IN 3D CADASTRE

Although the provisions of rights, restrictions and responsibilities have been included, they do not address the way they should be registered. The existing technical and legal system does not incorporate the issues such as properties overridden by other owner(s), properties of different owners overlapping on different floors, underground parking, overhead bridges, underground marketplaces and underground cable and utilities. The legal provision for adjudication and documentation of real estate is lacking. Existing legislation for 3D registration or the third dimension on the paper-based plans of subdivision cannot meet current demands. The technical aspects of 3D data capturing, representation, visualization, updating and modelling of cadastral objects have not been addressed by existing laws. Therefore, there will be some technical obstacles to the development and implementation of the 3D cadastre.

In the present context, various issues need to be addressed to develop a 3D cadastre system in Nepal. Inheritance of property in Nepal is a very sensitive issue. Different rooms of a house can be inherited by different individuals. In some cases, especially in Kathmandu Metropolitan areas, there are places where the ground floor of a building is used by a community, while the upper floors are owned by different owners. In some districts, particularly in remote hilly districts like Jumla, houses are built in such a way that the roof of a house owned by a family is used as a courtyard by the owner of the house built in the upper terrace of the ground (Bhatta, *et.al*, 2005). These are some issues that have not been well addressed by the existing registration system.

With the growing population and a dramatically increase in migration towards urban areas, high-rise residential buildings are becoming the only solution. In the last decade, urban centers have seen significant investment in the construction of such buildings. Middle income families are attracted towards purchasing apartments in these buildings. However, there is hesitation in investment due to lack of clarity about the security of ownership over such apartments. Existing legal provisions do not clearly mention about the rights of the owner of each unit in a multi-story building over common space areas. People are unsure about the future consequences if the building is damaged and whether they have any rights over the land on which the building. Therefore, there is a strong need for clear legal provisions in this regard.

In another scenario, urban centers in Nepal are becoming densely populated, leading to a lack of space for constructing adequate transportation and utility infrastructures. To address the needs of the growing population, these infrastructures must be expanded, requiring the utilization of space below or above the land surface. Acquiring space below and above the earth's surface will involve obtaining rights from the owners of the respective parcels. Without a proper system for registering such cases, efficiency will be compromised, highlighting the necessity of implementing a 3D cadastre system. The current legal framework does not adequately support the registration of overriding interests of different entities over a single piece of land, a task that can only be achieved through the implementation of a 3D cadastre system.

7. CONCEPT OF 4D CADASTRE

Use of land is related to the area over the ground (2D), the area above the ground (3D) and the span of time (4D) (Doner, et. al., 2010). For apartments and underground utilities, a 3D representation is relevant, while changes in legal status of a parcel can be recorded in the 4D. Parcel often undergo changes in ownership either in a whole or in part after parcel subdivision. The history of this information can only be maintained in the 4th dimension (time dimension). Time has always played an important role in maintaining the history in cadastral system but has been treated separately and independently from the spatial aspect (Oosterom, *et. al*., 2006). 4D registration in cadastral system is specifically needed for recording dynamic objects cases, time sharing cases and utilities registration cases (Oosterom et al., 2006). Parcel boundaries in the field can change over time due to river erosion and meandering. In some cases, cattle farmers lease land to graze cattle for many years and put up fences, which may need to be defined as temporary parcel boundaries for that farmer.

In other cases, a certain piece of land can be rented for a specific period of time, or a unit in a building can be shared on a weekly basis, which may need to be recorded. Similarly, the registration of utilities underground is also becoming a crucial issue. To record all of the aforementioned issues, 4th dimension is very necessary.

8. LEGAL ASPECT AND DISPUTE RESOLUTION THROUGH 4D CADASTRE

The time component (4th dimension) in cadastre is necessary to track the history of land transactions and to reflect the reality of rights over due course of time (Vuĉić, *et al*., 2014). When conducting the land transactions, they are based on the legal framework that existed at the time of the transaction. As the time passes, changes in laws are needed to meet the requirements of the present context, leading to amendments or reformulations of different land-related laws. Recently, questions have been raised about land transactions conducted in the past in relation to current rules and regulations. This situation has increased the number of land dispute cases and the fraudulent land transactions cases by oversight agencies.

In the context of Nepal, most of the fraudulent land transaction cases registered by oversight agencies, were conducted many years ago under laws that were legal at the time but are now deemed fraudulent under current land regulations. The challenge is that decisions made during those periods may be poorly documented or lost due to inadequate archiving practices. Additionally, successive generations of employees may be unaware of these historical transactions. These transactions were genuine at that time they were made. Thus, it's crucial to contextualize such transactions within the legal framework of the time they occurred. Therefore, when analyzing transactions, the time dimension needs to be considered and linked to the prevailing laws at that time. Recording the time dimension (4D) and linking it to the rules and regulations in place at that time will help reduce land disputes and cases of fraudulent land transaction by the oversight agencies.

9. CONCLUSION

Modern day property ownership and land use are rapidly being changed to the highest levels of complexity due to increasing urbanization and population growth. This underscores the need for a more advanced cadastral system capable of not only representing real-world objects in two or three dimensions (3D) but also recording the 4th dimension (time). Nepal's existing cadastral system, though it includes some basic legal provisions for 3D registration, predominantly relies on two-dimensional (2D) cadastral maps and lacks the essential technical and legal frameworks to fully accommodate 3D and 4D cadastre.

The proliferation of high-rise buildings with apartment ownership, underground structures, and extensive utility networks has created a demand for 3D cadastral registration, while the increasing cases of land disputes has highlighted the necessity of 4D cadastre. However, Nepal's current legal framework lacks clarity on issues such as ownership of common spaces in multi-story buildings, registration of overriding interests on a single parcel by different entities, and documentation and adjudication of complex real estate situations.

Nepal's cadastral system struggles with capturing, representing, updating, and modelling 3D cadastral objects. The existing paper-based and semi-analog systems are inadequate to meet the growing need for 3D and 4D cadastre. Precise measurement and documentation of all dimensions are crucial for accurate visualization and modelling of 3D property units.

To establish a robust 3D and 4D cadastre system in Nepal, a comprehensive approach is necessary. This includes updating the legal framework to incorporate clear provisions for 3D property rights, registration, and adjudication over time, developing technical standards and guidelines for 3D data capture, modeling, visualization, and management over time, providing training and capacity building, exploring the use of modern technologies such as 3D GIS, BIM, and VR tools to enhance the visualization and management of cadastral data. By addressing current challenges and adopting a holistic approach, Nepal can establish a more efficient, transparent, and equitable land administration system that meets the needs of a rapidly urbanizing population.

REFERENCES

Acharya, B. R. (2011). *Prospects of 3D Cadastre in Nepal*. 2nd International Workshop on 3D Cadastre. Held on 16-18 November, Delft, the Netherlands.

Atazadeh, B, Kalantari. M, Rajabifard, A. and Ho, S. (2017). Modelling Building Ownership Boundaries Within BIM Environment: A Case Study in Victoria, Australia. *Computers, Environment and Urban Systems*, 61, 24–38. DOI:10.1016/j.compenvurbsys.2016.09.001

Bhatta, G.P., Khanal, G.R., and Sharma, R. K. (2005). *Registration of 3rd Dimension: The Context of Nepalese Cadastre*. Nepalese Journal on Geoinformatics, (4), Kahtmandu, Nepal.

Dimopoulou, E., and Elia, E. (2012). *Legal Aspects of 3D Property Rights, Restrictions and Responsibilities in Greece and Cyprus.* 3rd International Workshop on 3D Cadastres, 25-26 October 2012, Shenzhen, China.

Doner, F., Thompson, R., Stoter, J., Lemmen, C., Ploeger, H., Oosterom, P. V., and Zlatanova, S. (2010). 4D Cadastres: First Analysis of Legal, Organizational and Technical Impact – With a Case Study of Utility Networks. *Land Use Policy*, 27 (2010) 1068-1081.

FIG. (1995). *FIG Statement on the Cadastre.* (Vol. 11). The International Federation of Surveyors (FIG).

FIG. (1999). *The Bathurst Declaration on Land Administration for Sustainable Development* (Vol. 21). The International Federation of Surveyors (FIG). https://www.fig.net/resources/publications/figpub/pub21/figpub21.asp

Kara, A., van Oosterom, P.J.M., Çagdas, V., Isıkdag, Ü., and Lemmen, C.H.J., (2020). 3-Dimensional Data Research for Property Valuation in the Context of the LADM Valuation Information Model. *Land Use Policy* (98), November 2020.

Karki, S., Thompson, R., & McDougall, K. (2010). *An Overview of 3D Cadastre from a Physical Land Parcel and a Legal Property Object Perspective:* XXIV FIG International Congress 2010.

Karki, S. (2013). *3D Cadastre Implementation Issues in Australia* [PhD Thesis]. University of Southern Queensland.

Khoo, V. H. S. (2012). *3D cadastre in Singapore*. In Proceedings of the 3rd International Workshop on 3D Cadastres: Developments and Practices (pp. 279-294).

Oldfield, J., van Oosterom, P., Beetz, J., and Krijnen, T. F., (2017). Working with Open BIM Standards to Source Legal Spaces for a 3D Cadastre. ISPRS International Journal Geo-Information, Nov. 2017 6 (11), 1–19.

Oosterom, P. V., Ploeger, H., Stoter, J., Thompson, R., and Lemmen, C. (2006). Aspects of a 4D Cadastre: A First Exploration. Shaping the change. XXIII FIG Congress, Munich, Germany, October 8-13, 2006.

Paulsson, J. (2007). *3D property rights: an analysis of key factors based on international experience*. Royal Institute of Technology (KTH), Stockholm, Sweden.

Stoter, J. E. (2004). *3D Cadastre* [PhD Thesis]. Netherlands Geodetic Commission.

Stoter, J. E., Ploeger, H., Roes, R., van der Riet, E., Biljecki, F., Ledoux, H., & Lemmens, M. (2017). Registration of multi-level property rights in 3D in the Netherlands: two cases and next steps in further implementation. *International Journal of Geo-Information*, 6(6), 158.

Vuĉić, N., Roić, M., and Markovinović, D. (2014). *Towards 3D and 4D Cadastre in Croatia*. 4th International Workshop on 3D Cadastre, 9-11 November 2014, Dubai, UAE.

Williamson, I. P., & Grant, D. M. (2002). *United Nations-FIG Bathurst Declaration on Land Administration for Sustainable Development: Development and Impact*. 12.

Author's Information

Name	:	Pravesh Yagol
Academic Qualification	:	Master of Science in Geospatial Technologies
Organization	:	Survey Department
Current Designation	:	Survey Officer
Work Experience	:	13 years
Published paper/article	:	7

Obituary

All the officials of Survey Department pray to the almighty for eternal peace to the departed soul of the following officials of the department and this department will always remember the contribution they have made during their service period in this department.

Sansar Nath Panday
Then Chief Survey Officer
17 Kartik 2080

Alina Bhandari
Assistant Surveyor
Survey Office, Jajarkot
18 Kartik 2080

Ram Narayan Sah
Then Surveyor
28 Magh, 2080

Sanju Rokaya
Assistant Surveyor
Survey Office, Kathmandu, Dillibazar
23 Falgun, 2080

Climate Change and Flood Vulnerability Analysis in the Narayani River of Nepal

Kiran Maharjan (Ph.D.)[1], Susheel Dangol[2]
kiran0maharjan@gmail.com, susheeldangol@gmail.com
[1]University of New South Wales, Australia, [2]Survey Department, Nepal

KEYWORDS

Climate change, Vulnerability, Flood analysis, Disaster

ABSTRACT

Flood disasters annually devastate livelihoods, particularly during the monsoon season, with no apparent reduction in impacts in low-lying regions of developing countries like Nepal. Given the increasing effects of climate change globally, this study aims to assess climate change effects and biophysical vulnerability of riverine communities to floods in the Narayani River of Nepal, elucidating the interrelationship between these phenomena. This paper presents an analysis of trends and extreme events of climatological variables, such as temperature, precipitation, and daily river discharge and hazard mapping and risk assessments in the river stretch of two Village Development Committees (VDCs) in the country's inner Terai region of Nawalparasi district for different return-period floods, with the aid of the HEC-RAS (Hydrologic Engineering Centre's River Analysis System) and HEC-GeoRAS. A long-term climatological data was collected from the Department of Hydrology and Meteorology, Kathmandu, and the analysis was performed using statistical softwares, SigmaStat, and SigmaPlot. In addition, flood conditions representing 2, and 100-year periods were determined using Gumbel's distribution. The study revealed a narrowing temperature range, with increasing minimum temperatures and decreasing maximum temperatures, precipitation, and river discharge. However, there was a notable increase in extreme events. The hazard mapping indicated the people's vulnerability to inundation and soil erosion along the low-lying riverbanks. The findings underscore the necessity for reliable technological and socio-economic vulnerability mapping to provide early warnings to at-risk populations. This paper argues that unplanned and mismanaged settlements in riverine areas may lead to population displacements, creating environmental refugees.

1. BACKGROUND

Flood disasters are a prevalent global phenomenon that pose intricate challenges stemming from a combination of human vulnerabilities, insufficient development planning, and climate variability (Bubeck et al., 2012). The absence of adequate development planning, changes in land use, haphazard construction of infrastructure in flood-prone areas, and river obstructions all elevate the risk of flooding occurrences. Noteworthy natural disasters such as the Indonesian Tsunami, Hurricane Katrina in the USA (Hoggan, 1997), and the floods in the UK in 2000 and 2007 (Wilby et al., 2008) serve as poignant reminders of the catastrophic consequences floods can inflict on both human lives and economies. Recent flood events in the southern slope of the Himalayas, affecting countries like Pakistan, Bangladesh, India, and other South Asian nations, have resulted in significant human casualties, displacement of populations, and extensive economic losses (Sahoo et al., 2019; Gaire et al., 2015).

Nepal, in particular, faces devastating floods annually, accounting for a significant portion of both human casualties and property damage (Bhattarai & Ghimire, 2023; Gautam et al., 2016). Historical flood occurrences in Nepal have shown that the most significant losses occur along river and rivulet channels, with devastating flood events, for instance, in the years 1993, 2002 in central Nepal, 2008 in the Koshi River, 2008 in western Nepal, 2012 in the Seti River, and 2017 all over the country highlighting the vulnerabilities along riverbanks (Shrestha et al., 2020). These events have resulted in substantial human casualties, property damage, and economic losses, emphasizing the urgent need for effective flood risk management strategies in the region (Devkota, 2021). The country's vulnerability to these disasters is also influenced by factors such as increasing population, poor economic conditions, and unplanned settlements.

The impacts of global climate change further exacerbate the fragility of Nepal's geomorphology. The frequency and intensity of extreme events like floods, and heavy precipitation are projected to increase in South Asia due to global warming (Hasson et al., 2015). Studies indicate that the warming trend in the Himalayas exceeds the global average, emphasizing the region's heightened susceptibility to climate variations (IPCC, 2007a; Meehl et al., 2007; Shrestha et al., 2016).

A combination of structural and non-structural measures is essential for effective flood hazard reduction to address the negative impacts of flooding. While structural measures like culverts, dams, and dykes are considered hard approaches to flood control, they may pose environmental and societal risks (Binns, 2020). In contrast, soft measures, including hazard mapping, risk zonation, and improved flood forecasting systems, are crucial for minimizing flood risks and enhancing resilience, enabling timely decision-making and response efforts (Kvočka et al., 2016; Wang et al., 2018; Binns, 2020; Mostafiz et al., 2022). Studies focusing on categorizing and prioritizing these measures are imperative for developing comprehensive flood control strategies.

While developed nations employ advanced flood forecasting models to manage flood risks effectively, developing countries like Nepal struggle to mitigate the adverse impacts of flooding (Chidi et al., 2022; Shreevastav et al., 2021). Although there are some efforts to mitigate floods involving flood mitigation strategies and green infrastructure like low impact development, localized floods often do not receive adequate attention from policymakers despite their severe impact on rural communities (Sudalaimuthu et al., 2022).

In Nepal, limited research has been conducted on soft measures, particularly in the Narayani River basin, to establish early warning systems and inundation mapping for effective flood control (Dhital et al, 2005; Gautam and Kharbuja, 2006; Dangol, 2014; Banstola et al., 2019; Bhattarai et al., 2019; Thapa et al., 2020; Chidi et al., 2022). Enhancing the understanding of flood risk management through a combination of hard and soft measures is vital for reducing the socio-economic impacts of flooding in vulnerable regions (Quirogaa et al., 2016). By integrating advanced modeling techniques, such as the HEC-RAS (Hydrologic Engineering Centre's River Analysis System) model, with innovative flood control strategies, countries can enhance their preparedness and response mechanisms to mitigate the devastating effects of floods on communities and infrastructure (Sarhadi *et al*., 2012).

This paper aims to analyze the patterns of climatological variables, including temperature, precipitation, and daily river discharge, in addition to performing hazard mapping and risk evaluations along the Narayani River segment within two former Village Development Committees (VDCs) situated in the inner Terai region of what was then Nawalparasi district (now Nawalpur district) in Nepal, being the locations of frequent flooding and severe losses and damages. The investigation focuses on assessing various return-period floods with the support of the HEC-RAS and HEC-GeoRAS tools. The paper firstly reviews literature on climate change and flood vulnerability, followed by a discussion of hazard mapping techniques, specifically in Nepal. The next section includes the methodology used for data collection and analysis of the climatological data and conducting hazard mapping. Next, the findings are presented via climatological pattern graphs and flood vulnerability maps for various return periods. The final section will provide the concluding remarks by providing suggestions on effective land-use planning strategies.

2. CLIMATE CHANGE AND FLOOD VULNERABILITY

Recent studies have emphasized the critical association between Nepal's vulnerability and changes in the water regime, particularly highlighting the impact of floods on human lives, infrastructure, and natural assets, especially during the monsoon season (see Khanal et al., 2019; Aryal et al., 2020; Thapa & Prasai, 2022 etc.). The primary trigger for floods is often attributed to high-intensity rainfall events. Understanding the link between floods and climate change necessitates an analysis of hydrological and meteorological data to assess the extent to which climate change contributes to these devastating flooding occurrences. The repercussions of floods, particularly on communities residing near riverbanks, result in displacements and tragic loss of life, underscoring the socio-economic vulnerability of these populations (Aryal et al. 2020). Despite the implementation of disaster risk reduction and adaptation strategies, the resilience of affected individuals remains a critical concern, as some strategies have proven inadequate in addressing the targeted disasters. Flood forecasting and warning systems emerge as pivotal nonstructural measures in comprehensive flood management, essential for minimizing flood-related damages and preserving human lives (Lin et. al., 1995). Additionally, hazard mapping is identified as a crucial nonstructural measure for disaster mitigation, providing valuable insights into vulnerable areas and populations (Mahato et. al., 1996). The delineation between biophysical and social vulnerabilities, as defined by various scholars, underscores the importance of understanding vulnerability in terms of human capacity to anticipate, cope with, resist, and recover from natural hazards, emphasizing the need for comprehensive approaches to disaster risk reduction and climate change adaptation (Blaikie et. al. 1994).

2.1 Climate change effects on floods

Recent studies have highlighted the intricate relationship between total precipitation and heavy or extreme precipitation events, such as floods, in various regions. While it is very likely that regions experiencing increased total precipitation also witness more pronounced heavy and extreme precipitation events, the opposite can also occur in regions where total precipitation has decreased or remained constant (Alfieri et al., 2013). Despite these findings, changes in extreme events have not received adequate attention, despite their significant implications (Alfieri et al., 2023). Climate change is increasingly manifesting through extreme events like droughts, floods, and heatwaves rather than gradual shifts in average conditions over extended periods (Schröter et al., 2015).

Changes in precipitation patterns can have significant implications, leading to severe water shortages or flooding. The accumulation of continuous yet fluctuating precipitation eventually leads to river flow surpassing a critical threshold, causing breaches in riverbanks or previously implemented flood mitigation measures, consequently resulting in inundation (Smit & Pilifosova, 2002; Bubeck et al., 2012). Additionally, the melting of glaciers can contribute to increased flooding and soil erosion (Siddique & Rahman, 2023). With global warming, extreme events such as droughts, hurricanes, tropical cyclones, typhoons, floods, and heavy precipitation events are expected to become more frequent and intense, despite slight increases in average temperature (Li et al., 2015). Observations have already shown more frequent and intense heatwaves and heavy precipitation events (Nie et al., 2010).

In Nepal, rising temperatures have been recorded at a rate of 0.6°C per decade between 1977 and 2000 (Shrestha et. al., 1999). Moreover, warming trends in Nepal and Tibet have been more pronounced at higher elevations (Talchabhadel *et al*., 2021). Many glaciers in Nepal are experiencing rapid deglaciation, with reported rates of glacial retreat ranging from several meters to 20 meters per year (Chand *et al.*, 2017). This rapid deglaciation poses a significant concern for regions dependent on the Himalayan Rivers (Eugster *et al.,* 2016). The country's hazard landscape varies elevation, with snow avalanches and glacial lake outburst floods (GLOFs) being predominant at very high altitudes, giving way to landslides, debris flows, and their outburst floods in the middle mountains, before riverine floods reign supreme in the lower valleys and plains (Nie et al., 2017).

2.2 Flood vulnerability mapping

The evolving field of flood vulnerability mapping and assessment has seen advancements in methodologies and technologies. Studies like those by Wang & Xie (2018) have explored the applications of remote sensing and GIS in water resources and flood risk management, offering insights into flood modeling and forecasting techniques. Tian et al. (2019) have conducted hazard assessments of riverbank flooding and backward flows, utilizing GIS and digital elevation model technology for flood inundation connectivity and evolution simulations. Merwade *et al.* (2008) have addressed the uncertainties in flood inundation mapping, highlighting the need to consider various uncertain variables in producing deterministic flood extent maps.

Numerous studies conducted since 1990 have been dedicated to identifying floodplains and assessing flood hazards across various regions globally. The Hydrologic Engineering Center's River Analysis System (HEC-RAS) model, developed by the U.S. Army Corps of Engineers (USACE), has emerged as a widely utilized tool for investigating flooding and associated hazards, as well as for mapping floodplains on a global scale (Chaudhary & Piracha, 2021). Integrating the HEC-RAS model with ArcGIS has proven effective in floodplain delineation and risk assessment in diverse geographical contexts (Zope et al., 2016; Shafique & Kim, 2018; Bakare et al., 2019; Muhadi et al., 2020; Atanga & Tankpa, 2021). The HEC-RAS model has been instrumental in simulating flood flows, determining inundation levels, and mapping flood hazards worldwide. For instance, studies have applied this model in regions such as Ottawa, Canada, Los Alamos, New Mexico, USA, Bhutan, Morocco, and Vietnam, showcasing its versatility in flood risk management and mitigation efforts (Earles et al., 2004; Yang et al., 2006; Adhikari, 2015; Mai et al., 2017; Azouagh, 2018). In Nepal, the utilization of the HEC-RAS model, along with its ArcGIS extension (HEC-GeoRAS), has enabled the mapping of flood hazards in critical river systems (Dangol, 2014; Dangol & Bormudoi, 2015). These studies underscore the pivotal role of geo-informatics in enhancing urban river management practices during flood events.

Flood vulnerability mapping in Nepal has been a subject of diverse methodologies and approaches, as evidenced by various studies. Gautam (2017) has emphasized the importance of vulnerability mapping in assessing social vulnerability to natural hazards in Nepal, advocating for decentralized frameworks and inter-district coordination. Additionally, research by Sarkar & Mondal (2019) and Basri et al. (2019) has underscored the importance of utilizing scientifically justified past flood occurrence data for estimating future flood vulnerability and mapping flood-prone areas using remote sensing techniques and Shrestha et al. (2020) have specifically delved into flood risk mapping and hazard assessment in specific regions of Nepal, providing insights into the distribution of flood risk areas and quantifying hazards and vulnerabilities. Aryal et al. (2020) have focused on model-based flood hazard mapping on the southern slope of the Himalayas, offering valuable insights for water resource management and flood control planning. Despite these advancements, there remains a gap in studies that incorporate climate change analysis, and flood inundation mapping using GIS in flood vulnerability analysis, particularly in Nepal. The interdisciplinary nature of flood vulnerability mapping necessitates a holistic approach that integrates diverse methodologies and technologies to effectively assess and mitigate flood risks in Nepal and other vulnerable regions.

3. METHODOLOGY

The research was carried out in the two then VDCs of Kolhuwa and Narayani, situated in the inner Terai region of what was called Nawalparasi district (now Nawalpur). These VDCs were frequently impacted by severe flooding events originating from the river.

3.1. Data collection

Secondary data were obtained from different organizations pertinent to the research. Data on precipitation, temperature, and water discharge were acquired from the Department of Hydrology and Meteorology (DHM), Nepal to investigate the correlation between climate change and flooding in the study area. Furthermore, topographical maps of the study site were obtained from the Department of Survey, Nepal to facilitate flood hazard analysis.

3.2. Analyzing the relationship between floods and climate change

To examine the relationship between climate change and flood occurrences in the study area, long-term climatological data including temperature and precipitation were obtained from the nearest weather station, Dumkauli, through the Department of Hydrology and Meteorology (DHM). Due to the considerable distance of other weather stations from the study sites, they were not included in the analysis. Daily discharge data for the Narayani River at Narayanghat were specifically acquired as this station is in close proximity and serves as a primary confluence of major rivers in the region. Subsequent data analysis was conducted using statistical software packages such as SPSS, SigmaStat, and SigmaPlot. A normality test (Kolmogorov-Smirnov) was performed in SigmaStat to determine the appropriate analytical approach, revealing that the data obtained from DHM were not normally distributed. Consequently, non-parametric analysis methods were employed for the study.

The study conducted trend and mean analyses on variables including temperature and precipitation in the study area, as well as daily discharge in the Narayani River. Analysis of extreme events, such as extreme precipitation and significant floods in the river, was performed to assess the occurrence of climate change in the study area. Correlation coefficients were calculated between the aforementioned variables to determine their significant relationships. Additionally, trend patterns of the variables for corresponding time periods were compared to further support the correlation between them.

3.3. Flood vulnerability analysis

The Hydrologic Engineering Center's River Analysis System (HEC-RAS) has been extensively employed for the computation of one-dimensional water surface elevations and profiles to facilitate flood level prognostication. This software model has gained credibility globally among various entities, including organizations, researchers, and professionals (Knebl et al., 2005). Renowned for its efficacy in river analysis, HEC-RAS has solidified its reputation, and continuous improvements to HEC-RAS have contributed to its ongoing relevance in river analysis (Dangol, 2008). Furthermore, HEC-GeoRAS has been utilized for the preprocessing and postprocessing of data, serving as an intermediary tool bridging HEC-RAS and Geographic Information Systems (GIS), allowing for the extraction of essential spatial information from topographic base maps to support comprehensive analysis (Knebl et al., 2005).

This study used the Sharma and Adhikari (2004)-estimated flood frequency analysis for the Narayani River at Narayanghat for the standard 2-year, and 100-year return periods directly from the flood frequency table. The study area covered 44.75 km^2, including the villages within the study area and a 6.65 km stretch of the river at the study site.

To estimate floods for return periods not explicitly provided in the frequency table, the relationship outlined by WECS and DHM (1990) was employed. This approach enhanced the flood analysis by enabling the extrapolation of flood estimates for additional return periods beyond those directly available from the frequency table.

This methodology aligns with the broader context of flood frequency analysis, where leveraging established relationships and methodologies from prior studies contributes to a more comprehensive understanding of flood occurrences and their implications for risk assessment and management. The integration of such relationships aids in extending the analysis to encompass a wider range of return periods, thereby enhancing the robustness of flood frequency estimations (see table 1). Following relations are used for analysis.

$$Qf = \exp(\ln Q_2 + s\sigma 1) \quad \ldots\ldots\ldots\ldots\ldots\ldots\ldots\ldots\, i$$

$$\sigma 1 = \ln (Q_{100}/Q_2)/2.326 \quad \ldots\ldots\ldots\ldots\ldots\ldots\, ii$$

where ‘s’ is the standard normal variate having different value for different return period;

Q is the flood discharge in m^3/sec;

f is flood return period; Subscript 2 and 100 denote 2-year and 100-year flood return periods respectively.

Table 1: Discharge values for different return periods

S.N.	***Return Period***	***Discharge (m^3s^{-1})***
1.	*2*	*9360.00*
2.	*10*	*12200.00*
3.	*20*	*13249.77*
4.	*50*	*14445.58*
5.	*100*	*15300.00*

4. RESULTS AND DISCUSSIONS

Flood hazard modeling was undertaken to assess the vulnerability of the area to flooding, while statistical analysis was employed to investigate the correlation between various meteorological factors and flood occurrences.

4.1. Relation between climate change and floods

4.1.1. Statistical analysis and results

Correlation analysis was conducted to explore the interconnections among various climatological variables. Spearman Rank Order Correlations, a non-parametric method, were employed to assess the relationships between the variables. The outcomes of the correlation analysis are presented in Table 2.

Table 2: Spearman rank order correlation.

S.N.	Variable	Precipitation	Min. Temp	Max. Temp
1	Daily discharge	0.534	0.331	0.755
	p-value	0	0	0
2	Precipitation	--------	0.171	0.480
	p-value	--------	0	0
3	Max temp	--------	--------	0.714
	p-value	--------	--------	0

The correlation analysis presented in Table 2 indicates significant positive correlations among all variables at a significance level of p=0. Notably, daily discharge exhibits a very high correlation with minimum temperature and a high correlation with precipitation. Given that the Narayani River is influenced by both rainfall and snowmelt, the correlation between precipitation and daily discharge is not as pronounced. Furthermore, daily discharge shows a positive correlation with maximum temperature, albeit to a lesser extent compared to other variables.

Likewise, precipitation demonstrates positive correlations with maximum temperature and a strong correlation with minimum temperature. Additionally, maximum temperature exhibits a high correlation with minimum temperature. The positive correlation between temperature and precipitation suggests a degree of interdependence between these variables, indicating a mutual relationship where one variable influences the other. As temperatures rise, precipitation levels increase, subsequently elevating daily discharge and, consequently, river discharge. This underscores the potential for temperature-induced flood events resulting from climate change.

4.1.2. Analyzing precipitation patterns

Table 3 illustrates a rise in mean precipitation levels from 6.49 mm in the period 1976-1985 to 7.2 mm in 1996-2006. Comparing these values to the mean precipitation over a thirty-year span (1974-2006) of 6.76 mm, it appears that the mean precipitation during 1996-2006 has increased. However, when considering the standard deviations, the mean precipitation values for the respective decades remain relatively consistent. Contrary to this tabular data, previous findings suggest a declining trend in precipitation, attributed to sporadic occurrences of intense precipitation events.

Table 3: Precipitation pattern from 1974-2006 in mm

Year	Min	Max	Mean	St. Dev
1974-1984	0	242.0	6.49	19.34
1985-1995	0	289.0	6.57	19.37
1996-2006	0	324.5	7.20	20.68
1974-2006	0	324.5	6.76	19.81

Data source: DHM, 2008

Moreover, the table indicates an upward trend in the frequency of heavy precipitation events, with the maximum intensity recorded at 242 mm in the initial decade, escalating to 324.5 mm in the third decade, with a consistent increase in the second decade as well. Consequently, although the mean precipitation levels do not exhibit a notable increase over the thirty-year period, there is a discernible rise in the occurrence of extreme precipitation events.

4.1.3. Analyzing discharge patterns

The trend of daily discharge within the Narayani River exhibits an upward trajectory. Table 4 delineates a progression in the mean daily discharge, escalating from 1539.96 m^3s^{-1} in the initial decade to 1573.13 m^3s^{-1} in the third decade. Concurrently, the maximum daily discharge within the river has surged from 10700 m^3s^{-1} in the first decade to 12100 m^3s^{-1} in the third decade. However, when juxtaposed with the mean daily discharge spanning 1971-2006, totaling 1570.53 m^3s^{-1}, the mean daily discharge for the period 2001-2006 showcases a decline. This rise in mean daily discharge is primarily attributed to the heightened occurrence of extreme flood events in recent years.

Table 4: Mean daily discharge in the Narayani River from 1971-2006 in m^3sec^{-1}.

Year	Min	Max	Mean	St. Dev
1971-1980	163	10700	1539.96	1716.52
1981-1990	160	11400	1574.39	1729.81
1991-2000	214	12100	1573.13	1751.87
2001-2006	163	11300	1450.99	1626.77
1971-2006	160	12100	1570.53	1729.37

Data source: DHM, 2008

4.1.4. Analyzing temperature patterns

The graphical representation in Figure 1 illustrates a declining trend in maximum temperature over a span of three decades from 1976 to 2006, while Figure 2 depicts an increasing trend in minimum temperature during the same period.

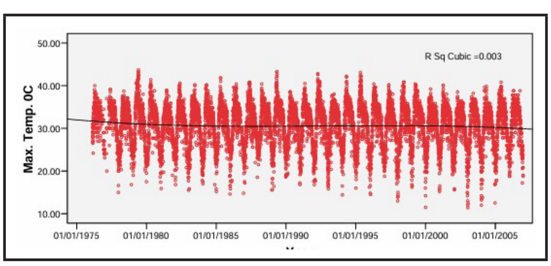

Figure 1: Trend of maximum temperature (1976-2006)

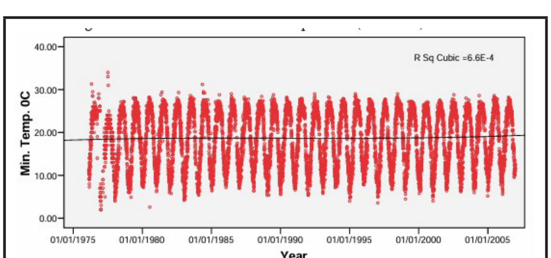

Figure 2: Trend of minimum temperature (1976-2006)

Table 5 presents a decline in the mean maximum temperature from 30.75°C in the period 1976-1985 to 30.35°C in 1996-2006. The mean maximum temperature for the decade 1996-2006, is also lower than the thirty-year mean maximum temperature spanning 1976-2006, which stands at 30.60°C. Conversely, the mean minimum temperature exhibits an increasing trend, rising from 18.63°C in 1976-1985 to 18.81°C in 1996-2006, with an intermediate value of 18.68°C in 1986-1995. The mean minimum temperature for the period 1996-2006 surpasses the thirty-year mean minimum temperature of 18.71°C for 1976-2006, indicating an increase of 0.18°C in the minimum temperature and a decrease of 0.40°C in the maximum temperature over the three decades. Consequently, the table also indicates a narrowing range between the maximum and minimum temperatures.

Table 5: Temperature patterns from 1976-2006.

Year	Temp	Min	Max	Mean	St Dev
1976-1985	Max	14.60	43.70	30.75	4.83
	Min	2.00	34.00	18.63	6.75
1986-1995	Max	14.40	43.30	30.74	4.92
	Min	4.00	29.00	18.68	6.49
1996-2006	Max	11.40	40.80	30.35	4.99
	Min	3.60	29.00	18.81	6.36
1976-2006	Max	11.40	43.70	30.60	4.92
	Min	2.00	34.00	18.71	6.47

4.2. Flood vulnerability analysis

The flood vulnerability maps were generated through the intersection of the land use map of the floodplain with the flood area polygon corresponding to each modeled flood event. This process facilitated the assessment of the physical vulnerability of people to flood disasters (see Figure 3 and 4; Table 6).

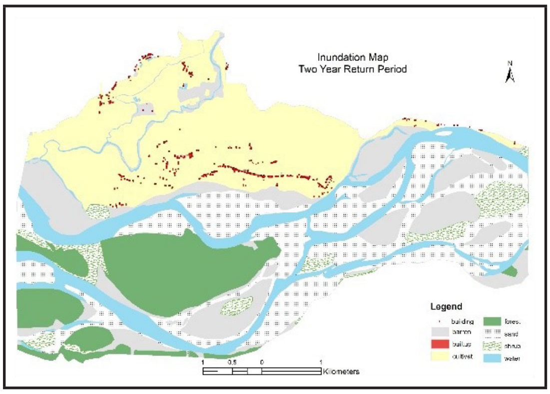

Figure 3: 2-year return period inundation area.

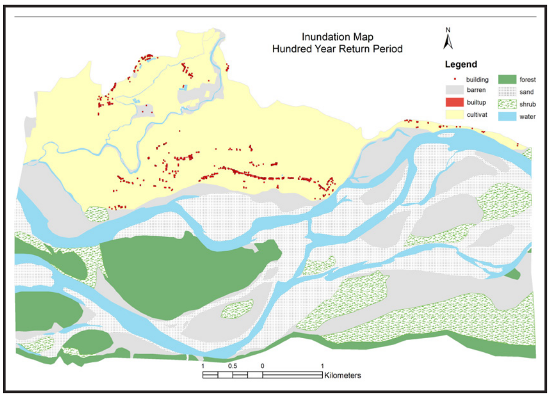

Figure 4: 100-year return period inundation area

Table 2 presents an overview of the impact of simulated floods on land use patterns. The evaluation of the flood-affected area reveals that a significant portion of cultivated land, sand area, barren land and forested areas are situated within the vulnerable zone. Specifically, during the 2-year return period, approximately 8.923 km^2 of cultivated land is submerged, a figure that escalates to 9.889 km^2 for the 100-year return period, rendering the land unsuitable for agricultural purposes. The extent of inundation spans from 27.179 km^2 to 32.641 km^2 across various land categories, encompassing shrub lands, forests, barren lands, and water bodies (excluding the Narayani River) over return periods ranging from 2 to 100 years. However, the data indicates that the inundation of forested and barren areas remains relatively stable despite increasing return periods. This phenomenon can be attributed to the elevated elevation of these forested and barren lands within the study area, placing them beyond the reach of flood inundation at higher return periods. Consequently, these lands are deemed resilient to inundation by floods during extended return periods.

Table 6: Land use vulnerability for different return periods

Land Use Class	Total vulnerable area (km^2)				
	2-yr	10-yr	20-yr	50-yr	100-yr
Barren	5.372	5.397	5.419	6.528	6.772
Built up	0.080	0.081	0.082	0.083	0.086
Cultivation	8.923	9.461	9.657	9.797	9.889
Forest	4.390	4.390	4.390	4.391	4.980
Sand	6.761	6.917	6.932	6.932	6.932
Shrub	1.384	1.384	1.384	2.006	3.713
Water	0.270	0.270	0.270	0.270	0.270
Total	27.179	27.899	28.135	30.006	32.641

The analysis reveals that cultivated land, forest areas, shrub lands, and barren land are subject to inundation by floods, leading to the degradation of cultivated land and a subsequent decline in food productivity and availability within the region. Despite owning agricultural land, many villagers are compelled to purchase food grains for their families, as their hard work and resources are compromised alongside the deterioration of their cultivated plots. Furthermore, the degradation of forest and shrub lands restricts villagers' access to essential natural resources in close proximity.

A considerable expanse of cultivated land falls within the vulnerable zone across various flood frequencies, necessitating the implementation of effective disaster risk reduction strategies to safeguard the area's productivity. Additionally, the study highlights that numerous residences constructed in floodplain areas are at heightened risk of flood hazards, including inundation and soil erosion. Natural calamities do not provide forewarning, underscoring the imperative need for the development of robust mechanisms to mitigate and alleviate the impacts of such disasters to enhance community resilience.

Table 7 illustrates that the count of houses submerged during the 2-year return period amounts to 477, progressively escalating to 529 in the 100-year return period. Assuming an average household size of approximately 6 individuals, the total population at risk due to flood inundations is estimated at 2862, 2970, 3024, 3084 and 3174 individuals for return periods of 2, 10, 20, 50, and 100 years, respectively. It is important to note that the figures denoting the number of houses susceptible to inundation are approximations, as they are derived from google maps and not field verified. Enhanced accuracy in these estimations can be achieved through the generation of large-scale building footprints for more precise calculations.

Table 7: Number of vulnerable houses for different return periods

S.N.	Return period	No. of vulnerable houses
1	2-year	477
2	10-year	495
3	20 year	504
4	50-year	514
5	100-year	529

5. CONCLUSION AND RECOMMENDATION

This paper presented an analysis of climatological variables for trends and extreme events and conducted hazard mapping and risk assessments in the river stretch lying in Nawalparasi district for different return-period floods, using the HEC-RAS and HEC-GeoRAS. It has contributed to the interdisciplinarity of flood vulnerability analysis by incorporating climate change analysis and flood inundation mapping using GIS.

The analysis of temperature trends revealed a gradual convergence between maximum and minimum temperatures. Concurrently, while there was a declining pattern in precipitation trends, there was a notable increase in the frequency of intense precipitation events. A similar scenario was observed in the daily discharge patterns of the Narayani River, where despite a decreasing trend, occurrences of high-volume discharges were conspicuous. These trend dynamics, coupled with the prevalence of extreme events, underscored the manifestation of climate change impacts within the study area. This escalation in the frequency of extreme events, alongside the uncertain trend patterns, signified a growing vulnerability to the effects of climate change.

Moreover, the proliferation of settlements along riverbanks accentuated the heightened vulnerability to such impacts, exacerbated by unplanned and mismanaged settlements. It is imperative that stringent measures, such as the implementation of effective embankments and the relocation of at-risk populations to safer locales, be promptly initiated to mitigate the vulnerability of individuals to flood hazards. Until such measures are implemented, the loss of lives, properties, and livelihoods will persist, exacerbated by incidents of inundation and riverbank erosion exacerbated by the effects of climate change. It is crucial to recognize that the low-lying areas along riverbanks are best suited for cultivation with adequate protective measures, rather than for habitation in a resource-poor country like Nepal. Therefore, construction of houses without proper planning and management should be avoided as far as possible.

Soft measures of flood hazard reduction techniques are very essential in the context of rivers of Nepal, as the Nepal government and the policymakers are usually unaware of localized floods despite their severe impacts on people, similar to what was argued by Sudalaimuthu et al., 2022. As many houses have been built in the low-lying riverbeds, the country urgently needs better flood hazard mapping and forecasting systems, along with timely decision-making and response efforts, for significant reducing flood risks and increasing community resilience, as suggested by Mostafiz et al., 2022.

Without stringent policies and reliable technological and socio-economic vulnerability mapping, developing accurate and prompt early warning systems for climate change disasters remains a challenge. This leaves a significant portion of at-risk populations in Nepal and similar developing countries precariously exposed, increasing the likelihood of environmental refugees.

REFERENCES

Adhikari, R. (2015). Application of HEC-RAS model in flood inundation modeling of Wangchu River, Bhutan. Journal of Bhutan Institute of Technology, 2(1), 1-8.

Alfieri, L., Broduch, Z., Ferraris, M., Jakobsen, N., & Dottori, S. (2013). Rainfall extremes and high-resolution inundation modeling in the Po Plain, Italy. Water Resources Research, 49(6), 3886-3899.

Alfieri, L., Dottori, S., & Mazzetti, C. (2023). Unveiling the misleading relationship between total precipitation changes and flood risk across Europe. Geophysical Research Letters, 50(2), e2022GL101290.

Aryal, A., Baniya, C. B., Shrestha, S., Pandey, B., & Shrestha, M. (2020). Assessment of flood vulnerability and its driving forces in the Gandaki River Basin, Nepal. Sustainability Science, 15(2), 377-396.

Asian Disaster Preparedness Center and United Nations Development Program (ADPC and UNDP). (2005). *Integrated Flood Risk Management in Asia. Bangkok: Asian Disaster Preparedness Center and United Nations Development Program*. Accessed on September 13, 2008.

Atanga, A. B., & Tankpa, V. T. (2021). Floodplain delineation and inundation mapping of Mayo-Danai River using HEC-RAS and GIS. International Journal of River Research and Applications, 37(1), 121-132.

Bakare, A. A., Ibrahim, A. L., Pradhan, B., & Yusof, M. L. (2019). Flood Susceptibility Mapping and Mitigation Strategies in Kelantan River Basin. *Malaysia. Environmental Earth Sciences*, 78(10), 290.

Banstola, N., Ngai, V., Adnan, S. F., & Tang, J. Y. (2019). *Assessing the Effectiveness of Flood Early Warning Systems (EWS) – A Case Study of the Gandaki River Basin, Nepal.* https://www.researchgate.net/publication/255947664_Effectiveness_and_Efficiency_of_Early_Warning_Systems_for_Flash-Floods_EWASE

Basri, H., Anuar, M. K., Abdullah, R., & Yusop, Z. (2019). Assessment of Flood Vulnerability Using Remote Sensing and Spatial Multi-Criteria Evaluation Approach. *Sensors,* 19(1), 180.

Bhattarai, T., & Ghimire, M. N. (2023). *Flood Hazard Assessment in Gandaki River Basin, Nepal.* https://www.mdpi.com/2076-3263/8/2/50

Binns, A. R. (2020). *Floodplain Ecosystems: A Short Review of Their Services and Management.* Wiley Online Library. https://link.springer.com/article/10.1007/s10750-022-04916-7

Blaikie, P. M., Cannon, T., Davis, I., and Wisner, B. (1994). *At Risk: Natural Hazards, People's Vulnerability and Disasters.* London: Routledge.

Bohle, H. G., Downing, T. E., and Watts, M. (1994). Climate Change and Social Vulnerability: Toward a Sociology and Geography of Food Insecurity. *Global Environmental Change*, 4(1), 37-48.

Bubeck, P., Newell, B., & Dessai, S. (2012). *Flood Risk, Resilience and Adaptation & Decision-Making Under Uncertainty in Europe.* https://www.merit.unu.edu/publications/uploads/1684850075.pdf

Buttle, J. M., and Xu, F. (1988). Snowmelt Runoff in Suburban Environments. *Nordic Hydrology*, 18, 19-40.

Chaudhary, A., & Piracha, A. M. (2021). Application of HEC-RAS Model for Flood Inundation Mapping in Chenab River, Pakistan. *Journal of Applied Environmental and Biological Sciences*, 11(1s), 31-39.

Chidi, Z., Ndomba, P., & Rabearison, J. (2022). Flood Vulnerability Assessment and Early Warning System: A Case Study for Data-Scarce Regions. *Natural Hazards*, 1-22. https://www.preventionweb.net/publication/flood-early-warning-system-development-case-study

Dangol, B. (2008). *Application of HEC-RAS Model for Flood Inundation Mapping in Rapti River, Nepal*.

Dangol, B. (2014). *Community Based Flood Risk Reduction Program, Budhikhola Watershed, Nepal*. https://www.scirp.org/journal/paperinformation?paperid=109886

Dangol, B., & Bormudoi, S. (2015). *Flood Hazard Assessment in The Gandaki River Basin Using HEC-RAS Model.*

Dangol, S. (2014). Use of Geo-informatics in Flood Hazard Mapping: A Case of Balkhu River. *Nepalese Journal on Geoinformatics* (13), pp 52-57, DOI: https://doi.org/10.3126/njg.v13i0.16937

Dangol, S., and Bormudoi, A. (2015). Flood Hazard Mapping and Vulnerability Analysis of Bishnumati River, Nepal. *Journal of Geoinformatics, Nepal* 14, pp 20–24, https://doi.org/10.3126/njg.v14i0.16969

Devkota, L. P. (2021). Flood Risk and Adaptation in Nepal. In A. Dutta & M. L. Khan (Eds.), *Natural Disasters in South Asia* (pp. 87–102). Springer Singapore. https://www.sciencedirect.com/science/article/pii/S2214581818300417

Dhital, M. R., Babel, M. S., & Wahid, S. (2005). Flood Hazard Assessment in The Narayani River Basin, Nepal. *Natural Hazards*, 35(1), 361-381. https://www.sciencedirect.com/science/article/abs/pii/S2212420923000158

Earles, J., Michelsen, P., & Weissmann, D. (2004). HEC-RAS Modeling of Flood Wave Propagation in The Ottawa River. *Canadian Water Resources Journal*, 29(1), 79-92.

Eugster, P., Frey, H., & Haeberli, W. (2016). Amending the Definition of Glaciers and Ice Caps in The Himalayan Region. *The Cryosphere*, 10(5), 1525-1530.

Gaire, S., Delgado, R. C., and Gonzalez, P. A., (2015). Disaster Risk Profile and Existing Legal Framework of Nepal: Floods and Landslide. *Risk Management and Healthcare Policy* (8), 2015.

Gautam, D. (2017). Assessing Social Vulnerability to Natural Hazards in Nepal: A District-Level Analysis Using a Composite Index. *International Journal of Disaster Risk Reduction*, 24, 401-410.

Gautam, D. K., and Kharbuja, R. G. (2006). Flood Hazard Mapping of Bagmati River in Kathmandu valley Using Geo-informatics Tools. *Journal of Hydrology and Meteorology*, 3(1), 1.

Hasson, S., Sanderson, M., & Ahmed, K. (2015). Changes in The Seasonal Cycle of Temperature Over Land and Ocean in The South Asian Monsoon Region From 1979 To 2012. *Journal of Climate*, 28(8), 3231-3248. https://journals.ametsoc.org/doi/abs/10.1175/JCLI-D-14-00808.1

Hoggan, D. H. (1997). *Floodplain Hydrology and Hydraulics.* The McGraw-Hill Companies, Inc.

IPCC (2007a). *Climate change 2007: Impacts, Adaptation and Vulnerability*.

Contribution of Working Group II to the Fourth Assessment Report of the Intergovernmental Panel on Climate Change, M.L. Parry, O.F. Canziani, J.P. Palutikof, P.J. van der Linden and C.E. Hanson (Eds.), UK: Cambridge University Press, Cambridge, pp. 976.

Islam, M., and Sado, K. (2000). Flood Hazard Assessment in Bangladesh Using NOAA AVHRR Data with Geographical Information System. *Hydrological Processes*, 14 (3), 605-620.

Khanal, N., Uchida, K., Hirabayashi, Y., Morimoto, T., Ngo, L. T., Dung, N. V., & Nishio, M. (2019). Flood Hazard Mapping Using Improved Inundation Modeling and High-Resolution Land Use Maps. *Journal of Hydrology and Hydromechanics*, 67(3), 321-331.

Knebl, M. R., Wright, N. G., Sonny, M. B., & Baker, V. W. (2005). *HEC-RAS River Analysis System User's Manual (Version 4.1).* https://www.hec.usace.army.mil/software/hec-ras/documentation/HEC-RAS%20User's%20Manual-v6.4.1.pdf

Kvočka, J., Kašpárek, L., & Hlavčová, K. (2016). Flood Risk Perception of Riverside Population in The Czech Republic: A Case Study. *Water Resources Management*, 30(14), 5525-5541.

Li, C., Zhang, Y., Li, X., Xu, H., & Yu, C. (2015). Assessing the Impacts of Projected Climate Change on Extreme Precipitation Over China. *Journal of Climate*, 28(23), 9203-9215.

Lin, C., Cheng, M. D., & Chau, K. W. (1995). Flood Forecasting Using Radial Basis Function Network. *Journal of Hydrology*, 185(1-2), 323-338.)

Mahato, R. C., Higaki, D., Thapa, T. B., and Paudyal, N. P. (1996). Hazard Mapping Based on The Few Case Studies in The Central Region of Nepal. In *Proceedings of An International Seminar on Water Induced Disaster* (pp. 260), 26-29 November. Kathmandu, Nepal

Meehl, G. A., Stocker, T. F., Collins, W. D., Friedlingstein, P., Gaye, A. T., Gregory, J. M., Kitoh, A., Knutti, R., Murphy, J. M., Noda, A., Raper, S. C. B., Watterson, I. G., Weaver, A. J., and Zhao, Z. C. (2007). Global Climate Projections. In Solomon, S., Qin, D., Manning, M., Chen, Z., Marquis, M., Averyt, K. B., Tignor, M. and Miller, H. L. (Eds.), Climate Change 2007: *The physical Science Basis*. Contribution of Working Group I to the Fourth Assessment Report of the Intergovernmental Panel on Climate Change. UK: Cambridge University Press. Cambridge and USA: New York, NY. Nepal Red Cross Society (NRCS). (2008).

Merwade, V., Romanowicz, R. J., & Raffiani, M. (2008). Uncertainty in Flood Inundation Mapping Using Coupled Hydrologic and Hydraulic Models. *Journal of Hydrology*, 359(3-4), 207-220.

Mostafiz, S., Rahman, M. M., & Oo, A. M. T. (2022). Flood Risk Assessment and Management Using a Combined Approach. *Journal of Flood Risk Management*, 15(6), e12827.

Muhadi, A., Ramli, A. F., Pradhan, B., & Sameen, A. M. (2020). Flood Susceptibility Mapping Using an Ensemble Machine Learning Approach in the Sekayu River Basin, Malaysia. *Sustainable Water Resources Management*, 6(8), 3231-3249.

Nie, D., Wu, H., Kim, J., Kakarla, R., & Robinson, A. (2010). An Assessment of Global Precipitation Changes from 1979 to 2008. *Geophysical Research Letters*, 37(7).

Nie, Y., Ngai, V., Kang, Y., Wu, J., & Wong, M. S. (2017). A Comprehensive Framework for Evaluating Flood Resilience of Urban Areas Using Big Data. *Earthquake Engineering & Structural Dynamics*, 46(12), 2251-2273.

Quirogaa, S., Booij, M. J., Correa, A. M., He, B., Liang, X., Mejia-Fernandez, A., & Zhao, G. (2016). Ensemble Hydrologic Prediction for Flood Risk Reduction Under Uncertainty in Complex River Basins. *Water Resources Research*, 52(6), 4638-4662.

Sahoo, B. K., Patel, N. R., Sinha, S., & Kumar, P. (2019). Flood Hazard Assessment and Vulnerability Mapping for the Kosi River Basin Using Geospatial Techniques. *Arabian Journal of Geosciences*, 12(3), 88.

Sarkar, S., & Mondal, P. (2019). Application ff Machine Learning for Flood Susceptibility Mapping in a River Basin Using Satellite Remote Sensing Data. *Journal of the Indian Society of Remote Sensing*, 47(6), 963-973.

Schröter, D., Cramer, W., Le Mouel, P., Van der Linden, A., Bussar, A., Bopfenspörger, T., & Estel, S. (2015). What Can Scenarios Tell Us About Future Biodiversity? *Ecology Letters*, 18(1), 34-45.

Shafique, M., & Kim, S. (2018). Floodplain Delineation and Inundation Risk Assessment Using HEC-RAS and GIS in the Lower Mekong River Basin. *Water*, 10(12), 1822.

Sharma, K. P., and Adhikari, N. R. (2004). *Hydrological Estimations in Nepal.* Nepal: Department of Hydrology and Meteorology.

Shreevastav, A., Singh, V. P., & Sharma, A. K. (2021). Flood Susceptibility Assessment Using Machine Learning Models in the Rapti River Basin, Nepal. *Arabian Journal of Geosciences*, 14(18), 1-17.

Shrestha, A. B., Wake, C. P., Mayewski, P. A., and Dibb, J. E. (1999). Maximum Temperature Trends in the Himalaya and its Vicinity: An Analysis Based on Temperature Records from Nepal for the Period 1971-94. *Journal of Climate*, 12, 2775-2787.

Shrestha, A., Babel, M. S., & Pandey, A. D. (2016). Exploring the Nexus of Climate Change, Water, And Security in the Hindu Kush Region. *Ambio*, 45(S3), 347-360.

Shrestha, S., Vaidya, S., Sharma, A., Nakarmi, S., & Basaula, M. (2020). Flood Hazard Assessment and Risk Mapping in the Trishuli River Basin, Nepal. *Natural Hazards*, 101(3), 829-850.

Siddique, A., & Rahman, M. M. (2023). Glacial Lake Outburst Floods in The Hindu Kush Region: A Looming Threat. *Journal of Mountain Science*, 20(3), 825-838.

Singh, M., and Singh, K. N. (1988). *Planning in Integrated Rural Environment.* Deep & Deep Publications.

Smit, B. and Pilifosova, O. (2002). *From Adaption to Adaptive Capacity and Vulnerability Reduction. Enhancing the Capacity of Developing Countries to Adapt to Climate Change.* London: Imperial College Press.

Smit, B., & Pilifosova, O. (2003). From Vulnerability to Adaptation: A Conceptual Framework. *Mitigation and Adaptation Strategies for Global Change*, 8(2), 223-251.

Sudalaimuthu, S., Johan, S. A., & Abdullah, A. M. (2022). A Review on the Role of Green Infrastructure for Flood Risk Mitigation. *Urban Forestry & Urban Greening*, 73, 107921.

Talchabhadel, R., Rai, S., & Aalto, J. (2021).

Elevation-Dependent Warming Pattern in The Himalayas. *Theoretical and Applied Climatology*, 143(1-2), 223-235.

Thapa, R., & Prasai, S. (2022). Spatiotemporal Flood Vulnerability Assessment in the Gandaki River Basin of Nepal. *Journal of Mountain Science*, 19(6), 1803-1822.

Thapa, R., Baniya, C. B., & Murthy, M. S. R. (2020). Flood Inundation Modelling Using HEC-RAS Integrated with GIS and Remote Sensing in Gandaki River Basin, Nepal. *Arabian Journal of Geosciences*, 13(23), 1-13.

Tian, Y., Wu, J., Liu, Y., Ge, Y., & Li, J. (2019). Assessing Flood Inundation Connectivity and Evolution Based on a GIS And Digital Elevation Model (DEM). *Natural Hazards*, 98(3), 1021-1041.

Vivian, R. (2003). *Nepal Country Case Study*. Regional Workshop on NAPA, Bhutan.

Wang, Y., & Xie, H. (2018). Flood Disaster Monitoring and Early Warning Based on Remote Sensing and GIS. *Sustainability*, 10(11), 3822.

Water and Energy Commission Secretariat and Department of Hydrology and Meteorology (WECS and DHM). (1990). *Methodologies for Estimating Hydrologic Characteristics of Ungauged Locations in Nepal.*

Wilby, R., Beven, K. and Reynard, N. S. (2008). Climate Change and Fluvial Flood Risk in the UK: More of the Same? *Hydrological Processes* 22(14):2511-2523, DOI: 10.1002/hyp.6847

World Meteorological Organization (WMO). (2005). Weather Climate, Water and Sustainable Development. *Annual Report WMO*-No 1000, p. 36.

Zope, A. E., Bhakar, R. P., & Khambete, N. D. (2016). Floodplain Delineation and Risk Assessment Using HEC-RAS Coupled with GIS and Remote Sensing Techniques. *Journal of Applied Water Engineering and Research*, 4(2), 142-156.

ACKNOWLEDGEMENT

The research was undertaken as a thesis for the Master of Arts in Humanities and Natural Resources in 2009. Consequently, the data utilized in this study predates this particular year, however, the google map used to overlay on the inundation maps is from April 2024. The author expresses gratitude for the assistance received from both individuals and organizations, who facilitated the provision of essential data and technical guidance essential for the successful execution of this research.

Author's Information

Name	:	Kiran Maharjan
Academic Qualification	:	PhD
Organization	:	University of New South Wales
Current Designation	:	Academic
Work Experience	:	6
Published paper/article	:	7

Price of Aerial Photograph

Data	Size	NRs. Rate	Remarks
Aerial Photo (Scan Copy)	23cm X 23cm	300	

Price of Image Data

Image of Topographic Map	NRs. Rate	Remarks
Digital orthoimage (at scale 1:5000)	Rs 3125	
Digital orthoimage (at scale 1:10000)	Rs 5000	
District Map (150 dpi in JPEG file)	Rs 200	
VDC Map (150 dpi in JPEG file)	Rs 50	

Price of Land Use Digital Data

District Level Data	Unit	Rate
Present Land Use	Per sq. Km.	5
GIS Data for Land Resource (Except Land Use Zoning Data)	Per sq. Km.	5
Profile	per district	200

Local Level Data	Unit	Rate
Present Land Use	Per sq.Km.	50
Soil Map Data	Per sq.Km.	50
Land Capability Data	Per sq.Km.	50
Profile	Per local level	1000

Price of LiDAR Data

Type	Unit	Rate
Point Cloud Data	Per sq. Km.	Rs 15000
Contour Data	Per sq. Km.	Rs 3000
Digital Surface Model Data	Per sq. Km.	Rs 4000

Type	Unit	Rate
Digital Terrain Model Data	Per sq. Km.	Rs 5000
Orthomosaic Data (RGB)	Per sq. Km.	Rs 6000
Full Data	Per sq. Km.	Rs 25000

Orthomosaic of Kathmandu Valley (39 sq. km) in RGB	Rs 5000 per sheet

Price of Digital Topographic Data Layers

LAYER	Rs/Sheet
Administrative	100.00
Transportation	200.00
Building	60.00
Landcover	300.00
Hydrographic	240.00
Contour	240.00
Utility	20.00
Designated Area	20.00
Full Sheet	1000.00

S.N	Data	Price
1	Seamless Data whole Country	
1.1	Digital data of all layers	Rs. 300000.00
1.2	Digital data compiled at scale 1:1000000	Free
2	Digital data of all layers compilled at scale 1:500000	Rs 1000 per sheet
3	Generalized Districtwise Data Layers	
3.1	Administrative Boundary	Free
3.2	Building	Rs. 15000.00
3.3	Contour	Rs. 65000.00
3.4	Transportation	Rs. 60000.00
3.5	Hydrographic	Rs. 70000.00
3.6	Landcover	Rs. 87000.00
3.7	Utility Line	Rs. 2000.00
3.8	Designated Area	Rs. 1000.00
3.9	Full Sheet	Rs. 2000.00
4	Rural Municipality (Gaunpalika) unitwise- all layers	Rs. 1000.00
5	Municipality (Nagarpalika) unitwise- all layers	Rs. 2000.00

Price of Printed maps

S.No	Maps	Unit	Rate (In NRs)
1	Political and Administrative Map of Nepal (2019)	Whole Nepal	150
2	Topographic Base Map (1992-2001)	Sheet	150
3	Topographic Map (1950s)	Sheet	50
4	District Map (1980s)	Sheet	50
5	Land Utilization Map (LRMP)	Sheet	50
6	Land Capability Map (LRMP)	Sheet	50
7	Land System Map (LRMP)	Sheet	50
8	Pysiographic Map of Nepal		50

Price of SOTER Data	Whole Nepal	NRs : 1000.00.

Comparison of the Direct Supervised Classification and Segment Mean Shift Classification: A Case Study of Hetauda Sub-Metropolitan City of Nepal

Menaka Hamal[1], Prof. Shahnawaz (Ph.D.)[2]
menakahamal@gmail.com, shahnawaz.shahnawaz@plus.ac.at
[1]Nutan GeoEnvironmental Consultancy Pvt. Ltd, [2]University of Salzburg

KEYWORDS

Segment Mean Shift, Supervised Classification, Land Use Land Cover, Training Samples, Point Sampling

ABSTRACT

Comparison between Land Use Land Cover (LULC) classification and methods is a common practice to assess their suitability and reliability in specific areas. In the case of Hetauda Sub-Metropolitan City in Nepal, Sentinel-2B satellite imagery was utilized to evaluate the accuracy of LULC classification through both direct supervised classification and segment mean shift classification. Direct supervised classification was conducted in ERDAS Imagine, while segment mean shift classification was performed in ArcGIS to identify six LULC classes: forest, agriculture, built-up area, bare area, grassland, and waterbody. Pre-processing steps such as layer stacking, mosaicking, data extraction, atmospheric and radiometric correction were employed to enhance the imagery. Training samples were chosen via visual interpretation based on local knowledge to train the Maximum Likelihood Classifier (MLC). The results revealed that the segment mean shift method achieved the highest overall accuracy at 90%, whereas direct supervised classification yielded 85%. Furthermore, kappa statistics indicated a strong level of agreement, with segment mean shift scoring the highest at 0.88 and direct supervised classification at 0.81. Individual class accuracies varied, with forest classification being the most reliable at 98% and waterbody classification at 71%. Overall, the segment mean shift method was deemed more accurate and suitable than the pixel-based direct supervised classification for LULC classification in Hetauda Sub-Metropolitan City, Nepal.

1. INTRODUCTION

LULC classification utilizing satellite imagery has been widely practiced on both local and global scales (Belward & Skøien, 2015). Advancements in sensor technology worldwide, coupled with the accessibility of various satellite images and user-friendly spatial analysis tools, have heightened interest and improved the accuracy of LULC information extraction (Phiri & Morgenroth, 2017). Among the techniques employed, supervised classification stands out, allowing users to select sample pixels based on their prior knowledge of the area. These samples serve to train other pixels, enabling the identification of the closest LULC information across the entire study area (Enderle & Robert, 2005; Lillesand et al., 2015). Recently, the segment mean shift classification, facilitated by ArcGIS, has gained popularity. This approach, recognized for its robustness in feature space analysis (Comaniciu & Meer, 2002), involves grouping pixels based on similar characteristics from adjacent pixels, resulting in super pixels or segments. These super pixels are then classified, either supervised or unsupervised, depending on the study's objectives (ESRI, n.d.-a).

Access to satellite imagery varies, with free options often offering lower resolution and limited temporal coverage (Hegarty-Craver et al., 2020). The Sentinel-2 datasets, however, provide an alternative as they are freely available every five days and relatively high resolution compared to other open-source options. These datasets encompass 13 spectral bands with varying spatial resolutions: four bands at 10 meters, six at 20 meters, and three at 60 meters, with a 12-bit radiometric resolution allowing for a potential range of brightness levels from 0 to 4095 (ESA, n.d.). Ensuring the reliability of remotely sensed maps prior to their application is crucial in image classification (Congalton, 2001). The assessment can be done through comparisons with reference points from the original imagery, ground truth point collection (Enderle & Robert, 2005), or the author's prior knowledge of the study area. In this study, a stratified random sampling method is adopted to generate reference points. These points are then distributed across each stratum using the Sampling Design Tool to calculate the confusion matrix and kappa statistics, thereby assessing the reliability of the classified maps.

Open-access satellite data, including Landsat, MODIS, ASTER, VIIRS, IKONOS-2, OrbView-3, among others, are obtainable from sources such as the USGS Earth Explorer and various web services. GEOS-R and NOAA-20 data can be acquired from the NOAA web portal, while Sentinel-2A, Sentinel-2B, and similar data are accessible via the ESA open access portal. For data processing and analysis, a range of remote sensing software is available and selected based on the study's requirements (Roy et al., 2017), such as ERDAS Imagine, ArcGIS, eCognition, and so on. While classification can be performed using open-source platforms like QGIS and other programming languages, this study utilized commercial software, specifically ERDAS and ArcGIS. ERDAS, recognized as raster-based software, is widely utilized for extracting information from images and executing multiple geospatial tasks (Intergraph, 2021), particularly renowned for pixel-based classification (Basayigit, 2015). Similarly, ArcGIS facilitates the management and analysis of diverse geographic information, allowing for the visualization of geographical statistics through layer-based maps, and is popular for both pixel and object-based analysis (ESRI, n.d.-a).

In thematic mapping, accuracy assessment holds significant importance, serving as a pivotal step to gauge the reliability of the generated products for subsequent applications (FAO, 2016). As emphasized by Lillesand et al. (2015), "A classification is not complete until its accuracy is assessed." Thus, to ensure the integrity of the classification results, this study adopted a point sampling approach for accuracy assessment. The determination of the desired number of test points was guided by the principle that each class should ideally have ten times the number of test points (MGL, n.d.).

The kappa is one of the commonly used statistics to test the degree of agreement by chance (Viera & Garrett 2005). The values range from 0 to 1 where 0 interprets no agreement between the classified and reference images and 1 gives the classified images and the ground truth images are identical (Cohen, 1960). So, the higher the kappa coefficient, the more accurate the classification is. The level of the agreement depends on the value of Kappa that gives the percentage reliability of the data. The value 0 to 0.20 gives the 0-4% reliability that interprets no agreement, 0.21 to 0.39 gives 4-15% reliability with the minimal agreement, 0.40 to 0.59 gives 15-35% reliability that interprets the weak level of agreement, 0.60 to 0.79 gives 35-63% reliability with the moderate agreement, 0.80 to 0.90 gives 64-81% reliability interprets the strong level of agreement and above 0.90 gives 82-100% that interprets the almost perfect level of agreement (McHugh, 2012).

Hetauda Sub-Metropolitan City is one of the recently emerged densely populated city due to its strategic location at the convergence of Nepal's historic East West Highway and Tribhuvan Highway, linking the Tarai region with the Kathmandu Valley. The city has witnessed a significant influx of migrants from various regions, including the Tarai, Mountain, Hill, and nearby rural villages, in search of employment opportunities, better education, and improved infrastructure. Rapid urbanization driven by population growth and land demand for construction purposes has led to the conversion of agricultural land into built-up areas. Additionally, natural water bodies have been transformed into ponds for fisheries and other agricultural activities, while forests and grasslands have faced depletion due to infrastructure development. The widening of riverbanks and occurrences of floods during the monsoon season further highlight the dynamic changes in the landscape (GoN, 2017).

This study outlines the significance of observing notable LULC changes within the city. It aims to assess the accuracy of land cover mapping using two distinct approaches: the segment mean shift supervised classification and direct supervised classification methods. The primary objective is to ascertain the current status of LULC in the expanded metropolitan area. The study endeavors to provide valuable insights to guide the formulation of land use policies by governmental and non-governmental organizations. Specifically, it seeks to address inquiries regarding the extent of LULC and, the appropriateness of classification techniques tailored to urban contexts, and the trends in LULC changes over the past decade within the metropolis.

2. METHODOLOGY

2.1 Study area

The Hetauda Sub-Metropolitan City is situated in the southern region of the Makwanpur district within the Bagmati Province of Nepal. The geographic coordinates lie between 27.541940 to 27.32417° N latitude and 85.89083° to 85.1900° E longitude. Spanning an area of 261.58 square kilometers, the elevation within the city ranges from 300 to 1,800 meters above sea level. The sub-metropolis is home to a population of 193576 individuals, comprising 95,678 males and 97898 females, residing in a total of 46566 households (CBS, 2021). The climate and terrain of the city are conducive to agricultural productivity and human habitation. It is located within the inner Terai region, experiences a dominant tropical climate, transitioning into sub-tropical conditions with increasing elevation, and eventually into a lower temperate climate at higher altitudes (DoA, 2018). According to the city profile of 2017, approximately 41.46% of the city is covered by forest, while agricultural land occupies another 41% of the total area. The remaining land includes areas classified as barren, built-up, bush, grasslands, orchards, ponds, sand, and water bodies (GoN, 2017).

2.2 Data acquisition

Two multispectral images from Sentinel-2B covering an area of 100 meters by 100 meters each, acquired on March 31, 2020, from the Copernicus Open Access Hub, specifically located at UTM grid codes – 45 RTL and 45 RUL (ESA, n.d.). The datasets were geo-referenced and orthorectified with UTM 45 N projection. Comprising a total of 13 spectral bands ranging from Visible and Near Infra-Red (VNIR) to Short Wave Infra-Red (SWIR), four bands with a spatial resolution of 10 meters were selected for the study: blue (456 – 532 nm), green (536 - 582nm), red (646 – 685 nm), and near-infrared (774 – 907 nm) (ESA, 2015).

2.3 Image preprocessing

Image preprocessing techniques were employed to improve the visualization and interpretability of features present in the imagery. Initially, single layers with uniform cell sizes were stacked in Erdas Imagine to create a multi-band image. Subsequently, multiple tiles of the multi-band imagery were merged using the mosaic tool. The mosaic image underwent enhancement to refine image quality. The radiometric calibration was performed to mitigate atmospheric distortion caused by cloud and aerosols. The point spread method was applied to reduce haze and enhance image sharpness. Additionally, the histogram equalization tool was utilized to minimize noise distortion and enhance image features.

2.4 Image segmentation

The image segmentation process was carried out for the segment mean shift supervised classification, following the mean shift approach (ESRI, n.d.-c). Utilizing the Segment Mean Shift tool in ArcGIS, the objects within the processed imagery were grouped into segments based on their shapes, spectral properties, and spatial characteristics. By iteratively adjusting the spectral values within the range of 15.5 to 20, the segments were refined to closely resemble real features within the scene. Ultimately, a spectral value of 18 was determined to be the most suitable for approximating the shape of objects in the imagery. Similarly, a spatial value of 15 was identified as providing the best fit for the objects present in the imagery. Through multiple iterations, the minimum segment size was established at 20, ensuring that super pixels smaller than this threshold merged with their closest neighbor segment (Figure 1).

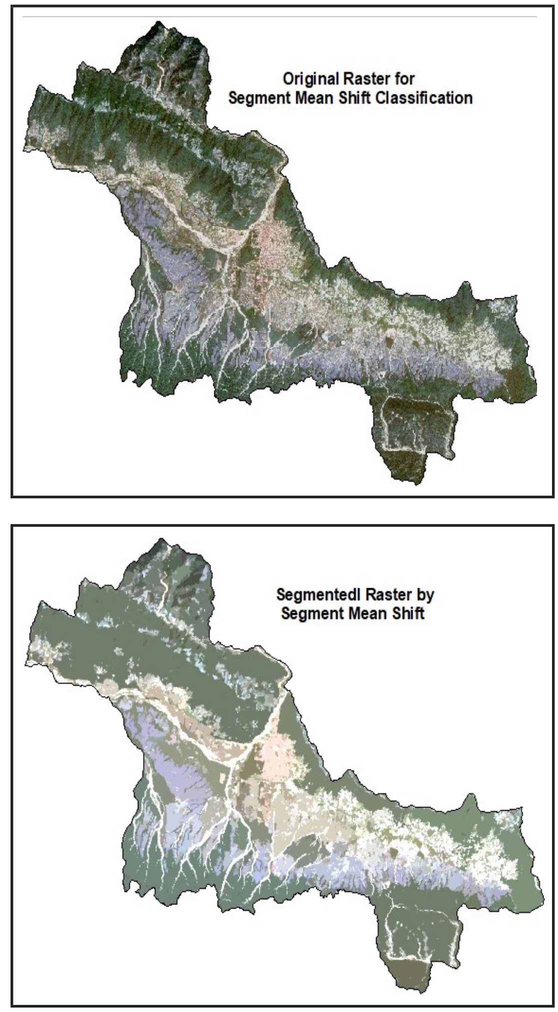

Figure 1: Original and segmented raster

2.5 LULC classification scheme

The LULC classes have been categorized depending on the desired objectives, available features on the image, and applicability of the ground coverage (Ai et al., 2020). The range of classes has been chosen for the LULC classification for a specific area (Basayigit, 2015). This study adhered to the predefined LULC classes utilized in prior land cover assessment by the city. As documented in the City profile of 2017, the classes included barren land, built-up areas, bush, cultivation, forest, grass, orchard, pond, sand, and water bodies. Building upon a scheme for this study, certain refinements were made to streamline classification processes. Specifically, the pond and water body categories into a water body class, while sand and barren land were consolidated under the barren land category. Furthermore, the bush and grassland designations were merged to form a unified grassland class. Similarly, the cultivation class was relabeled as agriculture. Consequently, the classification scheme employed in this study encompasses six distinct classes: Agriculture, Bare Area, Builtup Area, Forest, Grassland, and Waterbody.

2.6 Training samples

Training samples for the supervised classification must be both representative and complete (Lillesand, et al. 2015). The rule of thumb is that the more samples that can be used in training, the better the statistical representation of each spectral class (ESRI, n.d.-d). Adhering to this rule, the required samples were drawn based on the coverage of the area through visual interpretation using polygon tool in ERDAS across the scene considering the samples are normally distributed for the respective land coverage in the city. Considering the provided data. Based on this, Agriculture, Builtup Area, and Forest classes each have 47 training samples chosen for classification. Bare Area and Waterbody classes are represented by 35 training samples each, while Grassland has 21 samples allocated for training. Following the collection of training samples, a signature file was generated, encompassing essential parameters such as the mean values for each class, the count of pixels, and the variance and covariance matrix for the training class. This signature file served as a crucial input for training the Maximum Likelihood Classifier (MLC), facilitating the classification of pixels throughout the entire imagery based on the established signatures (Figure 2).

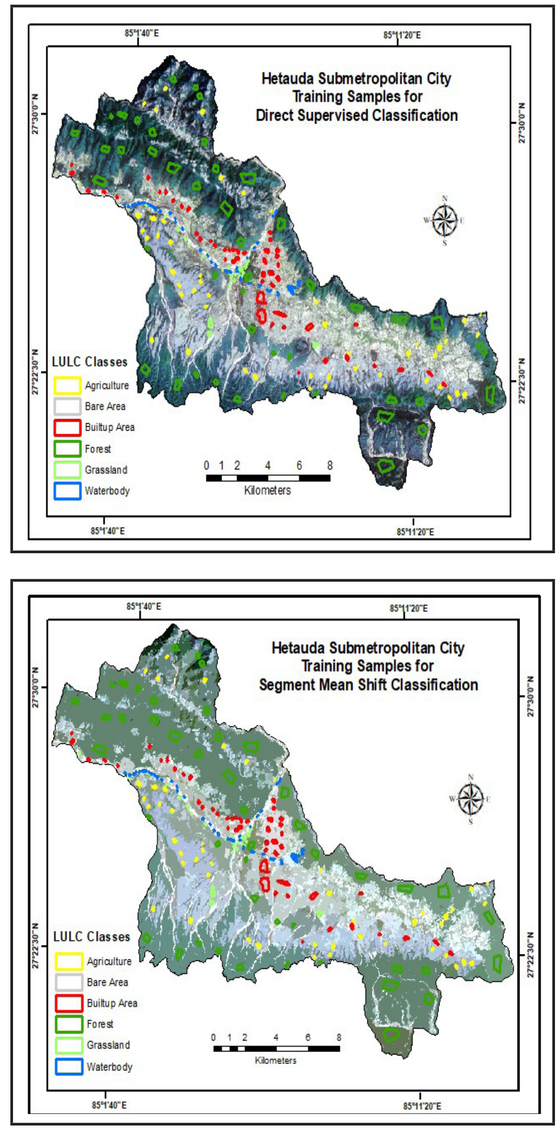

Figure 2: Training samples as thematic classes

2.7 Point sampling and accuracy assessment

To calculate the sample size, all classes were ranked based on their respective area coverage, ranging from lowest to highest. Subsequently, each rank was divided by the total number of ranks and multiplied by the total number of pixels to assign the sample size for each class. Consequently, the total number of pixels amounted to 6*6*10 = 360 for the classified scene (Table 1).

Table 1. A sample size of test points for accuracy assessment

Class	Ratio	Sample size
Agriculture	5	5/21*360 = 86
Bare Area	4	4/21*360 = 69
Built-up Area	3	3/21*360 = 51
Forest	6	6/21*360 =103
Grass	2	2/21*360 = 34
Waterbody	1	1/21*360 = 17
Total	21	21/21*360 = 360

After calculating the required sample points for each class, the stratified random procedure was implemented to allocates those points in each classified LULC using the Sampling Design Tool in ArcGIS. Then the allocated points over the classified image were verified individually with the location of the original image to find out the number of correctly classified pixels (Ruppert, et al. 2018). Then, every point of each stratum was checked with the visual interpretation whether those are matched with the location of the original imagery. The reference points were recorded against the classified points in the attribute table to compute the confusion matrix. The matrix provided the correctly classified and misclassified pixels, Producer's Accuracy (PA), User Accuracy (UA), Overall Accuracy (OA) and Kappa statistics (Anand & Bank, 2018). Then the, error of omission and commission was calculated based on those statistics. The whole classified map, as well as each LULC category, were compared by evaluating all the accuracy and errors.

3. RESULT AND DISCUSSION

3.1 LULC 2020

The metropolitan city is predominantly covered by forest, particularly in the northwest and southeast regions. Forest patches are noticeable at the center of the city, surrounded by agricultural land. The forested areas vary in density, with some being more spacious, attributed to natural forest cover and community-managed forests. Ongoing forest protection programs, both at the national and community levels, have led to the conversion of degraded land into forested areas (GoN, 2017). The majority of the built-up area is concentrated at the city center, with expansion occurring towards the periphery, driven largely by people's preference to settle near the east-west highway, particularly individuals migrating from outside of the city. Water bodies are primarily located at the center of the city and surrounding settlements, influenced by nearby flowing rivers and the growing interest of locals in fish farming. Bare areas consist of sand along the ridge of the riverbank, extending from north to west and into the city, as well as degraded land and dry streams sprawled across the southern part, adjacent to forests and agricultural areas. Sparse grass patches are scattered across forested and agricultural lands (Figure 3).

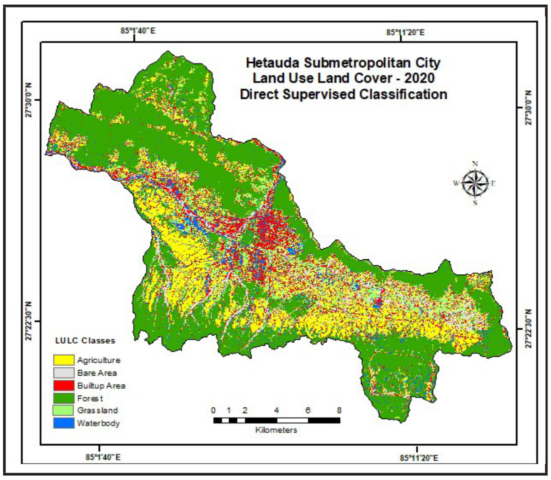

Figure 3: LULC 2020

In 2020, forest coverage was assessed at 127.8 square kilometers via direct supervised classification and 121.1 square kilometers through segment mean shift classification. Combined, forests accounted for 47.55% of the total area, emerging as the primary land cover type for the city. Agricultural land occupied 47 square kilometers in direct classification (18%) and 48 square kilometers in segment mean shift classification (18.3%). On average, it constituted 18.15% of the total area, ranking as the second most prevalent class. Built-up areas spanned 34 square kilometers in direct classification (13%) and 32.7 square kilometers in segment mean shift classification (12.5%). Collectively, they covered 12.75% of the total area. Grasslands extended over 24.8 square kilometers in direct classification (9.5%) and 34.5 square kilometers in segment mean shift classification (13.2%). On average, they constituted 11.35% of the total area. Within the city limits, a bare area measured 14.2 square kilometers in supervised classification (5.4%) and 13.8 square kilometers in segment mean shift classification (5.3%) in 2020. Combined, it accounted for 5.35% of the total land, marking it as the second lowest land cover category. Water encompassed 13.9 square kilometers, constituting 5.3% of the total land in direct classification, and 11.7 square kilometers, accounting for 4.5% of the total land in segment mean shift classification. On average, water coverage constituted 4.9% of the total area (Table 2).

Table 2. Area coverage in direct and segment mean shift classification 2020

LULC Classes	Direct Supervised Classification		Segment Mean Shift Classification		Both Classifications (Average)	
	Area Sq Km	Per-centage	Area Sq KM	Per-centage	Area Sq KM	Per-cent-age
Agriculture	47	18	48	18.3	47.50	18.15
Bare Area	14.2	5.4	13.8	5.3	14.00	5.35
Builtup Area	34	13	32.7	12.5	33.35	12.75
Forest	127.8	48.8	121.1	46.3	124.45	47.55
Grass	24.8	9.5	34.5	13.2	29.65	11.35
Waterbody	13.9	5.3	11.7	4.5	12.80	4.9

3.2 LULC 2010 and 2020

Over the past decade, there have been significant shifts in land use patterns within the city. **Agriculture,** once the dominant sector, has seen a substantial decline from 41.68% of total land area in 2010 to 18.15% in 2020 (Figure 4). This decline is attributed to the influx of migrants from other districts and rural areas, leading to increased construction activity and the conversion of agricultural land into built-up areas. The unplanned emergence of residential areas has further contributed to the expansion of built-up areas.

Similarly, the proportion of **bare areas** decreased from 7.39% in 2010 to 5.35% in 2020 (Figure 4). This decline attributed to an increase in households and occupation by landless squatters, resulting in its conversion to either built-up or agricultural land. The fluctuating patterns of rainfall throughout the seasons cause variations in river flow, characterized by increased flow levels during the summer and reduced or dry conditions during the dry season. These fluctuations contribute to the accumulation of exposed sediments along the riverbanks when water levels recede.

Conversely, there have been notable increases in **built-up** areas, almost doubling from 6.15% in 2010 to 12.75% in 2020 (Figure 4). This expansion attributed to various factors, including the influx of migrants who seek housing opportunities in the city. Additionally, private and individual land brokers play a significant role by acquiring agricultural land and converting it into residential plots with higher resale value, thus contributing to the urban sprawl. This trend of land conversion for profit-making has persisted over the years, further exacerbating the issue. Furthermore, the rapid development of infrastructure such as the east-west highway and linking roads has facilitated urbanization by encouraging construction along roadsides. Additionally, the presence of landless squatters has led to the encroachment of land, contributing to the escalating built-up area within the city.

Grassland has experienced a substantial increase from 2.34% in 2010 to 11.35% in 2020 (Figure 4). This increase attributed to the expansion of fallow land and the implementation of community-based forest programs within the city. Additionally, the proliferation of bushes in the area could be a consequence of illegal fires, particularly during April and May, as well as haphazard logging practices that make the forest space open for the grass

The **forest** cover has slightly increase from 41.46% in 2010 to 47.55% in 2020 (Figure 4), it remains a significant portion of the city's land area. The forest area become more spacious and dense due to existing natural forest and the conservation efforts made by the communities and the government agencies in the city. For years, forest protection programs have been diligently implemented both in national forests and community-managed forest areas. As a result of these sustained efforts, degraded lands have undergone a transformation from barren or bushy areas into thriving forests. This remarkable conversion underscores the effectiveness of conservation initiatives in restoring and regenerating forest ecosystems. By focusing on both national and local levels of forest management, these programs have played a crucial role in reclaiming degraded land and fostering the growth of vital forest habitats.

There has been a noteworthy increase in **water** bodies, rising from 0.97% in 2010 to 4.9% in 2020 (Figure 4). The rise in water bodies can be credited to the construction of ponds primarily intended for fishery purposes. The Bagmati River originates in the north and meanders westward through the heart of the city,

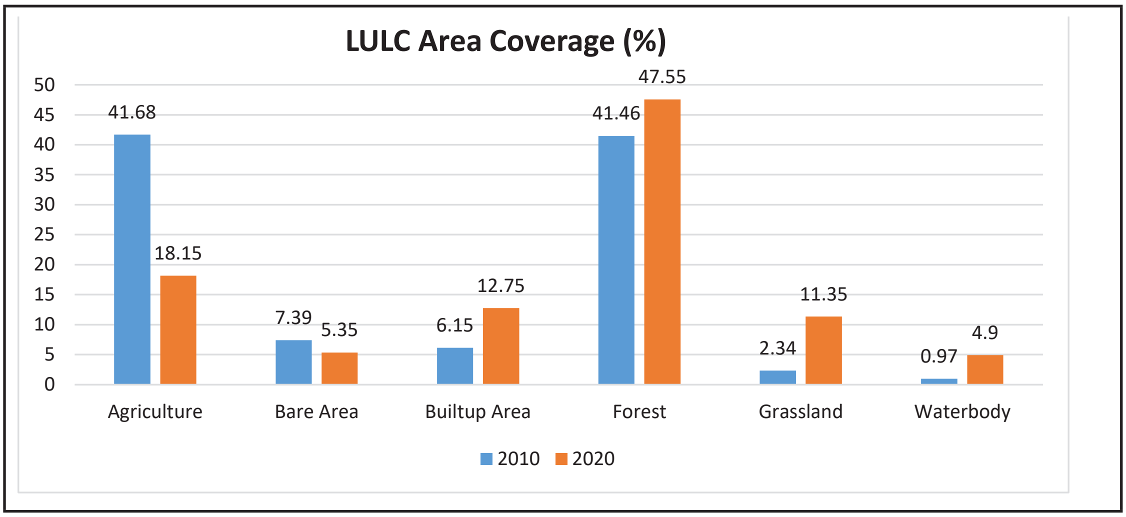

Figure 4: LULC of 2010 and 2020

3.3 Map accuracy

The accuracy of thematic maps in image classification is crucial before presenting them to users (Foody, 2013). The assessment output may vary depending on the application, but it relies on quantitative results to ascertain the map's reliability (Congalton, 2001). Thomlinson et al. (1999) suggest a minimum overall accuracy of 85%, with each class accuracy at 70%. Meeting these criteria indicates that the classified data is relatively accurate to the ground. Similarly, Anderson et al. (1992) propose an acceptable accuracy threshold of 85% for satellite land cover classifications, a similar accuracy limit echoed by Congalton (2001). Adhering to this accuracy limit, the reclassification of LULC data for the sub-metropolitan city was conducted to meet the minimum requirement. To find out the accuracy, the quantitative assessment - the confusion matrix was generated to assess how well the classification model is performing by comparing the predicted classes with the actual classes.

3.3.1 Accuracy of LULC (Direct Supervised Classification)

Out of a total of 360 pixels, 306 are accurately classified, yielding an overall accuracy of 85% (Table 3). The classification matrix reveals specific accuracies within different land cover categories: for forests, 101 out of 103 pixels are correctly identified, resulting in 93% producer accuracy and 98% user's accuracy. Agriculture exhibits 76 out of 86 correctly classified pixels, translating to 84% producer accuracy and 88% user's accuracy. In built-up areas, 37 out of 51 pixels are correctly labeled, leading to 66% user's accuracy and 73% producer accuracy. Similarly, bare areas showcase 55 out of 69 correctly classified pixels, reflecting 92% producer accuracy and 80% user's accuracy. Lastly, waterbodies have 12 out of 17 pixels correctly identified resulting 100% producer accuracy and 71% user accuracy. The kappa statistics of 0.81 which gives the 81% reliability interprets the strong level of agreement between classified and original map (Table 3).

Table 3. Statistics of accuracy assessment (Direct Supervised Classification)

Class Value	Agriculture	Bare Area	Builtup Area	Forest	Grassland	Waterbody	Total	UA
Agriculture	76	0	6	1	3	0	86	**0.88**
Bare Area	4	25	5	0	0	0	34	**0.74**
Builtup Area	3	7	37	3	1	0	51	**0.73**
Forest	0	0	1	101	1	0	103	**0.98**
Grassland	7	0	5	1	55	0	69	**0.80**
Waterbody	0	0	2	3	0	12	17	**0.71**
Total	90	32	56	109	60	12	360	
PA	**0.84**	**0.78**	**0.66**	**0.93**	**0.92**	**1.00**		
OA								**0.85**
Kappa								**0.81**

3.3.2 Accuracy of LULC (Segment Mean Shift Classification)

Out of a total of 360 pixels, 325 are accurately classified, yielding an overall accuracy of 90% (Table 4). The classification matrix reveals specific accuracies within different land cover categories: for forests, 101 out of 103 pixels are correctly identified, resulting in 94% producer accuracy and 98% user's accuracy. Agriculture exhibits 79 out of 86 correctly classified pixels, translating to 88% producer accuracy and 92% user's accuracy. In built-up areas, 46 out of 51 pixels are correctly labeled, leading to 90% user's accuracy and 79% producer accuracy. Similarly, bare areas showcase 56 out of 69 correctly classified pixels, reflecting 98% producer accuracy and 81% user's accuracy. Lastly, waterbodies have 12 out of 17 pixels correctly identified, translating 92% producer accuracy and 71 % user accuracy. The kappa statistics of 0.88 which gives the 88 % reliability interprets the strong level of agreement between classified and original map (Table 4).

Table 4. Statistics of accuracy assessment (Segment Mean Shift Classification)

Class Value	Agriculture	Bare Area	Builtup Area	Forest	Grassland	Waterbody	Total	UA
Agriculture	79	0	1	2	4	0	86	0.92
Bare Area	4	56	8	0	0	1	69	0.81
Builtup Area	3	1	46	1	0	0	51	0.90
Forest	2	0	0	101	0	0	103	0.98
Grassland	1	0	0	2	31	0	34	0.91
Waterbody	1	0	3	1	0	12	17	0.71
Total	90	57	58	107	35	13	360	0
PA	0.88	0.98	0.79	0.94	0.89	0.92		
OA								**0.90**
Kappa								**0.88**

3.3.3 Error of omission and error of commission

In the Direct Supervised Classification of LULC classes, the error analysis reveals varying levels of accuracy across different categories. Notably, Agriculture demonstrates a moderate level of omission error at 16% and a slightly lower commission error at 12%, indicating a relatively balanced performance in classification. Conversely, Bare Area exhibits a higher omission error at 22% compared to a commission error of 26%, suggesting a tendency to miss classifying areas as bare more frequently than misclassifying into this category. Builtup Area shows a higher commission error at 27% versus an omission error of 34%, indicating a tendency to misclassify non-built areas as builtup more often. Forest demonstrates a low omission error of 7% and a very low commission error of 2%, indicating high accuracy in classification. However, Grassland presents a higher commission error at 19% and a moderate omission error at 7%, indicating a tendency to misclassify other land cover types as grassland more frequently. Waterbody shows no omission error but a high commission error of 29%, indicating a tendency to misclassify other features as water bodies (Table 5).

In the Segment Mean Shift Classification of LULC classes, the error analysis highlights fluctuations in accuracy across different categories compared to Direct Supervised Classification. Notably, there is a decrease in the error of omission for some classes, such as Bare Area with 1.75% and Builtup Area with 20.69%, indicating improved accuracy in identifying these land cover types. However, this decrease is offset by an increase in commission error, particularly evident in Bare Area with 18.84% and Builtup Area with 9.8%. Conversely, Forest demonstrates a significant decrease in commission error at 1.94% while maintaining a low omission error at 5.61%, suggesting enhanced accuracy in classifying forested areas. However, Grassland shows a relatively higher commission error at 8.82% and a moderate omission error at 11.43%, indicating a tendency to misclassify other land cover types as grassland more frequently. Waterbody exhibits a decrease in commission error at 29.41% but no change in the omission error, suggesting an improvement in accurately identifying water bodies, albeit with a higher tendency for misclassification (Table 5).

Table 5: Omission and Commission Error

Error of LULC 2020				
LULC Classes	**Direct Supervised Classification)**		**Segment Mean Shift Classification**	
	Error of Omission	**Error of Commission**	**Error of Omission**	**Error of Commission**
Agriculture	16	12	12.22	15.3
Bare Area	22	26	1.75	18.84
Builtup Area	34	27	20.69	9.8
Forest	7	2	5.61	1.94
Grassland	7	19	11.43	8.82
Waterbody	0	29	7.69	29.41

4. CONCLUSION

The LULC classification of Hetauda Sub-Metropolitan City, utilized both direct supervised classification and segment mean shift methods with Sentinel 2B, Level-C, orthorectified data acquired on 31 March 2020, and 10-meter spatial resolution from the European Space Agency. Geo-registration at UTM 45 N projection, atmospheric correction for noise reduction, and histogram equalization for contrast enhancement were employed. Six LULC classes were identified: forest, agriculture, built-up area, bare area, grassland, and waterbody, with forest covering the largest area at 124.45 sq km, representing 47.55% of the total city area. Agriculture, built-up, bare land, grass, and waterbody covered 18.15%, 12.75%, 5.35%, 11.35%, and 4.9% of the area, respectively. Notably, forest, water, bare area, grassland, and the built-up area have increased since 2010, while agriculture has decreased significantly. The segment mean shift supervised classification achieved an overall accuracy of 90%, outperforming the 85% accuracy of direct supervised classification, with strong agreement shown by kappa statistics at 0.88 and 0.81, respectively. The forest class demonstrated the highest accuracy at 98%, while waterbody classification exhibited the lowest reliability. Thus, the segment mean shift method emerges as the preferred choice for LULC classification, considering both appropriateness and accuracy.

REFERENCE

Ai, J., , C., Chen, L., & Li, D. (2020). *Mapping Annual Land Use and Land Cover Changes in the Yangtze Estuary Region Using an Object-Based Classification Framework and Landsat Time Series Data*.

Anand, A., & Bank, W. (2018). *Unit 14 Accuracy Assessment* (pp. 59-77). Retrieved from https://www.researchgate.net/publication/324943246_UNIT_14_ACCURACY_ASSESSMENT.

Anderson, M. L., Heigh, R. I., Mccoy, G. A., Parent, K., Muhm, J. R., Mckee, G. S., Eversman, W. G., & Collins, J. M. (1992). *Accuracy of Assessment of the Extent of Examination by Experienced Colonoscopists*. 560–563.

Basayigit, L. (2015). *Comparison of Pixel-Based and Object-Based Classification. Land Reclamation, Earth Observation & Surveying, Environmental Engineering*, (March 2018).

Belward, A. S., & Skøien, J. O. (2015). *Who Launched What, When and Why: Trends in Global Land-Cover Observation Capacity from Civilian Earth Observation Satellites*. ISPRS

Journal of Photogrammetry and Remote Sensing, 103, 115–128. https://doi.org/10.1016/j.isprsjprs.2014.03.009.

Buja, K., & Menza, C. (n.d.). *Sampling Design Tool for ArcGIS - Instruction Manual* (pp. 1–16). Retrieved from http://www.arcgis.com/home/item.html?id=ecbe1fc44f35465f9dea42ef9b63e785.

CBS. (2021). The Population and Housing Census 2021. Central Bureau of Statistics. Kathmandu. Nepal

Clarke, M. R. B., Duda, R. O., & Hart, P. E. (1974). *Pattern Classification and Scene Analysis*. Journal of the Royal Statistical Society. Series A (General), 137(3), 442. https://doi.org/10.2307/2344977.

Cohen, J. (1960). *A Coefficient of Agreement for Normal Scales. Educational and Psychological Measurement*, XX(1), 37–46. https://doi.org/10.1177/001316446002000104

Comaniciu, D., & Meer, P. (2002). *Mean Shift: A Robust Approach toward Feature Space Analysis. IEEE Transactions on Pattern Analysis and Machine Intelligence*, 24(5), 603–619. https://doi.org/10.1109/34.1000236.

Congalton, R. G. (2001). *Accuracy Assessment and Validation of Remotely Sensed and Other Spatial Information. International Journal of Wildland Fire*, 10(3–4), 321–328. https://doi.org/10.1071/wf01031.

DoA. (2018). *Inter Provincial Dependency for Agricultural Development*. Department of Agriculture. Kathmandu. Nepal

Enderle, D. I. M., & Robert, C. W. J. (2005). *Integrating Supervised and Unsupervised Classification Methods to Develop a More Accurate Land Cover Classification.* Journal of the Arkansas Academy of Science, 59, 65–73.

ESA. (2015). *SENTINEL-2 User Handbook*. Retrieved March 1, 2021, from https://sentinels.copernicus.eu/documents/247904/685211/Sentinel-2_User_Handbook.

ESA. (n.d.). *Copernicus Open Access Hub*. Retrieved November 6, 2020, from https://scihub.copernicus.eu/dhus/#/home.

ESRI. (n.d.-a). *ArcGIS.* Retrieved June 19, 2021, from https://www.esri.com/en-us/arcgis/about-arcgis/overview.

ESRI. (n.d.-b). *Mosaic Operators*. Retrieved February 19, 2021, from https://desktop.arcgis.com/en/arcmap/10.3/manage-data/raster-and-images/mosaic-operators.htm.

ESRI. (n.d.-c). *Segment Mean Shift*. Retrieved March 18, 2021, from https://pro.arcgis.com/en/pro-app/tool-reference/spatial-analyst/segment-mean-shift.htm.

ESRI. (n.d.-d). *Understanding Segmentation and Classification*. Retrieved January 8, 2020, from https://desktop.arcgis.com/en/arcmap/10.3/tools/spatial-analyst-toolbox/understanding-segmentation-and-classification.htm.

ESRI. (n.d.-e). *Understanding Segmentation and Classification*. Retrieved March 18, 2021, from https://pro.arcgis.com/en/pro-app/tool-reference/spatial-analyst/understanding-segmentation-and-classification.htm.

Food and Agriculture Organization of the United Nations [FAO]. (2016). *Map accuracy assessment and area estimation: A practical guide (National Forest Monitoring Assessment*, Working Paper No. E(46)). Retrieved from http://www.fao.org/3/a-i5601e.pdf.

Foody, G. M. (2013). *Thematic Map Comparison. Photogrammetric Engineering & Remote Sensing*, 70(5), 627–633. https://doi.org/10.14358/pers.70.5.627.

Government of Nepal; Office of the Hetauda Sub-Metropolitan City[GoN]. (2017). *City Profile of Hetauda Sub-Metropolitan City*, 2017 (Vol. २०७४).

Hegarty-Craver, M., Polly, J., Neil, M. O., Ujeneza, N., Rineer, J., Beach, R. H., Lapidus, D., & Temple, D. S. (2020). *Remote Crop Mapping at Scale: Using Satellite Imagery and UAV-Acquired Data as Ground Truth*. Remote Sensing, 1–15.

Intergraph; Erdas. (2021). *Top 10 Reasons to Use ERDAS IMAGINE*, 8–9. Retrieved June 19, 2021, from https://www.esri.com/en-us/arcgis/about-arcgis/overview.

Lillesand, T. M., Kiefer, R. W., & Chipman, J. (2015). *Remote Sensing and Image Interpretation* (7th ed.). Vol. 53(9), 1689-1699.

McHugh, M. L. (2012). *Lessons in Biostatistics: Interpreter Reliability: The Kappa Statistic*. 276–282. https://doi.org/10.11613/BM.2012.031

MGL. (n.d.). *Accuracy Assessment of an Image Classification in ArcMap* [Video file]. Retrieved from Library. https://www.youtube.com/watch?v=FaZGAUS_Nlo&t=699s.

Phiri, D., & Morgenroth, J. (2017). *Developments in Landsat Land Cover Classification Methods: A Review*. Remote Sensing, 9(9), 967. https://doi.org/10.3390/rs9090967.

Roy, P. S., Behera, M. D., & Srivastav, S. K. (2017). *Satellite Remote Sensing: Sensors, Applications and Techniques. Proceedings of the National Academy of Sciences India Section A: Physical Sciences*, 87(4), 465–472. https://doi.org/10.1007/s40010-017-0428-8.

Ruppert, G., Hussain, M., & Heimo, M. (2018). *Accuracy Assessment of Satellite Image Classification Depending on Training Sample*. Journal Name, 28(4), 195–201.

Thomlinson, J. R., Bolstad, P. V., & Cohen, W. B. (1999). *Coordinating Methodologies for Scaling Landcover Classifications from Site-Specific to Global: Steps toward Validating Global Map Products*. (Report No. 4257(99).

Viera, A. J., & Garrett, J. M. (2005). *Understanding Interobserver Agreement: The Kappa Statistic*. 360–363.

Author's Information

Name	:	Menaka Hamal
Academic Qualification	:	MSc in Natural Resource Management
Organization	:	Nutan GeoEnvironmental Consultancy Pvt. Ltd
Current Designation	:	Managing Director
Work Experience	:	13 years
Published paper/article	:	5

CALENDAR OF INTERNATIONAL EVENTS

The 9th International Conference on Cartography & GIS
Date: 16-21 June 2024
Country: Nessebar, Bulgaria
Website: https://iccgis2024.cartography-gis.com

International Conference on Satellite Imagery and GIS Geography
Date: 03 Jul 2024
Country: Bangkok, Thailand
Website: https://itar.in/conf/index.php?id=2392469

International Conference on Geoinformatics and GIS
Date: 11-12 July 2024
Country: Ottawa, Canada
Website: https://waset.org/geoinformatics-and-gis-conference-in-july-2024-in-ottawa

Esri User Conference 2024
Date: 15 - 19 July 2024
Country: San Diego, California, U.S.A.,
Website: https://www.esri.com/en-us/about/events/uc/overview

International Conference on Geoinformatics and Remote Sensing
Date: 29-30 July 2024
Country: Istanbul, Turkey
Website: https://waset.org/geoinformatics-and-remote-sensing-conference-in-july-2024-in-istanbul?

31st International Conference on Geoinformatics
Date: 14 - 16 August 2024
Country: Toronto, Canada,
Website: http://www.geoinformatics2024.ca

35th International Geographical Congress
Date: 24 - 30 August 2024
Country: Dublin, Ireland
Website: https://igc2024dublin.org/

International Conference on Geoscience and Remote Sensing
Date: 12-13 September 2024
Country: Rome, Italy
Website: https://waset.org/geoscience-and-remote-sensing-conference-in-september-2024-in-rome

12th International FIG Workshop on LADM & 3D LA
Date: 24 - 26 September 2024
Country: Kuching, Malaysia
Website: https://gdmc.nl/3DCadastres/workshop2024/

International Conference on Geoinformatics and GIS
Date: 24-25 October 2024
Country: Bali, Indonesia
Website: https://waset.org/geoinformatics-and-gis-conference-in-october-2025-in-bali?

International Conference on Geomatics and Remote Sensing
Date: 04-05 November 2024
Country: Cape Town, South Africa
Website: https://waset.org/geomatics-and-remote-sensing-conference-in-november-2024-in-cape-town?

The International Conference on Space Science and Technology
Date; 20-21 Nov 2024
Country: Dubai, United Arab Emirates
Website: https://allevents.in/dubai/80002731887941

International Conference on Cartography
Date: 16-17 December 2024
Country: Rome, Italy
Website: https://waset.org/cartography-conference-in-december-2024-in-rome?

International Conference on Geoinformatics and GIS
Date: 21-22 January 2025
Country: Mandalay, Myanmar
Website: https://waset.org/geoinformatics-and-gis-conference-in-january-2025-in-mandalay?

International Conference on Cartography
Date: 15-16 February 2025
Country: Mumbai, India
Website: https://waset.org/cartography-conference-in-february-2025-in-mumbai?

The Global Space and Technology Convention (GSTC 2025)
Date: 27-28 Feb 2025
Country: Singapore
Website: https://www.space.org.sg/gstc/

International Conference on Geoinformatics and Remote Sensing
Date: 22-23 April 2025
Country: Tokyo, Japan
Website: https://waset.org/geoinformatics-and-remote-sensing-conference-in-april-2025-in-tokyo?

Joint Urban Remote Sensing Event (JURSE)
Date: 5 - 7 May 2025
Country: Tunis, Tunesia
Website: https://www.aconf.org/conf_194195.html

Integration of GNSS, Total Station, and Grid Controls: An Analysis of Combined Effect of Elevation of Topography and Map Projection Distortion to Solve the Distance Discrepancy

Shanker KC[1], Suresh Shrestha[1], Sandesh Upadhyaya[1], Stallin Bhandari[1]
Shankerkc01@gmail.com, Shrestha.suress@gmail.com, sandeshupadhya1@gmail.com, stallin.bhandari@gmail.com
[1]Survey Department

KEYWORDS

Control Survey Methods, Topography, Map Projection Distortion, Distance Discrepancy, GNSS, Total Station, Grid Controls, Integration

ABSTRACT

Heterogeneous measurements from various surveying methods need to be integrated to accomplish any survey project. The use of Global Navigation Satellite System (GNSS) and Total Station (TS) to establish a control framework along with utilizing existing national grid controls, for any survey project has been the standard practice. However, the successful integration of GNSS, TS, and existing grid controls could be challenging at times. Both survey professionals, and surveying stakeholders would benefit from the successful augmentation of heterogeneous measurements from GNSS, TS, and existing grid controls in order to provide a control framework for their survey project. In the past, the distance discrepancy/mismatch of GNSS-derived distance which is obtained from indirect measurements from GNSS survey and TS distance which is ground-based direct measurements, has created confusion. Herein, we have analyzed in detail, the combined effect of elevation of topography and map projection's distortion on the distance; demonstrate the magnitude of combined effect by numerical examples; tested this formulation with real-world GNSS and TS measurements. This way we proposed a solution to solve distance discrepancy/mismatch between various survey methods. The magnitude of the combined effect would be substantial with higher elevations and longer distances and could cross the threshold of specified/required accuracy. The effect would be more pronounced in mountainous regions suggesting combined effect should be properly taken into account. Taking combined effect into consideration brings the compatibility and comparability of GNSS, TS, and existing grid controls together. Thus, allowing both survey professionals and surveying stakeholders to utilize the mix of GNSS, TS, and existing grid controls to achieve required precision and accuracy in an economical, timely, and easy manner.

1 INTRODUCTION

The field of surveying and mapping gathers heterogeneous survey measurements from different surveying methods. The integration of such heterogeneous survey measurements should result required/specified precision and accuracy of the survey project in an economic manner in order to facilitate successful completion of survey project.

Control survey is the fundamental first step of every survey project. Nowadays, it has been standard practice that: major controls are established by the Global Navigation Satellite System (GNSS) survey method (Seeber, 2003) and further extension and densification of controls is done by Total Station (TS) survey methods. Similarly, the control points/network of any survey project starts from existing national grid controls as the reference points. In later case, the method of controls survey could be both GNSS-based and TS-based. In this study, we focused on this mix/integration of GNSS measurements, TS measurements, and existing grid controls and proposed a solution to make these measurements compatible and comparable with each other.

In Nepal, survey projects such as engineering surveys, cadastral surveys have been using a mix of GNSS and TS in order to establish the control framework. The GNSS-derived coordinates are from indirect GNSS measurements while the TS provides the ground-based direct measurements (Schofield & Breach, 2001). The computational way of GNSS measurements processing to get final coordinates differs from that of TS measurements. Due to this difference in nature, we have experienced the distance discrepancy between these two measurements. Similarly, the distance discrepancy occurred when taking existing grid controls and comparing them with ground-based TS measurements.

In this study, we analyzed the combined effect of elevation of topography (Torge & Müller, 2012) and map projection distortion (Krakiswky, 1973) on distance measurement together and proposed a solution on how measurements from GNSS, TS, and existing grid controls can be made comparable with each other. As we solve the distance discrepancy by considering the combined effect, survey professionals can easily and confidently use the GNSS method for major control framework and TS for further extension and densification. Similarly, the survey professionals can easily and confidently take existing grid controls from the Survey Department (SD) as reference controls for their survey project and extend and densify further controls using both GNSS and TS as per their will.

The use of GNSS to establish a control framework; the use of existing grid controls; and integrate these with TS measurements would motivate any surveying stakeholders to accomplish the control survey phase achieving specified/required precision in an economical, timely and easy manner.

The objective of this study is to provide a theoretical explanation behind making GNSS measurements, TS measurements, and existing grid controls (Ghilani, 2010; Ghilani & Wolf, 2012; Schofield & Breach, 2001) comparable and compatible with each other, specifically dealing with solving distance discrepancy we have been facing in the control establishment phase of engineering and cadastral survey projects. The detailed analysis of the combined effect into distance measurements has been done by providing demonstrative numerical examples and tested in GNSS and TS measurements from real survey projects. We discussed how this would solve the distance mismatch problems of real application scenarios. We argue this combined effect would be more pronounced in mountainous regions and also the way to deal with. In addition, this study makes a point that further well-designed research is necessary in order to have a comprehensive understanding of the problem.

This section presents the background of heterogeneous measurements from different surveying methods and technology (e.g. integration of GNSS and TS measurement for any survey project) and associated implications. Method section presents the theoretical aspect of distance reduction and map projection and elaborates on how change in elevation and change in scale factor can be taken into account in order to solve the problem that this paper is talking about. In the results section, numerical examples are presented to demonstrate the effect of elevation variation and distortion individually and their combined effect in various scenarios. Discussion section describes the potential problems and solution; necessity of further well-designed research in order to have well-rounded understanding of the problem that this paper is talking about. Finally, we conclude our paper.

2 METHOD

2.1 Geodetic reduction

Surveyors perform observations such as distance and angle measurement using TS, height difference measurement, etc. on the surface of topography. The immediate distance measurement from TS subject to geodetic reduction (Torge & Müller, 2012; Vanicek, 1986) and map projection (Krakiswky, 1973; Snyder, 1982) before using it for surveying and mapping activities. The ground distance is the distance measured at the surface of topography (see Figure 1). This ground distance is reduced to the surface of the reference ellipsoid by the geodetic reduction process (Torge & Müller, 2012; Vanicek, 1986). The reduced distance is called geodetic distance and also called ellipsoid distance. In this study, we only deal with geodetic distance reduction. Figure 1 below depicts the concept of geodetic distance reduction.

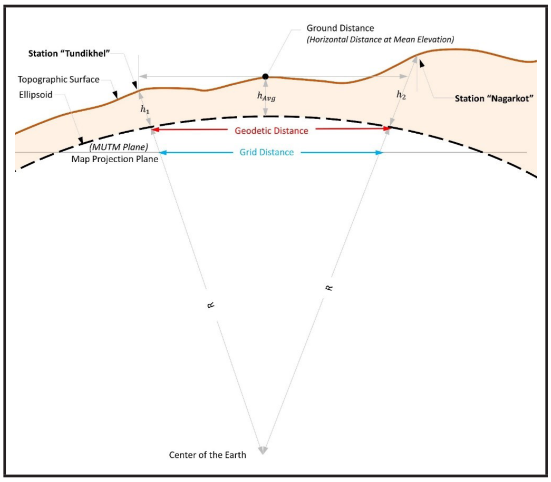

Source: Sickle, 2015

Figure 1: Distance between any two points at different surfaces. The ground distance is on the mean-elevation of topography; the geodetic (ellipsoid) distance is on the curved surface of the reference ellipsoid; and the grid distance is on the 2D rectangular grid plane.

Suppose we take two stations; "Tundikhel", and "Nagarkot" on the topography of Kathmandu Valley. The former is located in the valley and the latter is on the hilltop. The TS measurement provides horizontal distance at mean-elevation between them. The following relationship between ground distance on topography and corresponding geodetic distance on the surface of the reference ellipsoid exists (Torge & Müller, 2012).

$$s_0 = \sqrt{\frac{hd^2}{(1 + h_1/R)(1 + h_2/R)}} \qquad \text{(i)}$$

Where, *hd* is the horizontal distance at mean-elevation, h_1 and h_2 are the elevation of two stations, is the mean-radius of the Earth, and s_0 is the geodetic distance.

2.2 Conformal map projection

We are accustomed to the map. We can easily compute distance, azimuths, assess the size of features, etc. for our navigation and other objectives. Performing the same activities on the surface of the ellipsoid in terms of geodetic coordinates, distance, and azimuth would be a difficult task. The map is convenient. Therefore, the point on the curved surface of the reference ellipsoid is projected to the grid plane.

Grid plane is a flat 2D rectangular plane. The linear or polygon feature on reference ellipsoid is projected to grid plane with some distortion. Imagine, taking out a peel of an orange and try to make the peel flat. The peel becomes irregular, misshaped, with uneven bumps, wrinkles, etc. The peel now lacks uniformity, regularity, and smoothness as in its original form.

The angle between any two lines in the curved surface of the ellipsoid doesn't change between same lines in a flat grid plane through conformal map projection (Krakiswky, 1973; Shrestha, 2011; Snyder, 1982). Conformal map projection is the class of map projection that preserves the angular distance between lines. As a result, the conformal projection keeps the shape of any feature on the surface of the ellipsoid same in grid (map) plane. However, the length gets changed/distorted (see Figure 1). The navigational purpose map, the topographic map adopts this kind of projection.

The Transverse Mercator is a conformal cylindrical projection (Krakiswky, 1973; Shrestha, 2011; Snyder, 1982). The ellipsoid is supposed to be wrapped around by the developable surface. Here, the developable surface is a transverse secant cylinder, where the cylinder touches the ellipsoid along two meridians. These two meridians are called standard lines and the scale factor is unity along these lines.

The amount of distortion in length can be explained and quantified by scale factor (Krakiswky, 1973; Snyder, 1982). The scale factor is the ratio of map distance to geodetic (ellipsoid) distance (see Figure 1). The unit distance in the curved ellipsoid corresponds to the planar map distance by the amount of scale factor. Hence, the ellipsoid distance is scaled up/down by the scale factor to the map distance.

2.3 Modified Universal Transverse Mercator (MUTM) projection

In Nepal, we have adopted the MUTM projection. Each MUTM grid is made to cover a 3° span of longitude. As Nepal's total longitudinal span is about 9°, it requires 3 separate MUTM grids (Geodetic Survey Division, 1990; S. M. Shrestha, 2017).

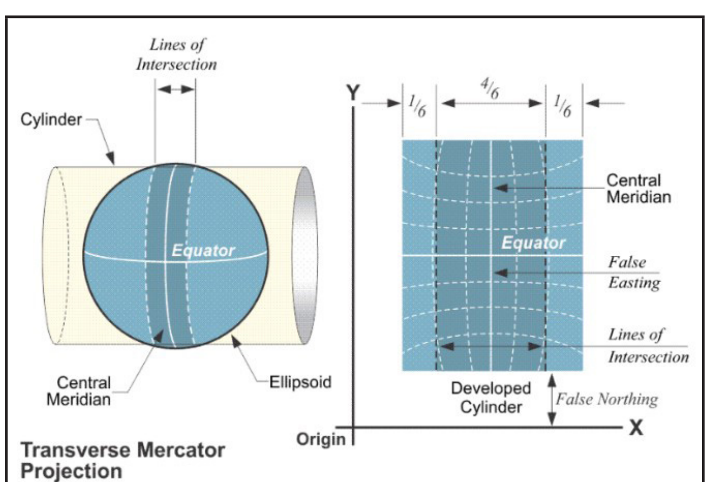

Source: Sickle, 2015

Figure 2: Description of transverse secant cylinder as developable surface and the MUTM grid

Table 1 shows the projection parameters of each MUTM grid zone adopted in Nepal.

Table 1: Nepal adopts 3 different MUTM grids: MUTM81, MUTM84, and MUTM87. Different longitude is chosen as the central meridian for each MUTM grid.

Parameters	**MUTM81 Grid**	**MUTM84 Grid**	**MUTM87 Grid**
Central meridian	81° E longitude	84° E longitude	87° E longitude
Origin of Longitude	81° E longitude	84° E longitude	87° E longitude
Origin of Latitude	0° N latitude	0° N latitude	0° N latitude
Scale Factor (along central meridian)	0.9999	0.9999	0.9999
False Easting	500000 m	500000 m	500000 m
False Northing	0 m	0 m	0 m
Reference Ellipsoid	Everest1830	Everest1830	Everest1830

Source: FINNMAP, 1993; Nepal & FINNMAP, 1997b, 1997a

The longitudinal edge of each MUTM grid lies 1°30′00″ away on either side of the central meridian. The secant lines, where the scale factor is unity and distortion is zero, lie 55′00″ away on either side of the central meridian (Geodetic Survey Division, 1990; Shrestha, 2017).

For a 1 km distance in an ellipsoid, it would be 10 cm less along the central meridian, 0 cm less along secant lines, and 18 cm excess along extreme bound lines, in a grid plane while applying MUTM projection.

2.4 Scale Factor Variation

The scale factor (k) varies at each point. The equation to compute the point scale factor can be expressed as (LINZ, 2008; Redfearn, 1948).

$$k = k_0(1 + Term1 + \mathrm{Term2} + \mathrm{Term3})$$

$$\mathrm{Term1} = \frac{\omega^2}{2}\psi\cos^2\phi$$

$$\mathrm{Term2} = \frac{\omega^4}{24}\cos^4\phi\,[4\psi^3(1-6t^2) + \psi^2(1+24t^2) - 4\psi t^2] \qquad \text{(ii)}$$

$$\mathrm{Term3} = \frac{\omega^6}{720}\cos^6\phi\,(61 - 148t^2 + 16t^4)$$

where, k=k_0 is scale factor at central meridian, $\omega=\lambda-\lambda_0$, is central meridian, and ϕ is latitude of point of interest.

The line scale factor (K) is the ratio of the planar grid (map) distance to the corresponding ellipsoidal distance between two points (see Figure 3). The rigorous formula to compute the line scale factor can be found in the same document (LINZ, 2008). Here we use an approximate formula (Sickle, 2015).

$$K = \frac{k_1 + k_2 + 4k_m}{6} \qquad \text{(iii)}$$

where, k_1 and k_2 are the scale factor at both stations and $k_m = (k_1 + k_2)/2$ is the mean-scale factor.

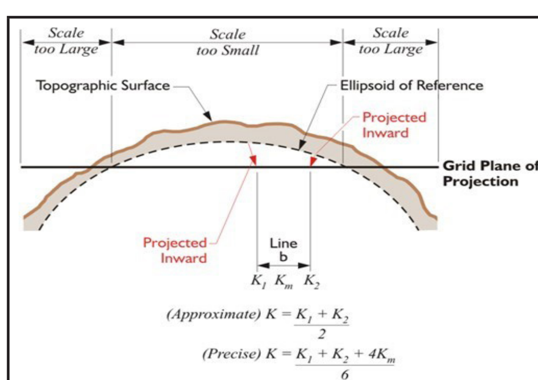

Source: Sickle, 2015

Figure 3: Point scale factor and line scale factor

2.5 Elevation factor, scale factor, and combined factor

The ground distance is reduced to the corresponding geodetic (ellipsoid) distance by elevation factor (see Figure 4).

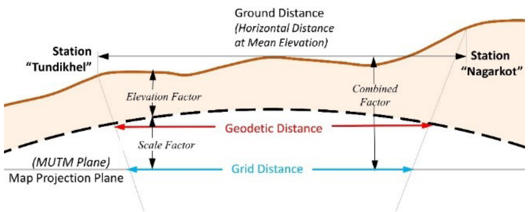

Source: Sickle, 2015

Figure 4: Description of how ground measured distance is converted to geodetic distance by elevation factor; how the geodetic distance is converted to grid (map) distance by scale factor; and when both elevation factor and scale factor effect together by combined factor.

Suppose the considered stations are at elevations of h_1 and h_2. We compute the mean-elevation (h_m) as in equation (iv). The horizontal distance at mean-elevation (h_m) is. To compute ellipsoid distance, we use for both stations' elevation in equation (i) above and rearrange. The resulting expression is equation (v) (Sickle, 2015; Torge & Müller, 2012)

On the right-hand side of equation (v), the second term is called elevation factor as shown in equation (vi).

$$h_m = \frac{h_1 + h_2}{2} \quad \text{(iv)}$$

$$s_0 = hd * \frac{R}{R + h_m} \quad \text{(v)}$$

$$Elevation\ Factor = \frac{R}{R + h_m} \quad \text{(vi)}$$

Next step is to project ellipsoid distance into a grid (map) distance by scale factor. For the distance between two stations in our case, the line scale factor K is computed by taking point scale factor k_1 and k_2 at both stations as given in above equation (iii) (Sickle, 2015).

The combined scale factor is given by the following expression.

$$Combined\ Factor = Elevation\ Factor * K \quad \text{(vii)}$$

The combined factor directly converts ground distance to grid (map) distance and the inverse combined factor converts back grid distance to ground distance.

3 RESULTS

3.1 Ground distance to geodetic distance and elevation factor

We have described the concept of geodetic reduction and elevation factor in method section. In the subsequent discussion, a numerical demonstration illustrating how ground measured distance is reduced to ellipsoid distance by elevation factor at various elevations of the topography, is provided. Figure 5 below shows the changes in elevation factor as the elevation changes. As the elevation of topography increases from zero elevation at sea level to higher elevation, the elevation factor goes decreasing. As a result, the distance measured at higher elevation reduced more compared to that measured at lower elevation. Figure 5 is for the unit distance. If we take the distance e.g. 100m, then the elevation effect on distance reduction is shown in Table 2.

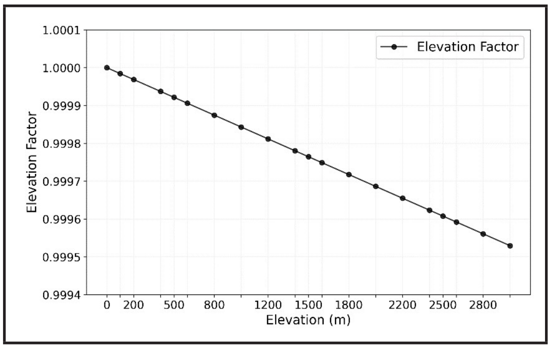

Figure 5: The effect of elevation in distance reduction.

Table 2: Ground distance is reduced to corresponding ellipsoid distance by elevation factor at various elevations of the topography. Different elevation factor applies to different elevations. Higher the elevation, higher the magnitude of the elevation factor.

Ground Distance (m)	Mean-Elevation (m)	Elevation Factor	Ellipsoid Distance (m)
100.00	0.00	1	100
100.00	100.00	0.9999843	99.998
100.00	200.00	0.99996861	99.997
100.00	400.00	0.99993722	99.994
100.00	500.00	0.99992153	99.992
100.00	600.00	0.99990583	99.991
100.00	800.00	0.99987445	99.987
100.00	1000.00	0.99984306	99.984
100.00	1200.00	0.99981168	99.981
100.00	1400.00	0.9997803	99.978
100.00	1500.00	0.99976461	99.976
100.00	1600.00	0.99974893	99.975
100.00	1800.00	0.99971755	99.972
100.00	2000.00	0.99968618	99.969
100.00	2200.00	0.9996548	99.965
100.00	2400.00	0.99962343	99.962
100.00	2500.00	0.99960775	99.961
100.00	2600.00	0.99959207	99.959
100.00	2800.00	0.9995607	99.956
100.00	3000.00	0.99952934	99.953

We take a distance of 100 m in topography at various elevations of range 0 m to 3000 m. We computed the elevation factor at each elevation according to equation (vi). Then, the 100 m ground distance is converted to the equivalent ellipsoid distance. We showed the result in the above Table 2. As the elevation increases, the higher the magnitude of elevation factor, thus the distance is reduced by a greater amount. At 0 m elevation, the distance remains same; at 1000 m elevation, the distance is reduced by 1.6 cm; at 2000m elevation, the distance is reduced by 3.1cm and at 3000m elevation the distance is reduced by 4.7cm.

This suggests that, in mountainous regions, the amount of reduction is big and should be careful when using grid coordinates with ground measurement. In addition to elevation effect, the scale factor amplifies the effect.

3.2 Ellipsoid distance to grid / map distance and scale factor

Conformal map projection converts the ellipsoid distance into grid/map plane distance by the scale factor. Here, we have shown the effect of scale factor that results various grid/ map distance for equal distance in ellipsoid by numerical example. Figure 6 below shows the scale factor effect to distance at different longitudes between central meridian and the edge of the MUTM zone. The scale factor is unity at 55′ away from central meridian, less than unity before 55′ and greater than unity after 55′.

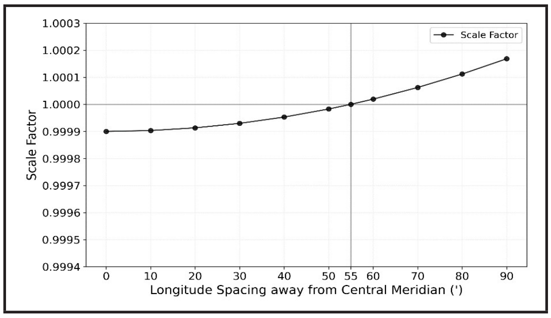

Figure 6: Scale factor variation away from central meridian.

Table 3: Scale factor variation in longitudinal direction at selected designed points and the effect while projecting ellipsoid distance into grid plane.

Ellipsoid Distance (m)	Longitude Spacing (')	Latitude (DD)	Longitude (DD)	Scale Factor	Grid Distance (m)
100.00	0	28.00	84.00000000	0.9999	99.99
100.00	10	28.00	84.16666667	0.99990332	99.99
100.00	20	28.00	84.33333333	0.99991326	99.991
100.00	30	28.00	84.50000000	0.99992984	99.993
100.00	40	28.00	84.66666667	0.99995304	99.995
100.00	50	28.00	84.83333333	0.99998288	99.998
100.00	55	28.00	84.91666667	1.00000029	100
100.00	60	28.00	85.00000000	1.00001936	100.002
100.00	70	28.00	85.16666667	1.00006246	100.006
100.00	80	28.00	85.33333333	1.0001122	100.011
100.00	90	28.00	85.50000000	1.00016857	100.017

We chose 84° E longitude as the central meridian which corresponds to the MUTM84 grid. We designed the point at every 10 ′

longitude interval resulting 11 points. These points have varying longitude away from the central meridian and reflect the scale factor variation of transverse Mercator projection (see Table 3). The secant lines is along 55′ away on either side of the central meridian. The scale factor is set to 0.9999 at the central meridian and increases outward, is unity at 55 ′ away and again increases outward up to the edge of the grid.

We choose a 100 m distance at every point and see the changes by scale factor. For a 100 m distance on the ellipsoid surface, the amount of distortion is -1.0 cm at the central meridian; 0 cm at 55′ away from the central meridian; and +1.7 cm at the extreme edge. This applies to either side of the central meridian. The scale factor effect will be bigger for larger distances such as 500 m, and 1000 m, resulting bigger distortion amount.

3.3 Ground to Ellipsoid to Grid and Combined Factor

The ground measured distance at a certain elevation is reduced to ellipsoid by elevation factor, and that ellipsoid distance is converted to grid /map distance by scale factor. The elevation factor varies as elevation varies and the scale factor varies as longitude varies in Transverse Mercator projection. When both the elevation factor and scale factor are combined, we call it a combined factor (see Equation vii). Figure 7 shows the combined effect.

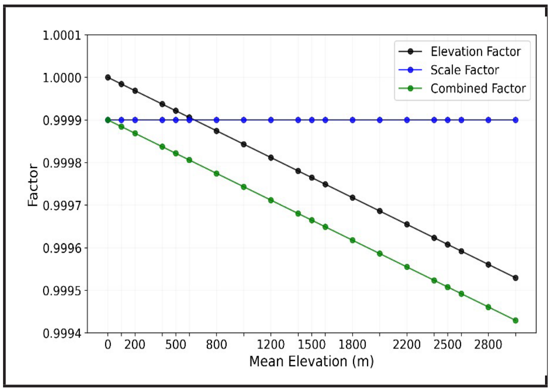

Figure 7: When the elevation factor (black line) combined with scale factor (blue line) results the combined factor (green line). This figure shows the combined effect for unit distance.

Table 4: The combined factor considers both elevation variation and longitude variation effect while plotting ground measured distance into grid plane or vice versa. The combined effect is larger compared to the individual elevation factor effect or scale factor effect.

Ground Distance (m)	Mean-Elevation (m)	Elevation Factor	Ellipsoid Distance (m)	Point Location (Lat, Lon)	Scale Factor	Combined Factor	Grid Distance (m)
100.00	0	1	100	28.0,84.0	0.9999	0.9999	99.99
100.00	100	0.9999843	99.998	28.0,84.0	0.9999	0.99988431	99.988
100.00	200	0.99996861	99.997	28.0,84.0	0.9999	0.99986861	99.987
100.00	400	0.99993722	99.994	28.0,84.0	0.9999	0.99983723	99.984
100.00	500	0.99992153	99.992	28.0,84.0	0.9999	0.99982153	99.982
100.00	600	0.99990583	99.991	28.0,84.0	0.9999	0.99980584	99.981
100.00	800	0.99987445	99.987	28.0,84.0	0.9999	0.99977446	99.977
100.00	1000	0.99984306	99.984	28.0,84.0	0.9999	0.99974308	99.974
100.00	1200	0.99981168	99.981	28.0,84.0	0.9999	0.9997117	99.971
100.00	1400	0.9997803	99.978	28.0,84.0	0.9999	0.99968032	99.968
100.00	1500	0.99976461	99.976	28.0,84.0	0.9999	0.99966464	99.966
100.00	1600	0.99974893	99.975	28.0,84.0	0.9999	0.99964895	99.965
100.00	1800	0.99971755	99.972	28.0,84.0	0.9999	0.99961758	99.962
100.00	2000	0.99968618	99.969	28.0,84.0	0.9999	0.99958621	99.959
100.00	2200	0.9996548	99.965	28.0,84.0	0.9999	0.99955484	99.955
100.00	2400	0.99962343	99.962	28.0,84.0	0.9999	0.99952347	99.952
100.00	2500	0.99960775	99.961	28.0,84.0	0.9999	0.99950779	99.951
100.00	2600	0.99959207	99.959	28.0,84.0	0.9999	0.99949211	99.949
100.00	2800	0.9995607	99.956	28.0,84.0	0.9999	0.99946075	99.946
100.00	3000	0.99952934	99.953	28.0,84.0	0.9999	0.99942939	99.943

In Table 4, we demonstrate the effect of the combined factor by a numerical example. We used 100 m ground measured distance at various elevations, used central meridian with a 0.9999 scale factor and computed the grid /map distance. The changes amount to +1.0 cm at 0 m elevation, +1.8 cm at 500 m elevation, and 2.6 cm at 1000 m elevation, 4.9 cm at 2000 m elevation and 5.7 cm at 3000 m elevation. The combined effect is larger. For topography having a higher altitude than 1000 m, the combined effect is greater than 2 cm in magnitude. The combined effect is 5cm at 2000 m elevation, which is a significant effect. The similar effect can be seen at the edge of each MUTM zone (see Table 5 below).

Table 5: The combined factor and its effect at the edge of the MUTM zone (e.g. at 85.5 ° E longitude).

Ground Distance(m)	Mean-Elevation	Elevation Factor	Ellipsoid Distance (m)	Point Location (Lat, Lon)	Scale Factor	Combined Factor	Grid Distance (m)
100.00	0	1	100	28.0,85.5	1.00016857	1.00016857	100.017
100.00	100	0.9999843	99.998	28.0,85.5	1.00016857	1.00015288	100.015
100.00	200	0.99996861	99.997	28.0,85.5	1.00016857	1.00013718	100.014
100.00	400	0.99993722	99.994	28.0,85.5	1.00016857	1.00010578	100.011
100.00	500	0.99992153	99.992	28.0,85.5	1.00016857	1.00009009	100.009
100.00	600	0.99990583	99.991	28.0,85.5	1.00016857	1.00007439	100.007
100.00	800	0.99987445	99.987	28.0,85.5	1.00016857	1.000043	100.004
100.00	1000	0.99984306	99.984	28.0,85.5	1.00016857	1.00001161	100.001
100.00	1200	0.99981168	99.981	28.0,85.5	1.00016857	0.99998023	99.998
100.00	1400	0.9997803	99.978	28.0,85.5	1.00016857	0.99994884	99.995
100.00	1500	0.99976461	99.976	28.0,85.5	1.00016857	0.99993315	99.993
100.00	1600	0.99974893	99.975	28.0,85.5	1.00016857	0.99991746	99.992
100.00	1800	0.99971755	99.972	28.0,85.5	1.00016857	0.99988608	99.989
100.00	2000	0.99968618	99.969	28.0,85.5	1.00016857	0.9998547	99.985
100.00	2200	0.9996548	99.965	28.0,85.5	1.00016857	0.99982332	99.982
100.00	2400	0.99962343	99.962	28.0,85.5	1.00016857	0.99979195	99.979
100.00	2500	0.99960775	99.961	28.0,85.5	1.00016857	0.99977626	99.978
100.00	2600	0.99959207	99.959	28.0,85.5	1.00016857	0.99976057	99.976
100.00	2800	0.9995607	99.956	28.0,85.5	1.00016857	0.9997292	99.973
100.00	3000	0.99952934	99.953	28.0,85.5	1.00016857	0.99969783	99.97

In mountainous regions (e.g. elevation greater than 1000 m and up to 2500 m), the play of elevation factor combined with scale factor results significant magnitude effect between ground measurement and grid measurement. This suggests to be careful and to well considering this combined effect while mixing both ground measurements from TS with grid/map measurements from existing grid coordinates and existing grid control points.

3.4 Application to integrated measurements from GNSS and TS

We test the effect to both elevation variation and scale factor with real measurement from GNSS observation and TS measured ground distance. We performed GNSS observation over 6 stations, forming 3 sides. We measured the ground distance of 3 sides using TS. The GNSS coordinates based on the global reference ellipsoid (Moritz, 1980) are transformed to local reference ellipsoid i.e. Nepal Datum ellipsoid (KC & Acharya, 2023; UK, 1985) by 7P transformation model (Adhikary, 2002; Manandhar & Bhattarai, 2002; K. G. Shrestha, 2011) and projected to MUTM84 grid. The inverse process: MUTM84 grid distance are scaled back to ellipsoid distance, and ellipsoid distance is scaled back to ground distance. The result is shown in Table 6 below.

Table 6: Inverse operation results the ground distance from MUTM84 grid coordinates and compared with actual TS measured ground distance. Both ground distances seem comparable.

Side	Grid Distance (m)	Mean-Elevation (m)	Elevation Factor	K	Combined Factor	Ground Distance (m)	Measured Ground Distance (m)	Difference Measured & Computed (m)
100-1002	157.219	161.096	0.99997471	0.99990038	0.9998751	157.239	157.237	0.002
1003-1004	300.311	164.941	0.99997411	0.99990097	0.99987509	300.349	300.361	-0.012
1005-1006	80.583	162.332	0.99997452	0.99990056	0.99987509	80.593	80.589	0.004

The ellipsoidal height is used to compute the elevation factor. Instead of the point scale factor, (k) the line scale factor (K) is used (see equation 3). We compared ground distance obtained from inverse operation with actual TS measured ground distance. The deviation is very small attributed to random errors, showing comparable results. Thus demonstrating the effect of elevation variation and scale factor variation is significant and needs to be considered accordingly when mixing TS and GNSS measurements in survey projects.

4 DISCUSSION

Cadastral survey is being carried out in the various parts of the nation. It has been standard practice that the required control network is established by the GNSS survey. Then, the traverse survey using TS is performed for further control densification by taking GNSS-established control points as the reference points. Here, the TS measurements are ground measurements while the GNSS-established control points have MUTM grid based coordinates. In order to make these heterogeneous measurements compatible with each other, the combined effect of both elevation and scale factor variation should be taken into account.

Recently, we faced the problem of mismatch/discrepancy between ground based TS measurements and grid coordinates (e.g. discrepancy in TS orientation) that occurred during the cadastral survey. This analysis of combined effects what might have been the case.

The combined effect would be more pronounced in the mountainous part. The high elevation nature of the mountainous part means the higher the effect of the elevation factor. Similarly, in mountainous regions, the length of the traverse leg or side or baseline tends to be longer. The longer the side, the elevation effect and scale factor effect would result in larger magnitude combined effect. For a traverse leg of 500 m in length at an elevation of 2000 m, the combined effect would be ~ 22 cm. Similarly, for a traverse leg of 1000 m in length and at elevation of 2000 m, the combined effect would be ~ 41 cm. these are substantial amount. This means that, while doing surveying works such as control point establishment by GNSS and later densification by TS as in our standard practice of cadastral survey, in hilly and mountainous parts, this combined effect must be taken into account.

The problem of mismatch/discrepancy between GNSS derived grid coordinates and ground based TS measurements have been a problem in engineering surveying works also. It has been found that the GNSS-derived measurements don't match with TS measurements between any two tower locations of transmission line projects. A similar has been found in reference control of hydropower projects. Here, taking the combined effect into account would bridge the gap between heterogeneous measurements.

Whenever the integration of GNSS and TS measurements needs to be utilized for any kind of surveying projects, this combined effect of both elevation and scale factor should be taken into account.

In the Terai lowland, the elevation factor would be very close to unity and would have very minimal effect, smaller than the tolerance specified/required by the survey project. Only taking the scale factor into account would suffice. This kind of practice has been in practice in the traverse survey of the India-Nepal border survey where only after the grid coordinates are scaled up by scale factor and compared with ground based TS measurements.

SD has established a horizontal control network of first, second, third, and fourth order categories (KC & Acharya, 2022). The fourth order control points are 200 m - 2000 m spacing distant (Geodetic Survey Division, 1990) and are MUTM grid coordinates. When we take TS measurements between any pairs of these fourth order controls, these TS measurements first should be corrected for combined effect, then only these measurements can be compared with MUTM grid coordinates. Otherwise, the discrepancy between the same pairs of fourth order controls would throw you off.

A survey project may have MUTM grid coordinates from past triangulation surveys, may have GNSS derived coordinates from GNSS control survey, and may have to do TS measurements further. This is exactly where the combined effect of elevation and scale factor becomes crucial and well taken care of.

A further well designed research study needs to be carried out in order to answer various questions such as 1) what would be the effective coverage region of the combined factor; 2) will the single combined factor work for the entire survey project area or do we need multiple factors, if so how to properly deal with that situation; 3) what if the same project area has very low and very high elevation region; 4) what if one only uses the GNSS survey during entire project period, would he/she need to take care of combined effect also.

5 CONCLUSION

The field of surveying and mapping science needs to deal with the mixture of heterogeneous measurements from different and various surveying methods. Integrating heterogeneous measurements that meet the precision and accuracy of survey projects could be challenging at times. Specifically, in this study, we focused on the integration of TS and GNSS measurements, particularly to solve the distance problem/discrepancy.

We analyzed the combined effect of elevation of topography and map projection distortion on distance; demonstrated the magnitude of the effect by numerical examples. We showed that by taking combined effect into consideration, ground based TS measurements can be seamlessly augmented/mixed with GNSS measurements. In fact, several surveying projects such as engineering surveys, cadastral and topographical mapping, etc rely on both TS and GNSS measurements for control establishment. We demonstrated that the combined effect would be larger in mountainous regions. However, considering the combined effect would eliminate the discrepancy between TS and GNSS measurements.

Our past experiences showed that, the distance discrepancy between GNSS-derived grid coordinates and TS measurements or existing grid controls and TS measurements has been a severe issue in the control survey part of engineering surveys and cadastral surveys in Nepal. This study has researched the problem with a theoretical aspect, further clarified by numerical examples, and evident by actual GNSS and TS measurements.

This study showed that by considering the combined effect of elevation and distortion, one can easily mix GNSS-derived coordinates, existing grid controls, and TS measurements smoothly in any survey project. By considering the combined effect, the indirect measurements/

coordinates from the GNSS survey are made comparable with direct measurements from TS. This caused increased confidence and motivation of surveying professionals to leverage the GNSS technology in addition to their existing technologies. Next, the integrity of existing grid controls provided by SD can be tested and can be used in any survey project. This would lead to the reduction of the cost of additional control establishment. Next, extending the control survey from existing national geodetic grid control or tie-in of control survey to the existing national geodetic control within the specified tolerance. This way, surveying projects can easily tie to the national grid.

We recommend further well-designed research in order to fully understand problem and devise a solution. The combined effect and mix of various surveying methods should be studied in categories: low-land, hilly, and mountainous regions. Research should be carried out to determine and answer: the effective region of combined factor, multiple combined factors for the same project; optimal combined factor and the guidelines to achieve uniformity.

This study would increase the understanding and clarity when dealing with heterogeneous measurements from GNSS, TS, and existing national grid controls; when making coordinates from indirect GNSS measurements compatible with direct TS measurements. Similarly, the surveying and mapping stakeholders would confidently use mix of existing grid controls, GNSS survey, and TS survey, tied to national grid controls. All these eventually would lead to successful completion of survey projects.

ACKNOWLEDGEMENT

We would like to acknowledge Er. Girija Pokhrel and Er. Kapil Katuwal for sharing their ideas on how scale factor variation effect is considered in border survey to switch between TS measurement and grid coordinates. We had insightful discussions on real life cases in the theme presented in this manuscript with Er. Jeewan Thapa, Er. Prabhas Yadav, and Er. Sundar Devkota. This discussion enhanced the clarity. We would like to appreciate Er. Dibbesh Lacoul's effort for organizing a webinar on grid-to-ground theme with Trimble geospatial resources.

REFERENCES

Adhikary, K. R. (2002). Global Positioning System on Cadastral Survey of Nepal. Nepalese Journal of Geoinformatics, 2, 58–62.

FINNMAP. (1993). Eastern Nepal Topographic Mapping Project, Report on GPS - Surveys. FM-International FINNMAP.

Geodetic Survey Division. (1990). Triangulation Instruction Book. Geodetic Survey Division.

Ghilani, C. D. (2010). Adjustment Computations: Spatial Data Analysis (5th ed.). Wiley.

Ghilani, C. D., & Wolf, P. R. (2012). Elementary Surveying: An Introduction to Geomatics (13th ed.).

KC, S., & Acharya, T. D. (2022). Advancements of Geodetic Activities in Nepal: A Review on Pre- and Post-2015 Gorkha Earthquake Eras with Future Directions. Remote Sensing, 14(7), 1586. https://doi.org/10.3390/rs14071586

KC, S., & Acharya, T. D. (2023). A Brief History of Advances in Geodesy with National Cases. Journal of Land Management and Geomatics Education, 5.

Krakiswky, E. J. (1973). Conformal Map Projections in Geodesy. Department of Geodesy and Geomatics Engineering, University of New Brunswick.

LINZ, O. of the S.-G. (2008). Standard for New Zealand Geodetic Datum 2000 Projections: Version 2 (Standard LINZS25002; Version 2). Office of the Surveyor-General. www.linz.govt.nz

Manandhar, N., & Bhattarai, M. P. (2002). An Overview on Time Series of Geodetic and GPS Network of Nepal. Nepalese Journal of Geoinformatics, 1.

Moritz, H. (1980). Geodetic reference system 1980. Bulletin Géodésique, 54(3), 395–405. https://doi.org/10.1007/BF02521480

FINNMAP. (1997a). Western Nepal Topographic Mapping Project Phase I Final Report of Ground Control Surveys Vol I: Report. HMG Survey Department of Nepal and FM-International FINNMAP.

FINNMAP. (1997b). Western Nepal Topographic Mapping Project Phase I Final Report of Ground Control Surveys Volume III: Definition of Gravimetric Geoid. HMG Survey Department of Nepal and FM-International International.

Redfearn, J. C. B. (1948). TRANSVERSE MERCATOR FORMULAE. Empire Survey Review, 9(69), 318–322. https://doi.org/10.1179/sre.1948.9.69.318

Schofield, W., & Breach, M. (2001). Engineering Surveying (6th ed.). Elsevier.

Seeber, G. (2003). Satellite Geodesy (2nd ed., Vol. 19, Issue 1). Walter de Gruyter. https://doi.org/10.1515/9783110200089

Shrestha, K. G. (2011). An Approach to Determine Coordinate Transformation Parameter for Nepal GPS Network. Nepalese Journal of Geoinformatics, 10, 9–14.

Shrestha, S. M. (2011). Concept of Map Projection and Coordinate System.

Shrestha, S. M. (2017). The Most Suitable Map Projection [Presentation].

Sickle, J. V. (2015). GPS and GNSS for Geospatial Professionals. Department of Geography, Penn State College of Earth and Mineral Sciences. https://www.e-education.psu.edu/geog862/

Snyder, J. P. (1982). Map Projections Used by the US Geological Survey (Second). Department of the Interior.

Torge, W., & Müller, J. (2012). Geodesy: DE GRUYTER. https://doi.org/10.1515/9783110250008

UK, G. D. D. of M. S. M. of D. (1985). Report and Results of a Geodetic Survey of Nepal 1981-84. Survey Department.

Vanicek, P. (1986). Geodesy, The Concepts. North-Holland Publishing Company. https://books.google.com.np/books?id=fnKdwgEACAAJ

Author's Information

Name	:	Shanker KC
Academic Qualification	:	BE in Geomatics
Organization	:	Geodetic Survey Division, Survey Department
Current Designation	:	Survey Officer
Work Experience	:	6 years
Published paper/article	:	5

Call for papers

The editorial board requests for papers related to geo-information science and earth observation for the publication in 24th issue of the Journal on Geoinformatics, Nepal.
Last date of submission is 30th March 2025.
For more information, please contact editorial board

Survey Department

P.O. Box 9435, Kathmandu Nepal
Tel: +977 1 4106508, 4106957, Fax: +977 1 4106757
email: info@dos.gov.np

Instruction and Guidelines for Authors Regarding Manuscript Preparation

- Editorial Board reserves the right to accept, reject or edit the article in order to conform to the journal format.
- The contents and ideas of the article are solely of authors.
- The article must be submitted in Microsoft Word by email.
- Editorial Board has no obligation to print chart/ figure/table in multi colour, in JPEG/TIFF format, the figure/picture should be scanned in a high resolution.
- Authors are also requested to send us a written intimation that the same articles is not sent for publication in other magazine/journal.

Page size: A4

Format: Single line spacing with two columns.

Margin: upper 1", left 1.15", right 1", bottom 1".

Length of manuscript: The article should be limited upto 6 pages including figures and references.

Body text font: Times New Roman "11".

Title: The title should be centrally justified appearing near top of 1st page in Cambria, "20" point (Bold).

Authors Name: Authors name should be in Times New Roman "10" with Upper and lower casing, centrally justified. There should be a gap of one lines with 11 pt between the title and author's name.

Authors Email: Authors email should be in Times New Roman "10" centrally justified. There should not be gap between the name and email.

Keywords: Four to five keywords on paper theme

in Times New Roman "10" with two spacing under

the Authors email left justified.

Abstract: Single line spacing after keywords, limited to around 300 words in Italic, Times New Roman "10".

Major heading (Level 1) should be flushed with the left margin in Times New Roman "10" bold font and with Upper casings. Color Dark blue. Numbering 1

Minor heading (Level 2) should be flushed with the left margin in Times New Roman "11" Bold font and with Upper and Lower Casing. Color Dark blue. Numbering 1.1

Minor heading (Level 3) should be flushed with the left margin in Times New Roman "11" Bold font, Italic and with Upper and Lower Casing. Color Dark blue. Numbering 1.1.1

Minor heading (Level 4) should be flushed with the left margin in Times New Roman "10" Italic and with Upper and Lower Casing. Color Dark blue. Numbering 1.1.1.1

BulletPoint: Use only (•).

Placement of photographs/tables: Photographs or tables should be pasted in appropriate place of manuscript pages with caption in their positions in Times new Roman "10" with Upper and lower casing.

Equations: All equations should be in Times New Roman, "11" and italic with consecutive equation numbers placed flush right throughout the paper.

References: References should be listed in alphabetical order at the end of paper in following sequence and punctuation. Author's last name, Author's initials, (Year of publication). *Title of references article in italic,* name of book or journal, volume number, country or city, name of publisher etc.

Citation: All papers are to be cited like (Rajabifarad, 2012), (Dangol & Kwak, 2014), (Zebenbergen, *et al*., 2018). Upto two authors, the last name should be cited for both and if more than two, then cite it as *et al*..

Primary Author's Information:

Name, Academic Qualification, Organization, Current Designation, Work Experience (in years),

Published Papers/Article (Number) and scanned copy of author's passport size photo.

Note: "Author should send the picture of all the figures kept in paper as separate file."

Landslide Susceptibility Analysis and Hazard Zonation in Nuwakot District, Nepal

Bikash Kumar Karna (Ph.D.)
bikashkumarkarna@gmail.com
Survey Department, Nepal

KEYWORDS

Bivariate analysis, Frequency ratio, Entropy index, Landslide susceptibility analysis

ABSTRACT

Landslide mostly occurred in highly rugged topography, erosional steeply sloping land form and fragile geological structural in mountainous region. Landslide susceptibility describe the likelihood relation of occurring landslide in an area controlled with their local terrain condition. Landslide susceptibility analysis (LSA) work is used to determine the spatial distribution of landslides prone area and applicable to predict the future landslides occurrences, which is vital for averting and mitigating regional landslide disasters. LSA. In this study, LSA is carried with the bivariate analysis incorporating twelve causative factors of landslide. The frequency ratio (FR) technique were used for computing the relative frequency (RF) as priority rank and entropy index (E) as weight of causative factor. Result of LSA shows that the probability of occurring landslides is 80 percent, with 27 percent of that risk being high risk, 38 percent being medium risk, and 15 percent being low risk. The prediction accuracy of the model is 87.89 percent, showing reliable and satisfactorily validation rates with good accuracy. So, the present study demonstrates that the quantitative assessment methods explored may have a promising potential for landslide assessment and prediction in the high hill and Himalaya regions.

1. INTRODUCTION

Landslides are global geomorphological phenomena occurring in all geographic regions in response to a wide range of triggering factors. It is linked to the combination of geological, geomorphological, and climatic factors in response to trigger mechanisms mostly represented by heavy rainfall events, seismicity, or human action. It occurs through the movement of a debris, rock or soil mass down the slope (Cruden, 1991) and plays an important role in landform evolution and cause serious destructive natural hazards (Seyedeh et al., 2011). It impacts directly and indirectly on a territory, causing fatalities and huge socioeconomic losses also due to rapid population growth and environmental degradation that requires correct land use policies and best practices for long-term risk mitigation and reduction.

Geographically, Nepal is a one of the most vulnerable countries in the world to landslide. Rugged topography, unstable geological structures, soft and fragile rocks, along with heavy and concentrated rainfalls during monsoon periods collectively cause severe land sliding problems and related phenomena in the mountainous part of Nepal (Dahal, 2012). Also, Nuwakot district covers mostly rugged terrain, erosional and past glacier land form and fragile geological structural mountainous region and consequently highly vulnerable to the occurrence of landslides. Landslide susceptibility describe the likelihood relation of occurring landslide in an area controlled with their local terrain condition (Joshi et al., 2017). The aim of this paper is to determine the spatial distribution and likelihood of landslides through landslide susceptibility analysis (LSA) in geographic information system (GIS) environment. LSA indicates the landslide-prone areas that can be used by policy-makers, and general public to avoid catastrophic landslides. It represents a fundamental step toward assessing landslide hazards and developing mitigation strategies (Dong et al., 2023). Therefore, conducting landslide susceptibility modeling and mapping research is essential.

2. STUDY AREA

Nuwakot District, a part of Bagmati Province, is one of the seventy-seven districts of Nepal. The district, is located at latitude from $27^{0}45'37.54''$ to $28^{0}05'27.72''$ and longitude from $84^{0}59'26.43''$ to $85^{0}29'57.87''$ having extent 1121 km^2. The demographic situation of this districts covers population of 263,391 and population density 235 per km^2 in 2021 (NSO, 2023). The district consists of 12 local units having two municipalities as Bidur and Belkotgadhi, and 10 rural municipalities as Kakani, Likhu, Panchakanya, Dupcheshwar, Suryagadhi, Tadi, Shivapuri, Kispang, Tarkeshwar, and Myagang. The location diagram of Nuwakot district is shown in Figure 1.

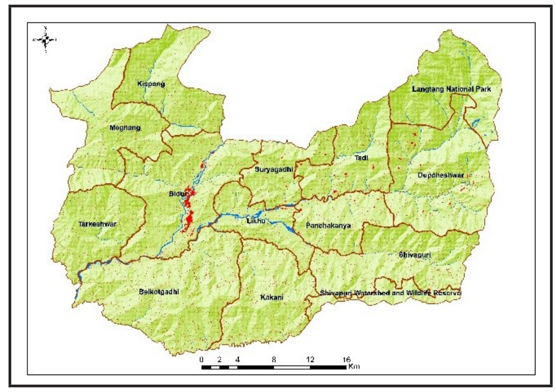

Figure 1: Study Area

3. METHOD AND MATERIALS

3.1 Data used

The data collected from secondary source that utilized to create the landslide inventory mapping, causative factors as criterion map and determine the potential site for susceptibility of landslide area. The detail of data and its source is shown in Table 1.

Table 1: Data & data sources

Data Type	Source	Year
ZY-3 Satellite Image	Survey Department	2024
Topographical map (1:25000 & 1:50000) and its digital layer	Survey Department	2023
Rainfall Data	Department of Hydrology and Metrology	2000-2023
Geological Map (1:50000)	Department of Mine and Geology	2022
Land System Map (1:50000)	Survey Department	2020
Past Landslide Data	District Disaster Committee, Nuwakot	2023

3.2 Method adopted

LSA was carried out using bivariate statistical analysis with frequency ratio (FR) technique in GIS environment. The FR technique has used to compute the weight and its influencing rate based on the possibility of landslide occurrence and relation with the characteristics of causative factors. The FR technique was used to establish the relationships between the distribution of landslide occurrence locations and each causative factor based on the reveal correlation between these factors. The weight for each causative factors of the landslide was firstly determined, then landslide susceptibility indexes map was generated by weighted summation of causative factor in GIS.

The conceptual framework of bivariate analysis based FR model associated with the parameters of LSA is explained in Figure 2.

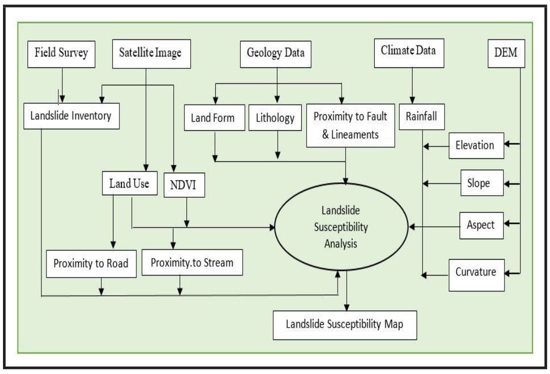

Figure 2: Landslide Susceptibility Analysis

The weight of each causative factor was defined as the natural logarithm of the landslide density in the class over the landslide density in the factor map as follows (Van Westen et al., 1997; Dou et al., 2015).

$$Wi = \ln(\frac{N_{pix}(S_i)/N_{pix}(N_i)}{\sum N_{pix}(S_i)/\sum N_{pix}(N_i)}) \quad \ldots \text{(i)}$$

where, Wi is the weight given to a certain causative class of factor parameter. Density class is the landslide density within the parameter class, Density Map is the landslide density of the entire factor map for all classes, Npix(Si) is the number of landslide pixels in a certain class and Npix(Ni) is the total number of pixels in all classes. The entropy index was used to estimate the difference between the average shares of single causative factor with proportion from the total causative factors used in the whole system. The entropy index (E) of each causative factor parameter was computed based on the information coefficient of parameter with the parameter value to total value ratio (Bednarik et al., 2010)

$$Eij = \frac{FR}{\sum_{j=1}^{n} FR} \quad \ldots\text{. (ii)}$$

The landslide susceptibility map (LSM) was computed from the values of parameters classes with influencing landslides as entropy index (E) and weight of causative factor based on FR together as follows (Nohani et al., 2019).

$$LST = \sum_{j=1}^{n}(W_j \, x \, E_i) \quad \ldots\text{. (iii)}$$

where, W.j is the weight of causative factor based on FR, Ei is the causative factor map product from FR value of i classes of causative factors j, and n is the number of causative factors and LST is the landslide susceptibility index for potential hazard for landslide risk.

In this study, the performance of LSE was validated through the receiver operating characteristic (ROC) curve and the area under the curve (AUC). Generally, ROC is used to quantify the quality of deterministic and probabilistic detections and to determine the accuracy of the LSA (Akgun et al., 2012). The ROC curve is drawn by plotting specificity on the X axis and sensitivity on the Y axis where sensitivity represents the false positive rate and specificity as the false negative rate based on the number of observed landslides predicted accurately compare to the predicted landslides. The AUC was used to identify the model accuracy based on the validation samples landslide and ability in predicting future landslides based on the training samples landslide. The range of the AUC ranges from 0.5 to 1 with the AUC of 1 representing perfect prediction and the closer the value of the AUC to this number, the better the performance of the model (Tehrany et al., 2013). In general, AUC of range between 0.9–1.0 is excellent, 0.8–0.9 is good, 0.7–0.8 is fair 0.6–0.7 is medium and 0.5–0.6 is poor (Kantardzic, 2011). In the model evaluation by AUC, there is two evaluation process based on the success rate and the prediction rate. The results for the success rate achieved on the basis of training data and the prediction rates attained by a set of validation data (Karna, 2024). The results of the success rate have represented the fitness of the model for the training data; used in model building and not useful in assessing the predicting power of the model (Nohani et al., 2019).

4. RESULT AND DISCUSSION

4.1 Landslide inventory mapping

Initially, landslide inventory map was prepared based on the past landslide occurrences. The accuracy of the data on past and present landslides were used for predicting future landslides. In this research, extensive field survey was conducted for collecting the past and present landslides and interpreted with help of topographical map and satellite images, and other relevant documents and reports. The total of 206 landslides sites (locations) were determined and mapped for preparing the landslide inventory map. The inventory data was randomly categorized into two parts; one containing about 70% of landslide occurrences (144 locations) for building the model, called training dataset and another about 30% of landslide occurrences (62 locations) which was not being used in the training step but applied for validating the model performance, called the validation dataset. The distribution of landslide area is represented in Figure 3.

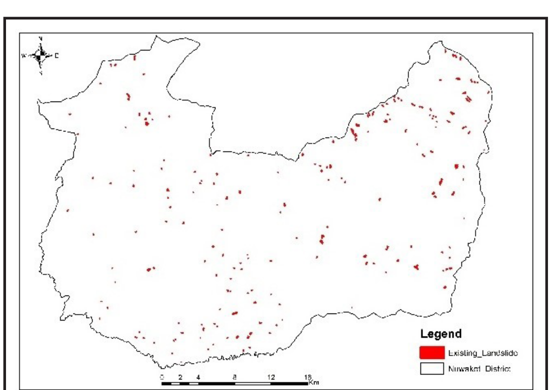

Figure 3: Landslide Distribution

4.2 Causative factor

For the assessment of susceptibility of landslides, identifying the landslide causative factors is essential. Landslide causative factors have some characteristics such as easy obtainability, representativeness, and practicality (Oh & Pradhan, 2011). In this research, twelve causative factors affecting the occurrence of landslides were determined for LSA based on the literature review and field surveys. The mechanism of landslide occurrence were identified and related to the factors of hydrology, geomorphology, geology, climatic etc. These factors includes: slope degree, slope aspect, curvature, elevation, proximity to fault line, lithology, land form, Normalized Difference Vegetation Index (NDVI), rainfall, proximity to stream, proximity to road, and land use. The map of these causative factors maps were prepared in GIS. Among these causative factors, the slope angle relates with shear stress and contributes to the displacement of the hill slope and the most significant in the occurrence of landslides. The surface of terrain with sufficient thickness of soil depends on slope angle and increased the slope angle depicts hill/mountain more unstable. The slope angles in the area under study area was directly derived from digital elevation model (DEM) and reclassified into five groups as 0–5, 5–15, 15–30, 30–45, and greater than 45 degrees.

The slope aspect is another significant factors has affected the occurrence of landslides due to various wetness of the aspect. It affected through the hydrological processes by evapotranspiration and influenced with soil moisture and vegetation cover. The information about the slope aspect was taken from DEM and divided into five categories as flat, north, east, south and west. Likewise, the curvature represents the morphological characteristics of the topography and controls surface runoff and factors on the impact of landslide occurrence. The curvature was straight derived from the

DEM and categorized into three classes of negative curvature as concave (≤0.05), zero curvature as flat (-0.05–0.05) and positive curvature as convex (≥0.05).

The heavy and concentrated rainfalls directly influences the occurrences of landslide as climatic factors. The rainfall intensity was derived from the mean rainfall intensity data from 2000-2023 at the surrounding metrological stations and categorized into three groups as less than 2000, between 2000 to 3000 and greater than 3000 mm per year. The intensity of rainfall and tectonics plate movement depends on the range of the elevation. So, the elevation also acts as influencing factor for the landslide occurrences indirectly. The elevation was represented through DEM and categorized into six groups' elevation range as 354–1000; 1000–2000; 2000–3000; 3000–4000; 4000–5000; and above 5000m from mean sea level.

The fault line indicates the tectonic racks that weaken the rock and cause discontinuities in the soil and rock. This indicates the likelihood that numerous landslides will be caused by seismic and geological processes. The fault line layer was derived from the geological map of the study area, then the distance from the fault was extracted using the multiple ring buffers with five classes of 0–100, 100–200, 200–500, 500-1000 and greater than 1000 m. The lithology represents the structure of work based on the different formations with various structures, compositions, and permeability, which influence the formation material (rock type) strength. The confluence of rock type with curvature and slope steepness are influenced remarkable occurrences of landslide. The lithological structure was also derived from the geological map of the study area, which consisted of 4 units as slate, gneisses, quartzite and schists. Landform mainly morphological identification play an important role in the occurrences of landslide because, for each individual slope the process that occurs is different, which in turn produces different materials (Malik et al., 2017). In addition, these differences of process and material have different effects on the frequency of landslide occurrences. The morphological landform was derived from land system map and it covers alluvial plains and fans, erosional terraces and tars, steeply sloping terrain, past glacier lower attitudinal mountain, and past glacier upper attitudinal mountain.

The NDVI represents the vegetation cover index in which greater the value, the more amount of vegetation cover and the root of vegetation leads to stabilization of the hill slope and reduction in landslide occurrences. The NDVI map was generated through ZY-3 MSS images. The range of NDVI values were categorized into four categories as less than zero as water body and high moisture condition and probability of high landslide occurrences; the value between 0.00 to 0.30 represented the built-up, bare soil and agriculture land with moderate landslide occurrences; between 0.30 to 0.45 represented the shrub land with low landslide occurrences and greater than 0.45 represented dense forest as very low occurrences of landslide. The water of the river are considered as an important factor in LSA having condition of wet land and high soil moisture. The water contains factor was extracted for the river layer through buffering in distance ranges and classified into five classes including distance less than100, 100–200, 200–500, 500-1000 and greater than 1000m. Existing landslides are typically found close to road systems, where they are caused by discontinuities in the rock and soil that are prone to landslides, or by cutting slope hills for roads that are steeper than 15 degrees. The distances to the roads was obtained from buffering in distance ranges and classified into four classes including distance less than 100, 100–200, 200–500, 500-1000 and greater than 1000 m. Land use acts as significant factor that caused by human beings and affects the probability to landslides in the study area. The land use map of study area in 2023 was created from topographical map and applied in LSA.

4.3 Computation of weight and entropy index

The entropy index (E) in terms of parameter weight of each causative factor was computed from association of FR values using equation (ii) and shown in Table 2.

Table 2: Entropy index and weight of Factors

S.N.	Factor	E Value	Weight
1	Proximity to Stream	0.08	8
2	Land Use	0.11	11
3	Lithology	0.06	6
4	Elevation	0.1	10
5	Proximity to Road	0.07	7
6	Curvature	0.06	6
7	Land From	0.07	7
8	Aspect	0.1	10
9	NDVI	0.1	10
10	Proximity to Fault line	0.07	7
11	Slope	0.1	10
12	Rainfall Intensity	0.07	7

4.3 Potential landslide susceptibility area

Potential landslide susceptibility area was produced based on the influencing weight and relative frequency derived from the FR of causative factors using equation (iii) is shown in Figure 4.

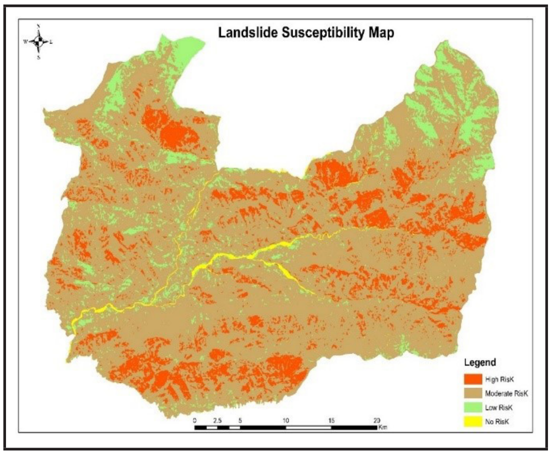

Figure 4: Landslide Susceptibility Map

From the landslide susceptibility analysis data, it's showed that the 80% of municipality extent land has occurred in the landslide risk in which the distribution of the high risk occupied 27%, medium risk occupied 38 % and low risk occupied 15%.

4.4 Validation of susceptibility model

The ROC curve with AUC for success rate was generated from the training dataset of landslide and potential landslide susceptibility map. Likewise, the ROC curve with AUC for prediction rate was generated from the validation dataset of landslide and potential landslide susceptibility map.

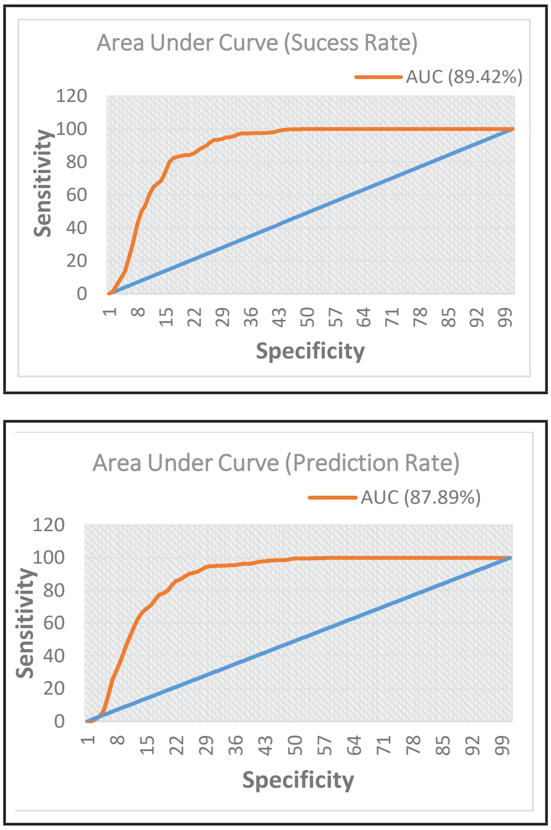

Figure 5: LSA Model Validation

The area under the curve of the success rate showed 0.89 and prediction rate 0.88 representing the prediction accuracy of the model is 87.89%. So, LSA is reliable and showed all satisfactorily validation rates with good accuracy.

4.5 Potential hazard zonation and impact

The impact of potential landslide assessment was carried out by the process of spatial overlay operation using zonal statistics of landslide susceptibility layer with land use layer 2023. The potential landslide risk in the land use categories is shown in Table 3. In overall risk, total 79.85 percent land has occurred in the potential landslide risk prone zone in Nuwakot district. The 84.39 percent of land under agriculture use is found in risky zone of the landslide. Also, 74.63 percent of forest land is occurred in the risk by landslide Likewise, 77.96 percent of built-up area, is found under the threat of landslide risk.

Table 3: Potential risk and impact on landuse

S.N.	Land Use Type	Landslide Susceptibility (area in Sq. Km)					Overall Risk (%)
	Description	High	Medium	Low	Total	%	
1	Agriculture	215.52	226.24	90.50	532.26	84.39	44.61
2	Forest	80.14	202.93	81.17	364.24	74.63	30.53
3	Waterbody	22.67	11.04	4.41	38.12	74.18	3.19
4	Built-up	5.13	8.37	3.35	16.84	77.96	1.41
5	Barren Land	0.77	0.34	0.14	1.25	88.82	0.11
	Total	324.23	448.92	179.57	952.72		79.85

5. CONCLUSION

LSA based on bivariate FR based quantitative technique is more appropriate to evaluate the probability assessment of landslides in the study area. The causative factors identified and applied in LSA is the local situation of Nuwakot District and might be used in other part of Nepal. The result of LSA shows that the steeply sloping terraces having rugged geological structure in the erosional land form area are occurred in high and medium risk of landslides. Also, landslide susceptibility depicts the most portion of the area in high risk that affected the serious threats to life, property, infrastructures and ecological system. The present study demonstrates that the quantitative assessment methods explored may have a promising potential for landslide assessment and prediction in the Himalayas.

REFERENCES

Akgun, A., Kıncal, C. & Pradhan, B. (2012). Application of remote sensing data and GIS for landslide risk assessment as an environmental threat to Izmir city (West Turkey). *Environ. Monit. Assess*, 184, 5453–5470.

Bednarik, M., Magulová, B., Matys, M. & Marschalk, M. (2010). Landslide susceptibility assessment of the Kral'ovany–Liptovský Mikuláš railway case study. *Phys. Chem. Earth Parts*, 35, 162–171.

Cruden, D. M. (1991). A simple definition of a landslide. *Bulletin of the International Association of Engineering Geology*, 43, 27–29.

Dahal, R. K. (2012). Rainfall-induced Landslides in Nepal. *International Journal of Erosion Control Engineering*, Vol. 5(1), 1-8.

Dong, A., Dou, J., Fu, Y., Zhang, R. & Xing, K. (2023). Unraveling the evolution of landslide susceptibility: a systematic review of 30-years of strategic themes and trends. *Geocarto International*, 38:1, 2256308, DOI: 10.1080/10106049.2023.2256308

Dou, J., Tien Bui D., Yunus, A., Jia, K., Song, X. & Revhaug I. (2015). Optimization of causative factors for landslide susceptibility evaluation using Remote Sensing and GIS data in parts of Niigata, Japan. *PLoSONE*, 10 (7), 1-29.

Joshi J., Bharadwaj, D., Paudyal,P. & Timalsina, N. (2017). Landslide inventory, susceptibility mapping and recommendation of the mitigation measures in Nuwakot District. *Journal* *of Nepal Geological Society*, 53, 107-118.

Kantardzic, M. (2011). *Data mining: Concepts, models, methods, and algorithms*. New York. John *Wiley* & Sons, Inc.

Karna, B. K. (2024). *Land suitability evaluation for land use planning in Shambhunath Mmunicipality of Saptari District, Nepal*. Ph.D. Dissertation. *Tribhuvan University, Nepal.*

Malik, R.F.; Sartohadi, J. (2017). Detailed Geomorphological Mapping Using the Step-Wise-Grid Technique in the Bompon Watershed, Magelang District, Central Java. *J. Bumi Indones*. 6, 1–16.

Nohani, E., Moharrami, M., Sharafi, S., Khosravi, K., Pradhan, B., Pham, B.T., Saro Lee, S. & Melesse, A. M. (2019). Landslide Susceptibility Mapping Using Different GIS-Based Bivariate Models. *Water*, 11, 1-22.

NSO. (2023), *National population and housing census 2021: National Report*. National Statistics Office, Kathmandu, Nepal.

Oh, H. J. & Pradhan, B. (2011). Application of a neuro-fuzzy model to landslide-susceptibilitymapping for shallow landslides in a tropical hilly area. *Computer. Geoscience*, 37, 1264–1276.

Seyedeh, Z. M., Ataollah, K., Karim, S., Seyed, R. M. & Ataollah S. (2011). GIS-based spatial prediction of landslide susceptibility using logistic regression model. *Geomatics, Natural Hazards and Risk*, 2(1), 33-50.

Tehrany, M. S., Pradhan, B. & Jebur, M. N. (2013). Spatial prediction of flood susceptible areas using rule based decision tree (DT) and a novel ensemble bivariate and multivariate statistical models in GIS. *Journal of Hydrology*, 504, 69-79. DOI: 10.1016/j.jhydrol.2013.09.034.

Van Westen, C. J., Rengers, N., Terlien, M. T. J. & Soeters, R. (1997). Prediction of the occurrence of slope instability phenomenal through GIS-based hazard zonation. *Geol Rundschau*, 86, 404–414

Author's Information

Name	:	Dr. Bikash Kumar Karna
Academic Qualification	:	Ph.D. Geography (Specialization: Land Use Planning)
Organization	:	Survey Department
Designation	:	Chief Survey Officer
Work Experience	:	25 Years
Published Articles/papers	:	13

Mapping and Analysing Suicide Locations of Lalitpur, Nepal

Dinesh Khatri[1], Dashrath Ghimire[1], Poshan Niraula[1]
dineshkc7373@gmail.com, ghimiredashrath@gmail.com, poshan.niraula@gmail.com
[1]Survey Department

KEYWORDS

GIS, Hotspot and Coldspots, Spatial dependence, Suicide

ABSTRACT

This research utilizes geospatial and statistical analysis to examine spatial patterns in suicide occurrences within the Lalitpur district of Nepal. The dataset comprises suicide locations collected from the Lalitpur Police Range (LPR) over a period of six fiscal years spanning from 2074/75 to 2078/79 (2017 AD to 2023 AD). Textual data undergo preprocessing and geocoding processes to derive locations for spatial analysis. The methodology employs Local Moran's I to identify spatial patterns and Getis Ord Gi to identify hotspots and coldspots of suicide incidents. Due to location approximations, spatial analyses are conducted at aggregated levels, including administrative units (wards level) and 1km x 1km grids. The study reports the identified hotspots and coldspots based on these analyses.*

1. INTRODUCTION

1.1 Background

Suicide refers to the act of intentionally taking one's own life. It is a complex and multifaceted issue that often results from a combination of factors, including psychological, social, and environmental influences (Karthick, 2017). It is often associated with mental health issues, such as depression, anxiety, bipolar disorder, schizophrenia, and substance abuse. However, it is essential to remember that there is no single cause for suicide, and it usually results from a combination of factors. It's crucial to approach discussions about suicide with empathy and understanding, as it is a matter of great importance for public health and mental well-being (Johnson, 1965).

According to the World Health Organization (WHO) around 700,000 people die by suicide every year globally. This amounts to approximately one death every 40 seconds. Suicide is a leading cause of death worldwide, especially among young people aged 15-29. Low and middle-income countries account for the majority of suicides globally (WHO, 2023).

According to New Spotlight online News Magazines the suicide rate has increased by 72 percent in a decade in Nepal from 11 persons a day in the fiscal year 2068/69 BS to 19 persons in the fiscal year 2078/79 BS. As many as 53,298 people committed suicide in the last 10 years, which is described in Table 1 (Spotlight Nepal, 2022).

Mapping suicide locations is akin to tracking a disease outbreak. Just as we locate clusters to understand disease spread, identifying where suicides cluster helps pinpoint high-risk areas. This targeted approach enables more effective prevention efforts and ensures that resources are allocated where they're most needed. Additionally, studying suicide locations can provide valuable insights into societal and environmental factors contributing to suicidal behavior (Too et al., 2017).

Table 1: Number of suicides committed per fiscal year in Nepal.

S.N.	Fiscal Year	Number of Suicides
1	2068/69	3977
2	2069/70	3974
3	2070/71	4504
4	2071/72	4332
5	2072/73	4680
6	2073/74	5124
7	2074/75	5317
8	2075/76	5754
9	2076/77	6279
10	2077/78	7149
11	2078/79	6830

1.2 Objectives

The main objective of this research is to map the suicide locations in the Lalitpur districts of Nepal and analyze these locations to identify possible spatial patterns.

The specific objectives of the tasks are as follows:

- To identify the datasets related to suicides in the study area including the location of the suicide and visualize the spatial distribution.
- To compute the spatial autocorrelation measures to study the pattern in these locations
- To identify the hotspots and coldpsots of the suicide location.

2. STUDY AREA

Lalitpur is one of the 77 districts of Nepal and covers an area of 396.92 km^2. It is located in the Kathmandu Valley, Bagmati Province of Nepal, a landlocked country in South Asia. The total number of people in the district is 551,667 (as per the census of 2021). The district is surrounded by Kathmandu and Bhaktapur district in the north, Kavrepalanchok district in the east, and Makwanpur district in the south and west. The altitude of Lalitpur district ranges from 1000 m to 3000 m above sea level. The district includes 6 local units, which are Lalitpur Metropolitan City, Mahalaxmi Municipality, Godawari Municipality, Konjyosom Rural Municipality, Bagmati Rural Municipality, and Mahankal Rural Municipality as shown figure (Figure 1).

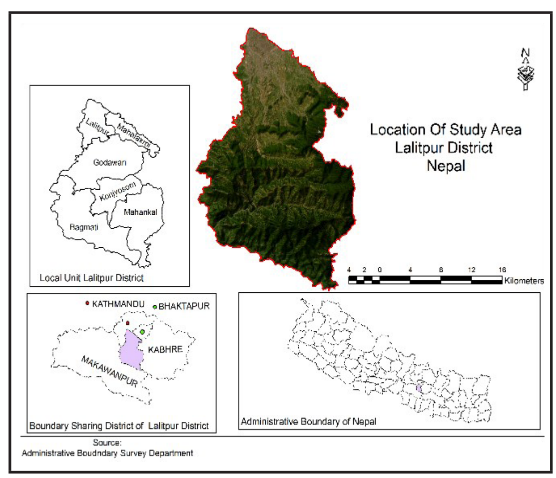

Figure 1: Study Area map.

The district has a diverse setup in terms of population distribution, as it has very densely populated regions within the Kathmandu valley as well as hilly and remote locations with sparsely populated regions. Along with this, there are only three police circles in this study area and all the incidents from these circles are aggregated by one police range making it easy to collect datasets.

3. METHODOLOGY

The methodology adopted for this research is described in this chapter. Figure 2 shows the overall methods adopted. The study involves the application of Geographic Information System (GIS) coupled with the spatial analysis techniques. The preliminary stage involved collecting data from the Lalitpur police range, which was in handwritten format. The collected data is then digitized, and the spatial locations are determined from the place names using tools like OpenStreetMap (OSM), Google Earth, and topographical base maps. These records had all the crime related events so collected data is subsequently filtered to isolate the suicide-related information. Then, spatial analysis is done on the suicide location by computing the Univariate local Moran's I and Getis ord method to compute the hotspots and coldspots. In the subsequent sections, the details are presented.

3.1 Data collection

The initial step involves collecting data from police stations, specifically in a handwritten format.

It should be noted that the DPR (District Police Range) Lalitpur records the suicides as a crime event within the study area. The crime data period covers fiscal years 2074/075 to 2079/080 (which is 2017 to 2023 AD) and specifically focuses on suicide incidents for each year. The process of gathering data for this study was to learn how many various sorts of reported crimes there were in the Lalitpur Police Range for each fiscal year. The dataset included information like the fiscal year, the precise type of crime, and the place names of the locations where these crimes took place. Official crime reports and records were used to extract the information. Once the information had been gathered, it was tabulated and structured to produce a comprehensive dataset that included both the temporal and geographic characteristics of crime occurrences. The ensuing research sought to map and examine the spatial distribution of different crime types throughout Lalitpur, and this information was crucial to that endeavor.

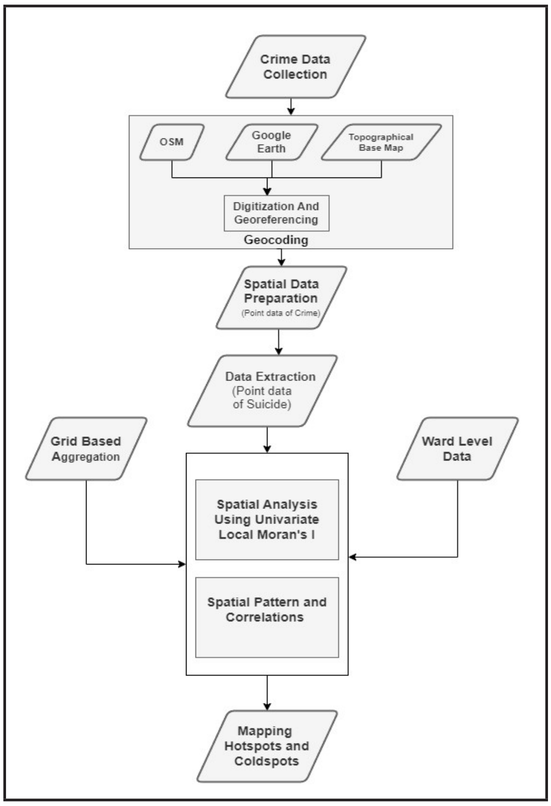

Figure 2: Overview of the adopted methodology

3.2 Geocoding

To enhance spatial analysis, Geocoding was performed manually using a combination of OpenStreetMap (OSM), Google Earth, and QGIS tools. This geocoding process involved associating precise geographic coordinates, such as latitude and longitude, with each recorded place names mentioned in the handwritten document. This meticulous geocoding effort facilitates accurate mapping and spatial analysis, enabling a comprehensive understanding of the distribution and patterns of suicide incidents across Lalitpur over the specified fiscal years.

These crime data for fiscal years 2074/075 to 2079/080 in the study area are digitized using QGIS. Figure 3 shows the spatial distribution of all the suicide incidents in the study area.

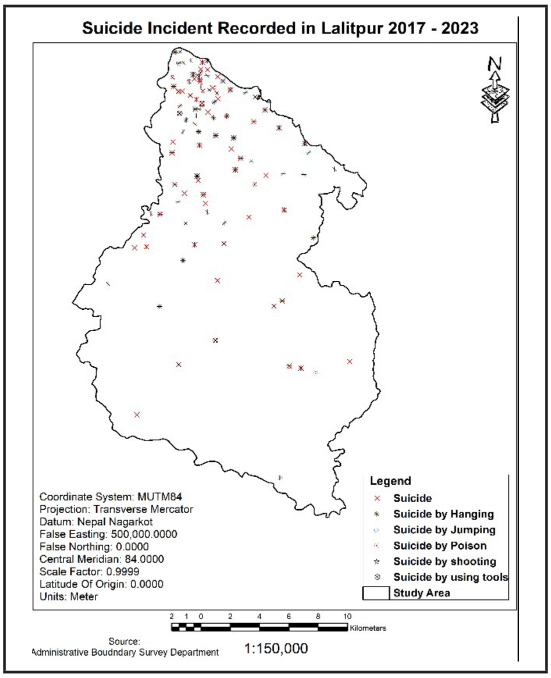

Figure 3: Suicide Incidents occurred in the study area between 2074/075 to 2079/080 BS.

3.3 Hotspot analysis

3.3.1 Hotspot and coldspots analysis

Hotspot and cold spot analysis are spatial mapping techniques used to identify clusters of high and low values, respectively, in a spatial dataset. In the context of suicide analysis, hotspot analysis pinpoints regions with significantly higher suicide rates, highlighting areas of concentrated risk. This information is crucial for targeted interventions and public awareness campaigns. Conversely, cold spot analysis identifies areas with unexpectedly low suicide rates, providing insights into effective prevention strategies and socio-cultural factors that mitigate risk. Together, these techniques offer valuable tools for understanding and addressing suicide at a community level.

3.3.2 Spatial autocorrelation

Spatial autocorrelation refers to the similarity or dissimilarity in values of a variable among nearby geographic locations. This concept is closely related to hotspot and coldspots analysis in the context of suicide research. Spatial autocorrelation quantifies the degree of clustering among these hotspots and coldspots, indicating whether neighboring areas exhibit similar suicide rates.

Local spatial autocorrelation statistics, like G statistics, focus on the relationship among the same property or magnitude across different areas. These statistics measure the local concentration or correlation among objects, providing insights into the spatial patterning of suicide risk.

Moran's scatterplot (Moran,1950) notes on continuous stochastic phenomena. Biometrika, 37(1/2), 17-23) Figure 4 classifies the nature of spatial autocorrelation into four categories, with positive spatial autocorrelation having similar values at neighboring locations, whereas negative spatial autocorrelation tends to have dissimilar values at neighboring locations. If the points in the scatter plot are clustered in the top right quadrant, it refers to some regions that has high attribute values compared to high neighboring values and so on.

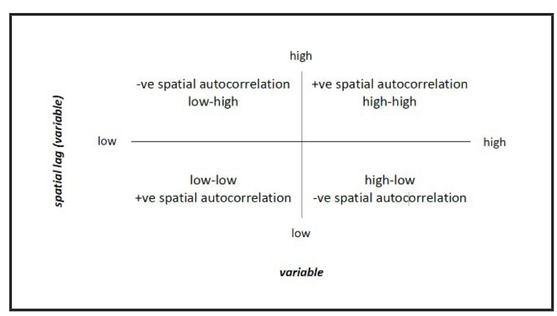

Figure 4: Moran's Scatterplot.

3.3.3 Getis-Ord

Getis-Ord Gi* (Getis,1992) is a local indicator of spatial association (LISA). LISA methods identify spatial clusters of similar values, either high or low. Getis-Ord Gi* uses a statistic called the Gi* statistic to identify clusters. The Gi* statistic is calculated for each grid cell in the study area. A positive Gi* statistic indicates a cluster of high values, while a negative Gi* statistic indicates a cluster of low values.

To compute the hotspot/coldspots the following equation of General G statistic is used:

$$G_i = \frac{\sum_{j=1}^{n} w_{ij} \cdot x_j - \bar{x} \cdot \sum_{j=1}^{n} w_{ij}}{s \cdot \sqrt{\frac{\sum_{j=1}^{n} w_{ij}^2}{n} - \left(\frac{\sum_{j=1}^{n} w_{ij}}{n}\right)^2}}] \qquad \text{(i)}$$

Where,

G_i = Getis-Ord general G statistic for location i,

n = stands for the total number of locations considered,

xj = number of suicides at location i

wij= spatial weight between locations i ∧ j

x = mean of all suicides across locations,

s = standard deviation of suicides across locations.

Z-score formula:

$$Z_i = \frac{G_i - \bar{G}}{s_G} \qquad \text{(ii)}$$

Where,

Z_i = Z – score for location i,

$\bar{G}$ = mean G statistic acreoss all locations,

s_G = standard deviation of G Statistics across all locations.

P-value formula:

$P(Z_i) = 1 - \phi(Z_i)$ *(iii)*

Where,

$P(Z_i)$ = P – value for location,

$\phi(Z_i)$= cumulative distribution function of the standard normal distribution evaluated at Zi.

3.3.4 Getis-Ord in aggregated data

Due to the lack of point coordinates for suicide locations, two aggregation methods were used for analysis: regular-shaped square grids (1kmx1km) and the lowest administrative units in Nepal. The lowest administrative units chosen were the wards of Village Development Committees (VDCs) instead of the current local levels, as the country is in a transition phase and there is still widespread understanding of VDC wards. This choice was made because VDC wards are smaller compared to the wards of the current local levels, and it was assumed that they would better represent the provided place names. A total of 436 grids covered the whole Lalitpur district as shown in Figure 5 and there are a total of 42 Village Development Committees (VDCs) encompassing 391 wards according to the old administrative boundary as shown in Figure 5.

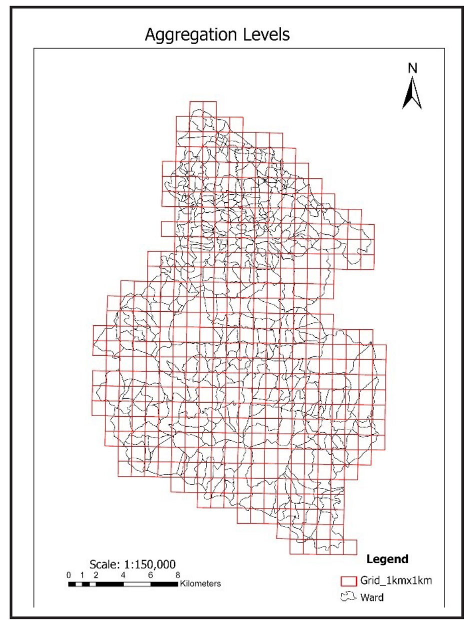

Figure 5: Grids of 1kmx1km with ward level of the study area.

4. RESULT

4.1 Exploratory data analysis

In the fiscal years 2074-075 through 2079-080, the Lalitpur police range office registered a total of 843 crime cases across 130 different locations. Among these cases, there were 562 instances of suicide, which accounts for approximately 66.66% of all the registered cases. Figure 6 illustrates the number of suicide incidents reported in each fiscal year alongside the corresponding count of unique locations. In the fiscal year 2074-2075, a total of 89 suicide incidents were documented, occurring in 14 distinct locations. Similarly, during the fiscal year 2075-2076, there were 92 recorded suicides, taking place in 19 separate locations. In the subsequent year, 2076-2077, 79 suicides were reported across 23 different locations. Moving to the fiscal year 2077-

2078, the number of suicides escalated to 108, distributed among 44 distinct locations. In the subsequent years, the pattern continues: 100 suicides in 59 locations for 2078-2079, and 94 suicides in 66 locations for 2079-2080.

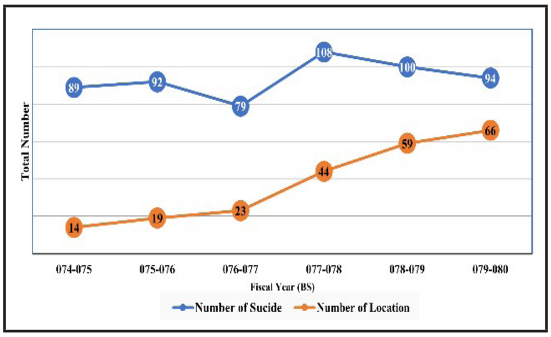

Figure 6: Suicide yearly chart.

To seek the movement, variation of variance is plotted for the time series data. The mean is 2.884422 and the maximum deviation of the mean is 9.0, which seems significant. A histogram of the data indicates that data seem slightly right skewed as well as multimodal as shown in Figure 7. This suggests the possibility of clustering in the suicide incidents.

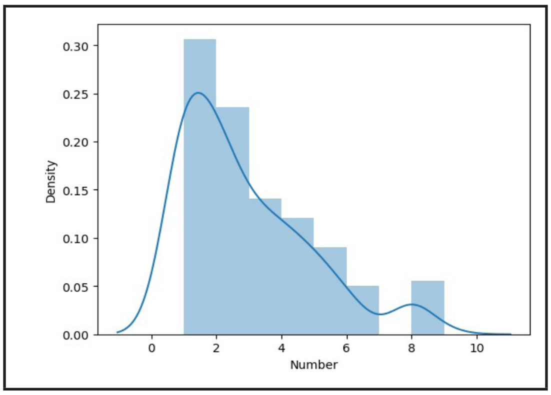

Figure 7: Histogram of Number of Suicide.

There were 562 suicide incidents recorded in the DPR in Lalitpur in 6 fiscal years. Suicide incidents are mapped with graduated symbols in which different sizes of features represent particular values of variables Figure 8.

It is evident from the spatial distribution of the suicide location that there are more suicide events in the Northern part of the district which is expected because the Northern part is a highly populated urban area whereas the southern part is a hilly region with a lower population density. Also since the southern region is more rural suicide cases may be under-reported as well.

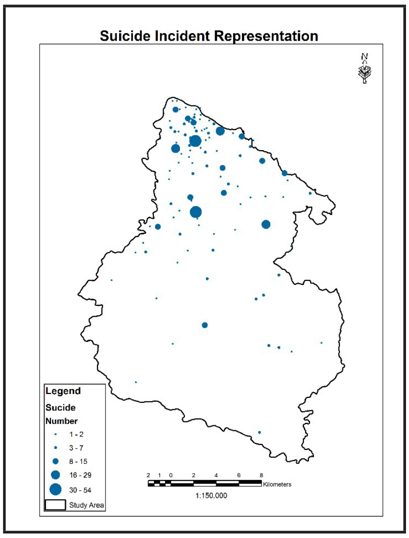

Figure 8: Area Representing Higher Rate of Suicide.

4.2 Spatial autocorrelation

In Figure 9 the Univariate Moran's I value of 0.313 in Lalitpur District's suicide data indicates a significant positive spatial autocorrelation.

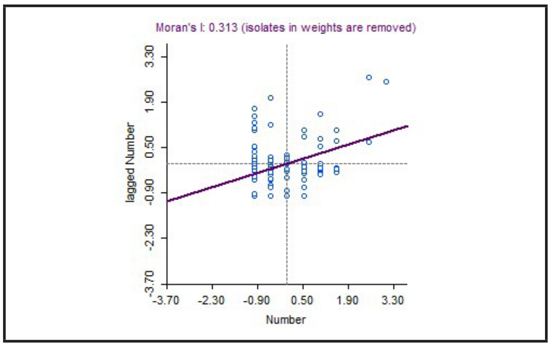

Figure 9: Univariate Local Moran's I.

This means that areas with similar suicide counts tend to be geographically clustered. The concentration of values in the upper right corner reflects the trend of high values grouping with high values and low values grouping with low values in neighboring locations. This spatial pattern has important implications for understanding the dynamics of suicide within the district, highlighting the role of geographic proximity in influencing suicide rates.

In Figure 10, the Local Indicators of Spatial Association (LISA) cluster map at the ward level is presented and the respective significance values are shown. Among these wards, 140 don't have any statistically significant (p-values greater than 0.05) spatial clustering. This implies that there is no clear pattern of neighboring regions or areas displaying similar suicide rates, suggesting a relatively random distribution across these wards.

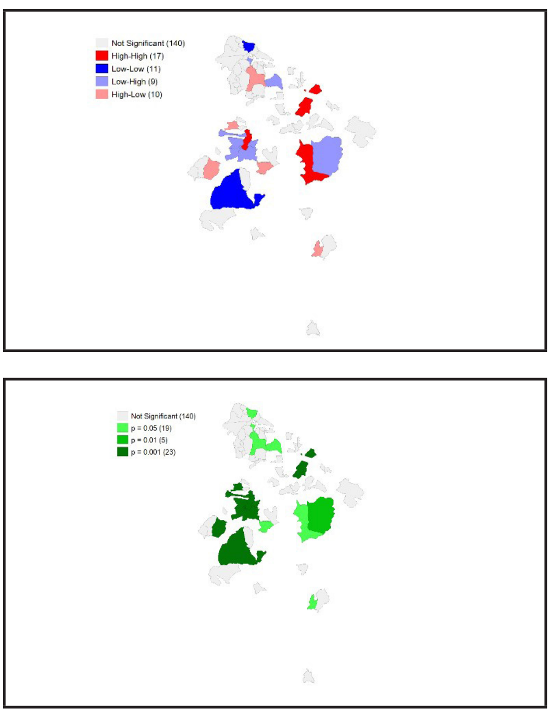

Figure 10: LISA Clusters of ward levels (top) and the respective significance level (bottom)

However, in 14 wards (significant at the 0.05 level), there is evidence of non-random clustering or dispersion of suicides. This suggests that certain areas have a higher concentration of suicide cases compared to what would be expected by chance alone. Moreover if we check at the significance level at 0.01 p value there are 5 wards with significant pattern. In these specific areas, the clustering or dispersion of suicides is particularly significant and unlikely to be attributed solely to random chance.

Overall, these findings shed light on the spatial dynamics of suicide occurrences, and highlights that there are few wards (at least 5) that have statistically significant clusters.

4.3 Hotspot and coldspots

We employed the Getis-Ord Gi* method to elucidate the distribution of hotspots and coldspots at the ward level. Our analysis revealed that within this framework, there are 7 wards categorized as coldspots. These include Bhattedanda ward 8, Harisidhi ward 9, Kaleshwar ward 2, Lalitpur sub metro ward 10, Lele ward 8, Nallu ward 8, and Pyutar ward 1. These wards exhibit relatively lower values in terms of the suicide.

On the other hand, 4 wards emerged as hotspots, signifying areas with notably higher values. These hotspots encompass Chapagaun ward 2, Godawari ward 6, Lubhu ward 4, and Lubhu ward 5. These wards showcase concentrations of the phenomenon in question that stand out from their surroundings. For a visual representation of these results, please refer to Figure 11.

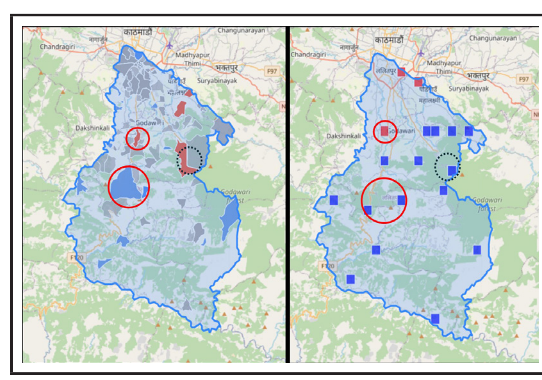

*Figure 11: Hotspots And Coldspotss at Old Ward Level (left) and at 1km*1km grids (right). Here, regions highlighted by circles are discussed in section 5.1 (Basemap: Openstreetmap)*

In the grid-based aggregation using a 1km x 1km grid to identify hotspots and coldspots within the study area, we made significant observations. Our analysis revealed 3 grids categorized as hotspots, encompassing 6 distinct locations: Asarang, Balkumari, Chyasal, Thecho, Tananitol, and Tikathali.

In contrast, our study identified 15 grids as coldspotss, each aligned with specific locations: Badikhel, Bhardeu, Bhattedanda, Bistachhap, Ghusel, Gimdi, Godamchaur, Iti Tole, Kaleshwor, Lakuribhanjyang, Nallu, Patlechhap, Pulchwok, Pyutar, and Tinpane Tower.

5. DISCUSSION AND CONCLUSION

5.1 Discussion

The study on suicide locations in Lalitpur faces challenges due to the aggregated nature of dataset. The data collected from the police stations is handwritten and includes the local name of suicide location thus it lacks precise coordinates, making it difficult to pinpoint exact suicide locations. Relying only on place names instead of actual coordinate limits the research's depth. Similarly, without detailed data, factors like demographics, socioeconomics, and culture that influence suicide rates remain unexplored. Therefore, while the study is a good start, its findings should be interpreted cautiously due to data limitations.

We have identified hotspots and coldspots using two different levels of aggregation and have observed similarities as well as differences in the identified hotspots. Figure 11 illustrates this, with solid red circles indicating similarities and dotted black circles representing dissimilarities. For instance, in both aggregation methods, the regions around Chapagaun and Thecho are identified as hotspots. However, there are discrepancies such as the ward near the Godawari forest being classified as a hotspot while the surrounding grids are considered coldspots. This demonstrates the significant impact of aggregation levels on such analyses. Therefore, we recommend carefully selecting the aggregation levels when performing hotspot and coldspots analyses.

Similarly, the temporal dimension was not considered in this study; all suicides were aggregated at the end of the study period, i.e.the 2078-79 fiscal year. Therefore, a future study could investigate the temporal dependencies associated with each of these suicide cases. Conducting spatio-temporal hotspot analysis would be a valuable approach to explore these dynamics.

5.2 Conclusion

In this study, we conducted an analysis of suicide locations in the Lalitpur district of Nepal, utilizing Geographic Information System (GIS) techniques and spatial analysis methods. The aim was to map suicide incidents, identify spatial patterns, and pinpoint hotspots and coldspotss within the study area.

The findings reveal several key insights into the distribution and clustering of suicide incidents. Over a span of six fiscal years (2074/075 to 2079/080 BS), a total of 562 suicide cases were reported, accounting for approximately two-thirds of all registered crime incidents in the Lalitpur police range. Exploratory data analysis demonstrated a concentration of suicide events in the northern, more densely populated areas of the district, compared to the sparser southern regions.

Spatial autocorrelation analysis using Univariate Moran's I indicated a significant positive spatial autocorrelation in suicide rates, revealing geographic clusters of similar suicide counts. Local Indicators of Spatial Association (LISA) cluster maps further highlighted statistically significant clusters of high and low suicide rates at the ward level, with specific areas exhibiting non-random spatial clustering.

Hotspot and coldspots analysis using the Getis-Ord Gi* method identified distinct wards and 1km x 1km grids as hotspots and coldspotss, underscoring areas with notably higher or lower suicide rates relative to their surroundings. The study revealed differences in hotspot identification based on aggregation levels, emphasizing the importance of careful consideration in spatial analysis.

Despite these insights, the study encountered challenges due to the aggregated and handwritten nature of the dataset, limiting the precision of location data and hindering deeper exploration of underlying socio-demographic factors influencing suicide rates. Future research should aim to incorporate finer-scale data and explore temporal dependencies to enhance understanding of suicide dynamics in the study area. In conclusion, this study contributes valuable spatial perspectives to the understanding of suicide patterns in Lalitpur district, Nepal. The findings underscore the importance of targeted intervention strategies and public health initiatives aimed at addressing suicide risk factors in specific geographical areas, thereby supporting efforts to promote mental well-being and prevent future suicides within the community.

ACKNOWLEDGEMENT

We extend our sincere thanks to all contributors and stakeholders involved in the completion of our research on mapping and analysing suicide locations in Lalitpur, Nepal. Special appreciation goes to Jawalakhel Police Station and Kathmandu Valley Police Office for their support and provision of necessary information and resources.

REFERENCES

Johnson, B. D. (1965). *Durkheim's one cause of suicide.* American Sociological Review, 875-886.

Getis, A., & Ord, J. K. (1992). *The analysis of spatial association by use of distance statistics*. Geographical Analysis, 24(3), 189-206.

Moran,P.A.P.(1950). *Notes on continuous stochastic phenomena*. Biometrika, 37(1/2), 17-23.

S Karthick and S Barwa (2017). *A review on theoretical models of suicide*. International Journal of Advances in Scientific Research.

Solange N´u˜nez-Gonz´alez, A Gabriela Lara-Vinueza, Christopher Gault, and J Andr´es Delgado-Ron (2018). *Trends and spatial patterns of suicide among adolescent in ecuador, 1997-2016*. Clinical Practice and Epidemiology in Mental Health: CP & EMH, 14:283.

Spotlight Nepal (2022). *Suicide rate has increased 72 percent in Nepal.* https://www.spotlightnepal.com/2022/09/26/suicide-rate-has-increased-72-percent-nepal/. (Accessed: August 27, 2023).

Too, L. S., Pirkis, J., Milner, A., & Spittal, M. J. (2017). *Clusters of suicides and suicide attempts: detection, proximity and correlates*. Epidemiology and psychiatric sciences, 26(5), 491–500.

World Health Organization (WHO) (2023). *Suicide*. https://www.who.int/news-room/fact-sheets/detail/suicide. (Accessed:August27,2023).

Author's Information

Name	:	Er Dinesh Khatri
Academic Qualification	:	BE in Geomatics
Organization	:	Survey Department
Current Designation	:	Surveyor
Work Experience	:	6 years
Published paper/article	:	1

Nepal Remote Sensing and Photogrammetric Society (NRSPS)

Executive Committee

Susheel Dangol, *President*
susheeldangol@gmail.com

Er. Sanjeevan Shrestha, *Vice President*
shr.sanjeevan@gmail.com

Er. Janak Parajuli, *Secretary*
janak.parajuli1@gmail.com

Raj Kumar Thapa, *Assistant Secretary*
thapark2013@gmail.com

Er. Tina Baidar, *Treasurer*
tina.baidar13@gmail.com

Members
Dr. Chhabilal Chidi
chidichhabilal@gmail.com

Jagat Raj Poudel
jagatrajpoudel@hotmail.com

Roshani Sharma
anjarija@gmail.com

Girija Pokharel
girija.pokhrel12@gmail.com

E-mail: nrspsociety@gmail.com

Earth Observation Newsletter:

Editorial Board

Pravesh Yagol, *Editor-In-Chief*

Prabesh Shrestha, Member

Shanker K.C., *Member*

Thakur Lamichhane, *Member*

The society begin its activities for current fiscal year by providing its vote in capacity of country member of International Society for Photogrammetry and Remote Sensing to change the Ordinary Membership name of Spain and Vietnam, and Associate Membership of Kenya. It conducted a Feature Extraction Challenge aimed at existing graduate and undergraduate students at various universities. With the aim of generating funds, it also organized a Friendly Futsal Tournament on Ashwin 11, 2080 for the first time and awarded the top two teams along with top performers with medals, trophy, and certificates. It conducted its Annual General Assembly on Ashwin 17, 2080 where annual progress and budget were presented, and upcoming plans were decided. The society also declared to support the research activities of existing graduate and undergraduate students by providing a Research Grant gross sum of NPR 50,000/-.

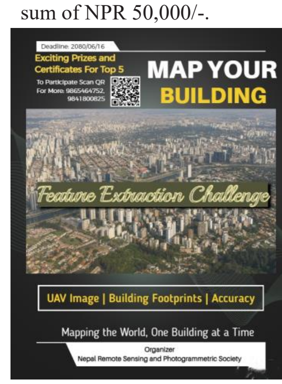

In collaboration with Kathmandu University Geomatics Engineering Society, the society provided a three-day training on Google Earth Engine to the Geomatics Engineering students during Dec 21-23, 2023. President of the society, Mr. Susheel Dangol and executive members participated in the 7th Global Surveyor's Day, organized by Nepal Institution of Chartered Surveyor and Survey Department on 21st March 2024 (8th Chaitra 2080).

Twelfth issue of "Earth Observation" newsletter is also planned to publish this year which will be made available to www.nrsps.org.np.

Modified One-Point-and-Area Algorithm for Sub-division of Irregular Parcels

Amrit Karmacharya[1], Janak Parajuli[1], Shrisha Makaju Shrestha[1]
akarmacharya8@gmail.com, janak.parajuli1@gmail.com, makajushrisha@gmail.com
[1]Survey Department

KEYWORDS

Polygon Sub-division, Irregular-shaped parcel, One-point-and-area, Land parcels, Cadastre, Concave parcel

ABSTRACT

Parcel sub-division is a crucial part of the Land Administration, and its techniques depend on the user requirements and other constraints. Splitting of a parcel based on a given area is one of such constraints whose subdivision has been popularly carried out using the trial-and-error method which is less accurate and time-consuming. For more accurate and direct subdivision, Habib developed algorithms based on popular eight cases. Among them, when the area to be split is known, a point or line is selected as a reference. In case if it has to be a point, then a one-point-and-area method is used for subdivision while a move-line-and-area method is used if line segment is used as reference. It was found that Habib Algorithm worked well for convex shapes, however it could not account for the concavity of irregular-shaped parcels. It was found that the approach for the calculation of the area considered only the cases of convex shapes. Therefore, the researchers observed the issues of clinging and retracting were identified. Thus, this study proposes an effective algorithm for the division of an irregular parcel using an improved version of One-Point-and-Area method used in Habib Algorithm. An additional stage of generating a convex hull was introduced to guide the iteration process, the formula to calculate area was adjusted to compute only the interior area and finally, the determination of the partition polygon was also done through an iterative improvement process rather than the existing one-step process. Experiments showed that the proposed algorithm accurately divided both irregular-shaped parcels and convex parcels. In the case of convex parcels, the result was found to be the same as Habib's method. Due to the addition of an extra stage of generating a convex hull and extra iterations in the final stage, the proposed algorithm consumed more time. However, it was found negligible in regard to the volume of parcels involved in splitting at a time. Overall, the proposed algorithm accurately solved the issues of clinging and retracting irregular polygons and without changing the results in convex polygons. So, it was concluded to be a suitable replacement of Habib Algorithm, and its implementation will provide more accurate results in parcel sub-division problems.

1. INTRODUCTION

Land partition involves dividing large pieces of land into smaller parcels based on specific requirements. Ideally, the parcel is staked out on the ground (Habib, 2020) and land professionals draw plans according to the measurements taken from the ground which are provided to legal offices (land revenue office and survey office) for authorization. However, practically, landowners first split the parcel shape in maps and stake out them on the ground accordingly. This splitting is done commonly using the following guidelines and tools for land subdivisions. (Easa, 2008)

1) Partition line goes in a direction through a specific point (One point and Line method).
2) The partition line goes through two specific points (Two points/Join Points method).
3) The partition line runs through a determined vertex and cuts a specified area (One-Point-and-Area method).
4) The partition line starts in a supposed direction and cuts a fixed area (Move line cut area).
5) The partition line starts in a supposed direction and fixed distance from an edge (Offset distance from edge method)

While using each one or a combination of the above methods, technical professionals generally carry out either the trial-and-error method or the direct method. The trial-and-error procedure assumes a tentative partition line and then establishes the exact one by relying on an iterative approach (Habib, 2020). It is a time-consuming approach susceptible to human errors. Direct methods determine partition lines using geometric and trigonometric characteristics where points are considered to have 0-dimensionality, lines have 1-dimensionality, and polygons have 2-dimensionality. This method has a variety of tools and approaches for subdivision although it is not always guaranteed to give the required results. The cases of parcel sub-division where the partition line (1-dimensionality) is determinable using points (0-dimensionality), angles (1-dimensionality), or their combination (e.g. One point and line, Two Points, offset distance from edge) can be handled by simple trigonometric calculations. However, the sub-division where a required area is given (2-dimensionality) and the partition line (1-dimensionality) is to be determined such that one of the split areas equals the input area is tricky, although in some cases, it might be the only method applicable. Take a parcel to be split into two halves for inheritance purposes for example. Here, the original and required areas are known and a common point is selected to provide road access to before splitting the parcel. Now, the task is to find a point on the other side which will divide the original parcel in half. Unlike tools such as Join Points, One point and a line, and offset distance where desired output can be achieved in a single operation, the One point and area and move line and area tools require some hit and trial operations before finding the desired output.

1.1 Background

Parcel sub-division is a spatial operation and the shape of the polygon is an important factor impacting its efficiency (Zhang et al., 2021 In the real world, parcels with arbitrary shapes such as being (1) (Habib, 2020), highly irregular, complex, concave, or convex, self-intersecting, or even hollows can be found. As seen in Figure 1, categorically, the parcels can be distinguished into four groups (Cogo et al., 2023) rectangular, axis-aligned, convex, and irregular.

The rectangular shapes have exactly four edges and all their angles are 90°. Axis-aligned shapes, as the name suggests, are seemingly aligned with either of the axes (X, Y, or Z) and can have angles dividable by 90°. All angles in convex polygons are always smaller than or equal to 180°. Other shapes not belonging to the above categories are irregular-shaped parcels. In this research, a concave-shaped parcel is treated as an irregular one.

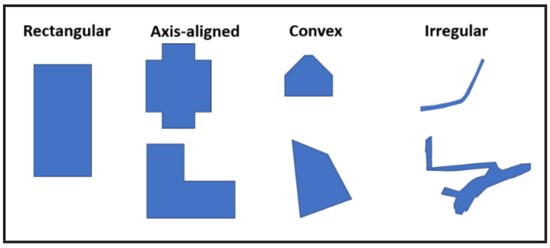

Source: Cogo et al., 2023

Figure 1: Categorization of Shape

The suggested algorithm determines the location of vertices at various partition levels. It is a straightforward, precise process and only requires the coordinaters for the peoperty corners. Among the eight scenarious, one is where the partition line runs through a determined vertex and cuts a specified area. This scenario is also knbown as the One-Point-and-Area mehtod.

As shown in Figure 2, coordinates P_1, P_2…. Pn represent a tract of land for which the coordinates of each point are known. Line P_1P' passes through point P_1 and intersects the polygon at point P' to separate the tract into two parts. It is required to compute the coordinates of the point, where the clipped part (shaded polygon) has the required area, A_S. In this case, the remaining triangular area A_1 is solved by subtracting the area of a portion A_2 from the area of the shaded part, which was specified only by the known vertices.

$A_1 = A_S - A_2$ (i)

For $A_1 > 0$, using their coordinates, the distance between the points P_1 and P_4 is computed by (Habib, 2020)

$$d_1 = \sqrt{(x_{p_1} - x_{p_4})^2 + (y_{p_1} - y_{p_4})^2} \quad \text{(ii)}$$

Then distance d_1 is obtained from equation 3. Once, d_1 and bearing of P_4P_5 is computed Coordinates of P' can be determined.

$$A_1 = \frac{1}{2}(d_1 d_2)\sin\theta \Rightarrow d_1 = \frac{2A_1}{d_2 \sin\theta} \quad \text{(iii)}$$

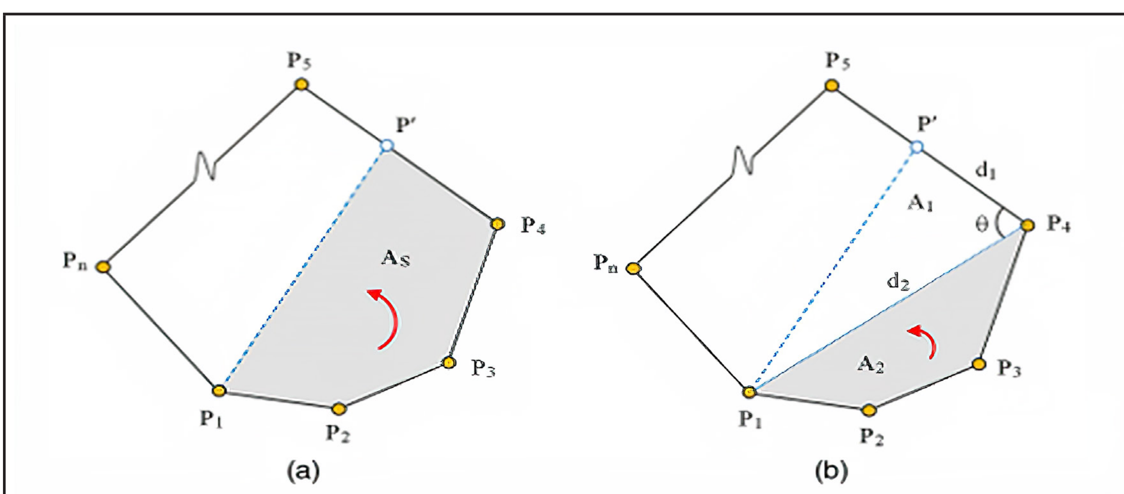

Source: Habib, 2020

Figure 2 Steps in One point and area method

1.2 Statement of the problem

In the One-Point-and-Area method, the Habib algorithm uses the SAS (Side-Angle-Side) formula for area calculation of convex-shaped polygons and modifies it to determine the distance d_1 from the vertex. However, when the partitioning line is passed through a concave section, the Habib algorithm does not give the required result. Splitting of the concave section in parcels was found to be suffering two issues, namely the issue of clinging and the issue of retracting.

Consider a clinging case of an axis-aligned parcel for example as in Figure 3. The triangle $P_1P_2P_3$ covers 250 sq. units., when it must be split by areas less than 250 sq. units such as 100, the resulting polygon was found to be clinging along line P_2P_3 as observed in Figure 3a. This might be the desired result in some cases, although the solution can be as in Figure 3d in other cases. On the other hand, for split areas greater than 250 sq. units such as 300, the resulting polygon was found to be retracting along line P_3P_4. This result was found incorrect for two reasons, first, the result was self-intersecting. Second, the result included a portion outside the original polygon. The expected solution for this case should be as presented in Figure 3e.

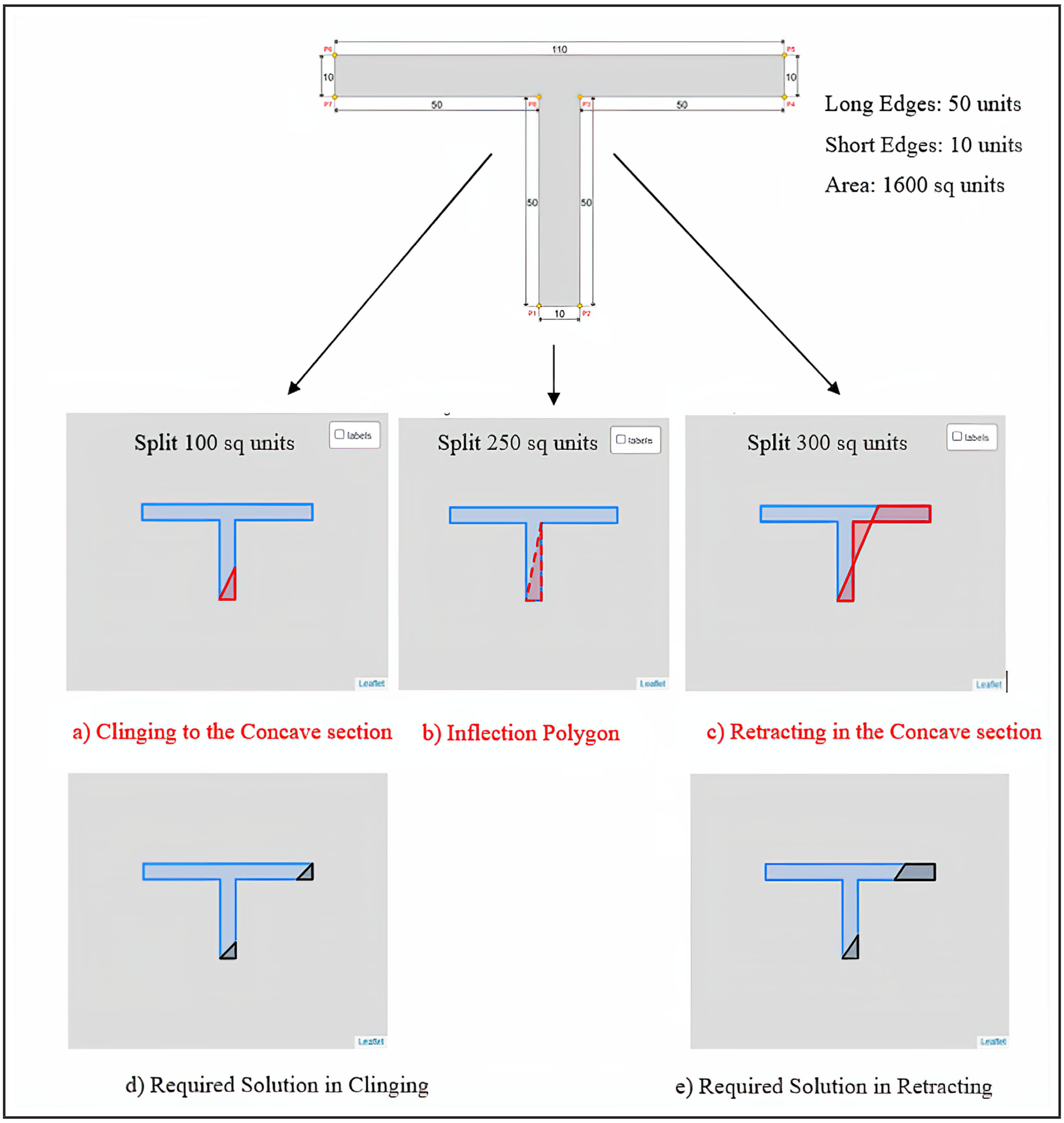

Figure 3: Problems in the Concave Section

1.3. Research objectives

The main objective of this project is to formulate an algorithm for the One-Point-and-Area method to accurately split an irregular-shaped polygon given a required area. In addition to this, the research is attempting to address the following research questions: -

1) How does the existing algorithm perform parcel subdivision in cases of irregular-shaped parcels, particularly the concave-shaped ones?
2) How can existing algorithms be improved to address the issues raised by irregular-shaped parcels, namely the clinging and retracting cases?

1.4 Significance of the study

In practice, while splitting parcels either using trial and error or direct method, two issues of high concern were found. When the trial-and-error method was followed, the professionals lacked the necessary tools due to the specific nature of splitting tasks. As already mentioned, this was normally time-consuming and susceptible to human errors. On the other hand, the direct method was also found to have its shortcomings. This method which employs trigonometric concepts, was found fast and accurate on normal convex parcels, it could not produce accurate results when the shape of the parcel was irregular. Apart from this, irregular-shaped parcels were also observed to bear legal and practical complexities such that the time and effort required in the trial-and-error method seemed justifiable. Hence, an alternative approach for sub-dividing irregular-shaped parcels was not found to be prioritized. In addition, to the knowledge of the author, very limited, if not no research has been done which could accurately split all the cases of irregular-shaped parcels. The authors believe that there is a necessity for such a method which can generate more accurate results efficiently than existing algorithms.

As such, the application of this research is expected to be significant for the following.

1) The proposed algorithm can accurately split both regular and irregularly shaped parcels.
2) In some specialized cases of irregular parcels where the retracting edge caused an error, the proposed algorithm removes those errors.

2. LITERATURE REVIEW

There a few research on parcel sub-division one of which is the "Proposed Algorithm of Land Parcel Sub-division" by Maan Habib (Habib, 2020). It focuses on the algorithm and steps for parcel subdivisions in land surveying and the legal change of property boundaries. The proposed algorithm provides a simple and relatively accurate solution for land partitioning using closed-form and direct procedures. The mathematical model is based on the coordinates of parcel vertices and specific constraints to fulfill site requirements. Another study, Zlatanova et al. (2014) related to land parcel sub-division is "SpaceSub-divisionTestbed: A Graphical Tool for Arbitrary Shaped 2D Polygon Sub-division" which provides methods and graphical tools for sub-division of both regular and arbitrary shapes (Cogo et al, 2023). The tool provides support for indoor applications and offers a practical approach to handling sub-division problems.

To the knowledge of the authors. scientific studies dealing with the automated partitioning of the process of parcel sub-divisions using vector data format are scarce. In an early work, Wakchaure (2001) created a standalone GIS tool to create a sub-division layout at the single parcel level for build-out analysis. The tool partitioned a parcel into subplots recommending a possible pattern for development, but it was not automatic, and the accuracy was also unreliable. In another research, Stevens et al. (2007) hinted at the development of an algorithm for automatically creating small land parcels which could be integrated into the vector-based City model of urban growth. An agent-based model of urban growth called Agent City, embedded a land sub-division module into its upgraded version of model (Jjumba & Dragićević, 2012). They stated that the module would initially divide the larger land parcel into city blocks and then the blocks into cadastral lots. Land Parceling System (LandParcelS) designed as a GIS-based software module during land consolidation integrated support system (LACONISS) for land planning and decision making (Demetriou et al, 2012). LandParcelS automates the process of parcelization, generating a set of new parcels that represent an alternative plan for land reallocation. The system generates new parcels based on optimization of their shape, size, land value, and road access. However, it is not capable of creating roads and is also inappropriate for subdividing parcels into city blocks and then city blocks into housing lots. Wickramasuriya et al. (2011) developed a GIS-based sub-division tool capable of generating urban sub-division layouts including both streets and lots. The tool carries out the partition of both rectangular and irregularly shaped parcels aiming to optimize the output by creating the highest number of lots and the lowest number of streets possible. Yet the model does not offer options for different sub-division styles and performs poorly in terms of shape and size of resultant lots adjacent to the boundary of irregular parent parcel. The tool cannot extend the road network if the candidate parcel is disjointed from the existing roads.

In addition, the authors found a few other procedural modeling tools that perform automatic polygon sub-division. These tools apply sub-division algorithms on a variety of input spaces. A circumscribed rectangle structure was used for diagonal polygon sub-division by Nikanorova and Romanovsky (Nikanorova & Romanovsky, 2020). Mkrttchian et al. (2023) proposed a trigonometric algorithm for subdividing non-convex polygons into sets of convex polygons. Vanegas et al. (2009) performed parcel sub-divisions using oriented bounding boxes. Dahal and Chow (2014) introduced a GIS toolset for the automatic subdivision of parcels. The toolset performs sub-division by using bounding boxes and contains special divisions for irregular T- and L-shapes. Adao et al. applied a rule-based approach using bounding boxes for the automatic sub-division of building interiors (Adao et al., 2014). They later extended this approach to irregular shapes in a tool by performing the fake-concave technique, which allows the user to specify parts of convex shapes as disposable parts for deletion after the sub-division is complete (Adao et al., 2014).

3. METHODOLOGY

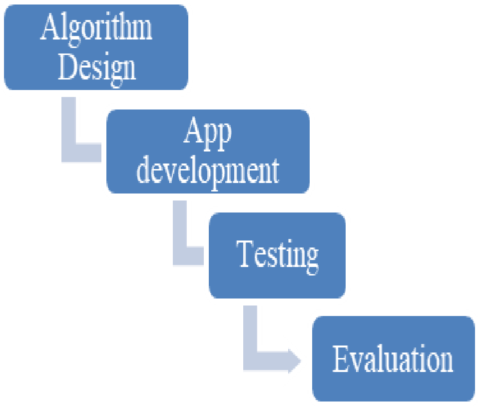

Figure 4: Workflow Diagram

This study modifies the existing Habib One-Point-and-Area algorithm to address the issues arising in subdividing irregular-shaped parcels. We add a guiding layer in the algorithm and upgrade the One-Point-and-Area metho, addressing the problems with clinging, retracting, and interior area calculation during the sub-division process.

3.1 Working model

The existing Habib algorithm was acquired from and reconstructed using HTML/CSS/Javascript.

3.2. Data

A dataset was created by collecting existing examples from the literature and creating new data. The data was formatted in GeoJSON format since it is the popular human readable industry standard (Fosci & Psaila, 2023).

3.3 Algorithm design

The Habib algorithm was found to be lacking a method to handle concave sections of parcels. It used two formulae namely SAS and Shoelace or Gauss to calculate areas which do not correctly account for retracting cases of concave section. SAS formula was found to include exterior area i.e. the area falls inside the triangle but outside the polygon whereas, Shoelace considered exterior area as negative and hence over-compensated the value while determining a new point. This is why the Habib Algorithm could not compute areas accurately upon using both formulae.

Hence, this research is focused on modifying Habib's One-Point-and-Area algorithm to accurately handle concave sections. The algorithm could be divided into three stages:

1) Collect input and Initialization by rearranging the vertices such that the input point was at the start of the polygon vertices list and the verticeswere arranged anticlockwise.
2) Iteratively refining to Find the Last Partition Polygon and determining the pair of vertices in which the required point lies.
3) Finally calculate the exact partition point and generate the desired polygon result.

The mentioned issues arose in the second stage as the iteration was guided by each edge respectively. The algorithm did not have any way to detect concave sections, and the issues were exacerbated as the said formulae for area calculation did not handle concave sections as well.

To solve this problem, three modifications were made. An additional stage to generate a convex hull was added after the first stage which was used during iteration to find the pair of vertices where the new point should lie. Another modification made was in the approach of calculating the area by improving it such that it only gave the interior area, thereby rectifying the errors made by SAS and Shoelace or Gauss formulae, finally the last stage to generate the desired polygon was done iteratively. Thus, we propose an improved version of the Habib algorithm that consists of four stages.

1) Same as Habib Algorithm

2) Generating a convex hull which guides the third process. If the start point did not lie on the convex hull, then it was added at the start of the convex hull.

3) Determining the pair of vertices upon which the required point was supposed to lie. For this, an iterative approach was used to form an initial partition polygon using the first three vertices of the convex hull. The intersection of the formed polygon and the original polygon gave internal area. If the area of the intersection was less than the required area, another vertex from the convex hull was appended to the end of the partition polygon, and the process was repeated.

4) Finally, the partition polygon was improved using the same technique as in the Habib algorithm. With the information on the LastPartitionPolygon and the area difference, the Habib algorithm was used to find a new vertex. The SAS formula included the exterior area, although only the interior area was necessary which made the exterior area greater than the interior area. As the area and distance were inversely proportional, the computed distance was minimized which meant the new point was still not correct. Hence, an iterative approach was employed to minimize the difference by appending the new vertex to LastPartitionPolygon and re-computing the interior area until the area was accurate.

3.4 Overview of algorithms

Habib One-Point-and-Area Algorithm	Proposed One-Point-and-Area Algorithm
1. Get input and rearrange vertices. 2. Iterate over vertices to find the last partition polygon. 3. Derive partition polygon	1. Get input and rearrange vertices. 2. Generate convex hull and identify vertices on convex hull. 3. Iterate over convex hull to find last partition polygon. 4. Iterate to derive partition polygon

Table 1 Overview of Algorithms

Algorithm: **Proposed One-Point-and Area**

Input: {**polygon**: [list of coordinates of corners $P_0P_1P_2\ldots P_n$],
A_s: Required Area,
P_s: Start Point}

Output: Partition Polygon

1: Initialize
- 1a. Polygon = rearranges vertices such that P_s is at start and vertices are anticlockwise,

2: Make Convex Polygon
- 2a. Generate Convex Hull $[C_0C_1C_2\ldots C_n]$
- 2b. If P_s not in Convex Hull, add P_s in convex hull
- 2c. LastPartitionPolygon = [polygon of convex hull $P_sC_1C_2$],
  I = Intersection of LastPartitionPolygon and original Polygon
  A_2 = interiorarea of I,
  $P_{Last} = C_{2,}$
  $P_{Next} = C_3$

3: Find Last Partition Polygon
- 3a. $A_1 = A_s - A_2$
- 3b. If $A_1 = 0$, I is required polygon, goto 4g
  $A_1 < 0$, add next vertex from convex hull to LastPartitionPolygon. Update A_2, P_{Last} P_{Next}. goto 3a
  $A_1 > 0$, goto 4

4: Derive Partition Polygon
- 4a. d_2 = distance (Ps , P_{Last})
- 4b. Θ = angle $P_sP_{Last}P_{Next}$
- 4c. $d_1 = 2 * A_1 / (d_2 * \sin\Theta)$
- 4d. $X_{p'} = X_{plast} + (X_{pnext} - X_{plast})*d_1/$ distance $(P_{Next} - P_{Last})$
  $Y_{p'} = Y_{plast} + (Y_{pnext} - Y_{plast})*d_1/$ distance $(P_{Next} - P_{Last})$
- 4e. $P' = [X_{p'}, Y_{p'}]$
  PartitionPolygon $= [P_sC_1C_{2\ldots}\ P_{Last}\ P']$
  I = Intersection of PartitionPolygon and original Polygon
  A_3 = interiorarea of I,
- 4f. $A_1 = A_s - A_3$
- 4g. If $A_1 = 0$, I is required polygon
  $A_1 < 0$, goto 4c

Algorithm 1 Proposed One-Point-and-Area Algorithm

3.5 Software interface design

Both Habib and the proposed algorithm were designed and implemented in an HTML/CSS/Javascript application using Leafletjs and Turfjs on local server. The software had three map views: first view for presenting results from Habib algorithm, second one for results from proposed algorithm, the final one for overlapping results from both algorithms for visualization and differentiation. Test polygons were preloaded in a GeoJSON file which could be selected from the "Select Polygon" dropdown. After the selection of a polygon its total area was displayed, and the polygon vertices populated the "select point" dropdown menu. Selecting Point and entering required area (less than polygon area) and clicking "Perform Split" displayed the results in the map views. The map views were synchronized allowing the zoom or pan tasks on one of the views were synchronized to other views respectively.

3.6 Testing and analysis

As mentioned previously, the application was tested using a test polygon as a sample. For simplicity in area calculation and verification, a T-shaped axis aligned figure was used as a case of an irregular polygon. Being a geometrical figure, it was easy to verify the area and polygon as well as it also provided the concave sections. The shorter edges were 10m and the longer edges were 50m long. The WKT representation of the polygon was:

Polygon ((0 0, 0 50, -50 50, -50 60, 60 60, 60 50, 10 50, 10 0, 0 0))

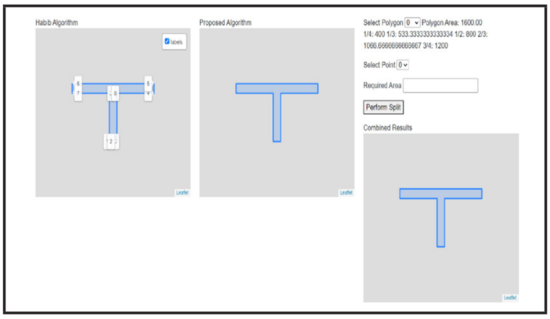

Figure 5: Software Interface

It consisted of 8 vertices and 8 edges with a total area of 1600 sq. m. and a perimeter of 340 m.

Case Study

Case 1: No clinging and no retracting

Taking the lower left point (1) as the selected point and the required area to be 40 sq. m., the outputs from the two algorithms were found to be the same and accurate (Figure 6) as concave section in this case only affected areas more than 47 sq. m

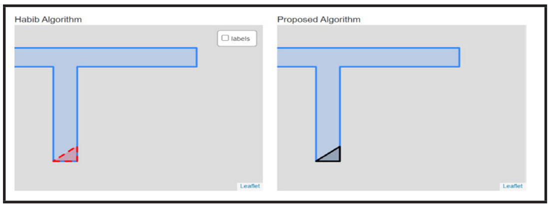

Figure 6 Output at Required Area 40 sq.m.

Case 2: Clinging Parcels

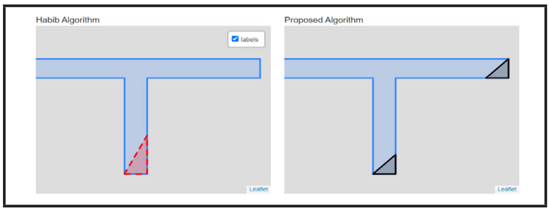

Figure 7: Output at Required Area 100 sq. m.

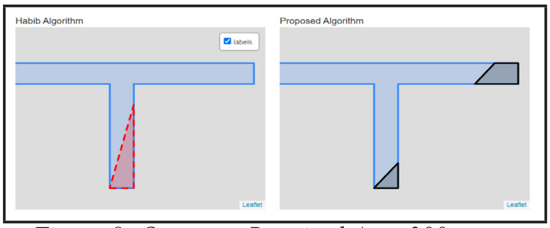

Figure 8: Output at Required Area 200 sq. m.

Again, taking the lower left point (1) as the starting point and this time area is 100 sq. m., the area computed by both algorithms was found to be different (Figure 7). The Habib algorithm could not remove the clinging, while the proposed algorithm successfully removed it.

In addition, if the required area was changed to 200 sq.m., then the proposed algorithm just followed correct the polygon edges.

Case 3: Retracting Parcels

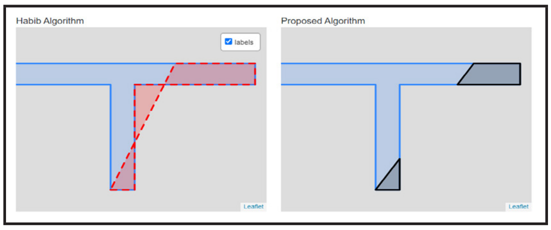

Figure 9: Output at Required Area 300 sq. m.

In this case, to split 300 sq.m, the Habib Algorithm could not acknowledge the concave section in contrast to the proposed algorithm (Figure 9). The output from the Habib Algorithm was found to be inaccurate since the polygon was intersecting with itself and part of it lay outside the original polygon. Since the result of the proposed algorithm was accurate, this case depicts the advantage of the proposed algorithm over the Habib Algorithm.

4. RESULT AND DISCUSSION

4. 1 Experiments and observations

Experiments were carried out on the sample polygons from the dataset with the required area for subdivision taken as 1/4th, 1/3rd, 1/2, 2/3rd, 3/4th of the parcel area as they were the most common in inheritance cases. Points were selected randomly, and consideration was made such that the sub-divisions were roughly equitable. To evaluate the difference in result, the angle made by the partition line with the parcel was computed. The base of the angle was the line joining selected point and the second vertex (first vertex is the selected point itself) on the convex hull of the parcel. Although the Habib algorithm did not require a convex hull, it was considered here to make it comparable with the proposed algorithm. All the angles were considered in degrees.

1) Selected point: 1, Selected Polygon: 2

Figure 10 displays clinging issue in a parcel with an inner cavity along vertices 15-21.

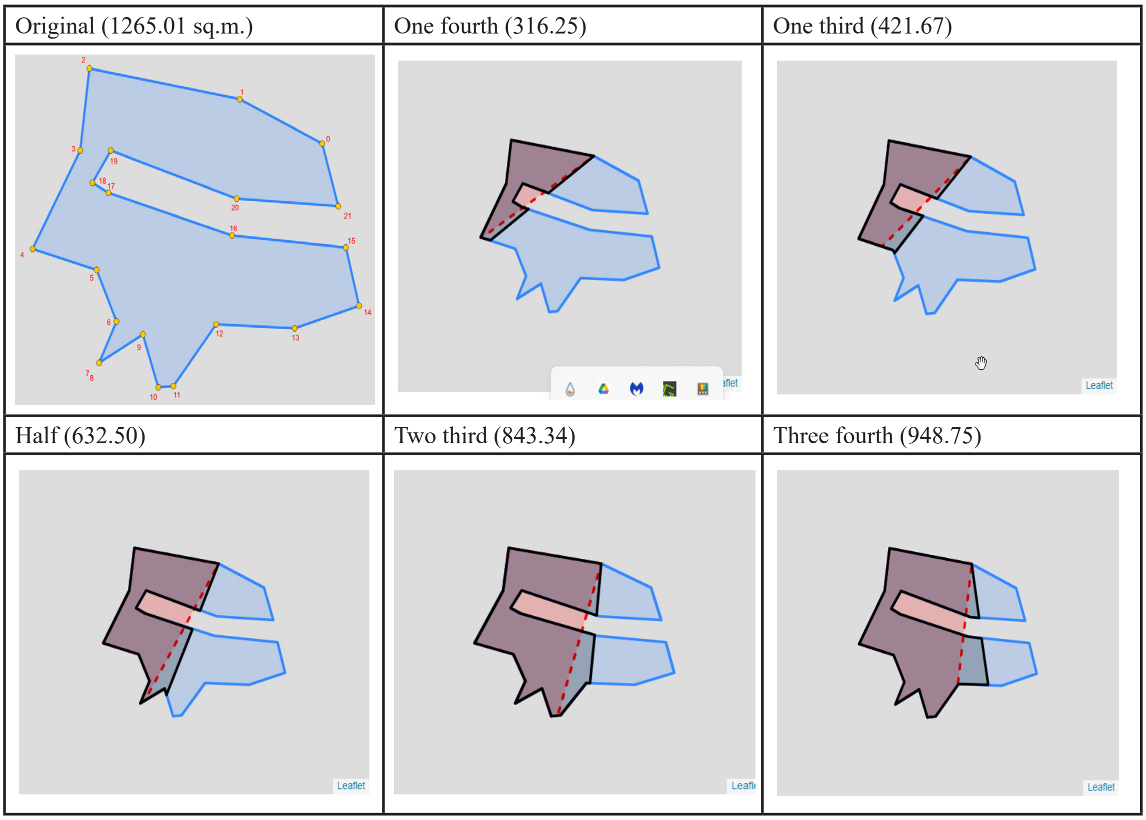

Figure 10 : Subdivision on First Irregular Parcel

Area computation using Habib algorithm included portion inside this cavity in contrast to the proposed algorithm which successfully excluded it. This can be observed visually.

3) Selected point: 17, Selected Polygon:6

Parcel in Figure 11 contained much irregularity. The point for sub-division was selected such that both cases of clinging and retracting could be observed. On splitting 1/4th and 1/3rd of the parcel area respectively, clinging was observed because of which the partition line in Habib Algorithm moved forward. The retracting issue was seen in case of splitting half area of the parcel which is discussed in the section to come. Clinging along convex section were observed while splitting the 2/3rd and 3/4th area were, the partition line in Habib Algorithm remained backward since it included the exterior area as well. In contrast, the proposed algorithm compensated for this by moving forward.

4) Selected point: 10, Selected Polygon: 8

In Figure 12, while splitting 1/4th and 1/3rd of parcel area, retracting issue was noticed. In these retracting cases, Habib algorithm considered the exterior area as negative since they were self-intersecting. This negative area was then compensated by forward moving partition point. In the case of splitting half of the parcel, both cases of retracting and clinging on convex section were detected. The exterior area of clinging was greater than the exterior area of retraction. This made partition point move forward making angle difference positive. Overall, it can be observed that the proposed algorithm addressed the clinging issue in both concave and convex sections as well as the retracting issue. It provided accurate results in all cases while Habib Algorithm could not accurately address the above issues

Original (2882.08 sq.m.)	One fourth (720.52)	One third (960.69)
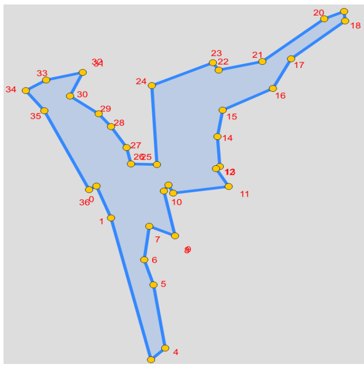	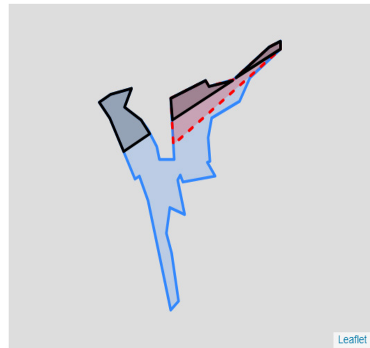	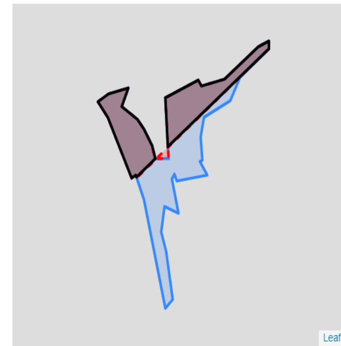
Half (1441.04)	Two third (1921.38)	Three fourth (948.75)
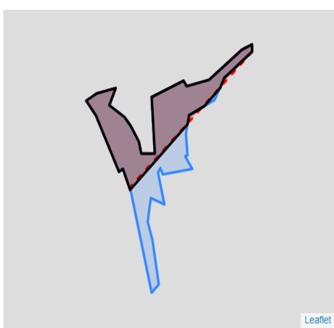	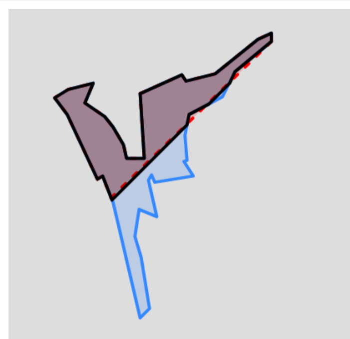	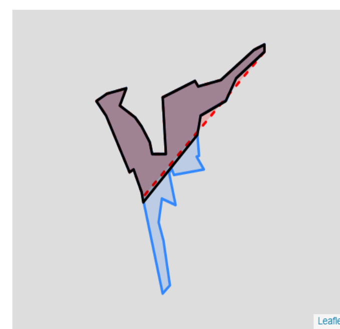

Figure 11: Sub-division on Second Irregular Parcel

Original (2404.41 sq.m.)	One fourth (601.10)	One third (801.46)
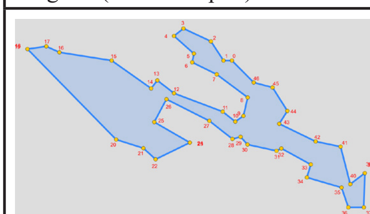	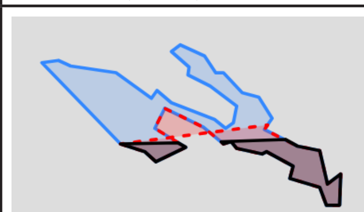	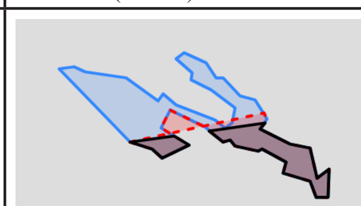
Half (1202.20)	Two third (1602.94)	Three fourth (1803.30)
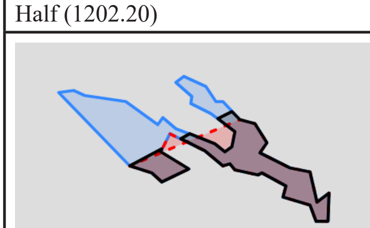	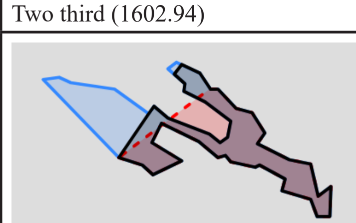	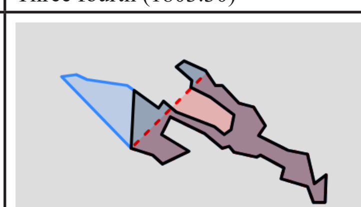

Figure 12: Sub-division on Third Irregular Parcel

4.2 Performance

For evaluating the performance, the Microsoft Edge browser (Version 120.0.2210.144 (Official build) (64-bit)) was used. All the dependencies were made local and other programs were terminated. For each reading, the browser was hard reset so that the variables did not stay in memory.

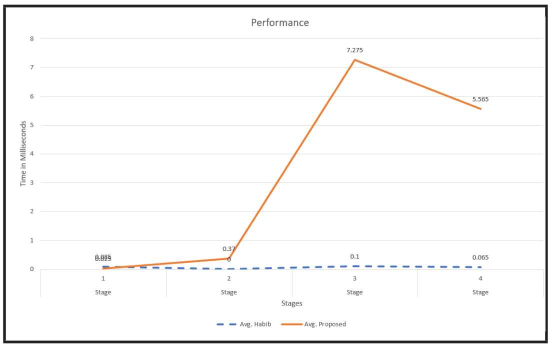

Figure 13 Average time taken in the operating stages for both algorithms.

It can be observed from the Figure 13 that the proposed algorithm, overall, was found slower than its counterpart. The time taken for the first stage of collecting input was found to be nearly similar in both cases. The second stage was not application to Habib algorithm as it completely lacked this stage. In the case of third and fourth stages, time taken by proposed algorithm was found significantly higher than that by Habib Algorithm since the former included an expensive intersection operation. Although, it was expected that the additional stage (2nd stage) would have much impact to the performance of proposed algorithm, it was observed that the highest effect was put forth by 3rd and 4th stage. In the fourth stage, Habib Algorithm performed singular execution of the "derive partition polygon" function whereas proposed algorithm executed it multiple times. Due to this, it was expected that this stage would have largest impact on increasing the computation time, however it was not the case. Overall, the third stage was detected to have the highest performance lag which was counter intuitive.

4.3 Limitation

This study has focused on solving the issues that arose while using the Habib algorithm for parcel splitting. Sub-division of multi-polygonal parcels (parcels with hollow) although has not been tested thoroughly in this research, we expect the concepts to apply to those issues as well. This research has used visualization as a method for evaluation. Other measures of polygon features like concavity, amplitude of vibration, and roundness have not been useful. Those measures compare singular polygons, but the results of the proposed algorithm are mostly multi-polygons. So, the comparisons are inconclusive.

5. CONCLUSION AND RECOMMENDATION

This research presents a modified version of the one-point-and-area method for parcel subdivision, particularly applicable for splitting irregular-shaped parcels. We have proposed to add an extra stage to generate a convex hull and use it to guide the iteration process. The area calculation formula computes the interior area and excludes the exterior area. The single-step process of deriving the partition point is kept in a loop because of the change in the formula of area.

The results from the experiments show that the final partition polygons generated are devoid of clinging and retracting issues. The algorithm handles clinging, retracting, and a combination of both issues. Although the proposed algorithm consumed more time, the quantitative increase in processing time was in milliseconds which is negligible. Normally, these algorithms are not used in bulk but are carried out on a single parcel. Due to this, compounding of increased computation time is not applicable. Hence, the algorithm can be s suitable for the One-Point-and-Area subdivision method.

While this study has limitations in performance, there is room for improvement. As a future work, in stage 3 for finding the "Last Partition Polygon", the initial guess of the last partition polygon can be improved based on the ratio of the required area to the original parcel area. Since stage 3 had taken the most time, authors believe that it can be improved significantly. Another is depending on the area difference if the required area is higher than half of the parcel area. The parcel vertices can be reversed, and the process be started from another direction. This trick has the potential to reduce computation by half in the worst cases. Multi-processing can be leveraged for the iteration of the third stage.

In the fourth stage for deriving a partition polygon, if iteration is to be done then the partition point derived in the last iteration can be removed as it has no effect on accuracy, but it takes computation resources. Intersection operation can also be limited to smaller parts of the original parcel, instead of the whole original parcel. This reduces the number of vertices that participate in the computation of intersection and reduces processing time.

Since this study is based on geometric properties and a Cartesian coordinate reference frame, this study can be implemented elsewhere relevant. Based on the results of the experiment and the discussions, the proposed algorithm is found to be an effective solution for parcel sub-division. It can handle all cases of parcel splitting using one point and including irregular parcels. The same concept can also apply to move-line-and-method as well.

REFERENCES

Adão, T., Magalhães, L., Peres, E., & Pereira, F. (2014). Procedural generation of traversable buildings outlined by arbitrary convex shapes. *Procedia Technology*, *16*, 310–321.

Cogo, E., Krupalija, E., & Rizvic, S. (2023). SpaceSubdivisionTestbed: A Graphical Tool for Arbitrary Shaped 2D Polygon Subdivision. *Proceedings of the 7th International Conference on Computer Science and Application Engineering* (pp. 1–5). doi:10.1145/3627915.3629605

Dahal, K. R., & Chow, T. E. (2014). A GIS toolset for automated partitioning of urban lands. *Environmental Modelling & Software*, *55*, 222–234. doi:10.1016/j.envsoft.2014.01.024

Demetriou, D., Stillwell, J., & See, L. M. (2012). *LandParcelS: A module for automated land partitioning*. School of Geography, University of Leeds.

Easa, S. M. (2008). Unified direct method for land subdivision: circular sides permitted. *Journal of Surveying Engineering*, *134*(2), 55–60. doi:https://doi.org/10.1061/(ASCE)0733-9453(2008)134:2(55)

Fosci, P., & Psaila, G. (2023). Soft Querying Features in GeoJSON Documents: The GeoSoft Proposal. *International Journal of Computational Intelligence Systems*. doi:10.1007/s44196-023-00325-3

Habib, M. (2020). Proposed algorithm of land parcel subdivision. *Journal of Surveying Engineering*, *146*(3), 04020012. doi:10.1061/(ASCE)SU.1943-5428.0000322

Jjumba, A., & Dragićević, S. (2012). High Resolution Urban Land-use Change Modeling: Agent iCity Approach. *Applied Spatial Analysis and Policy*, *5*(4), 291–315. doi:10.1007/s12061-011-9071-y

Mkrttchian, V., Revazyan, N. x, & Khachatryan, V. (2023). Sub division of the object into solid polygons and its applied and economic aspects. *Alternative*. Retrieved from https://api.semanticscholar.org/CorpusID:259034257

Nikanorova, M. Y., & Romanovsky, Y. R. (2020). On Subdivisions of Polygons. *Journal of Mathematical Sciences*, *251*, 524–530. Retrieved from https://api.semanticscholar.org/CorpusID:228884101

Stevens, D., Dragicevic, S., & Rothley, K. (2007). iCity: A GIS–CA modelling tool for urban planning and decision making. *Environmental Modelling & Software*, *22*(6), 761–773. doi:https://doi.org/10.1016/j.envsoft.2006.02.004

Vanegas, C. A., Aliaga, D. G., Benes, B., & Waddell, P. (2009). Visualization of simulated urban spaces: Inferring parameterized generation of streets, parcels, and aerial imagery. *IEEE Transactions on Visualization and Computer Graphics*, *15*(3), 424–435.

Wakchaure, A. S. (2001). An ArcView tool for simulating land subdivision for build out analysis.

Wickramasuriya, R., Chisholm, L. A., Puotinen, M., Gill, N., & Klepeis, P. (2011). An automated land subdivision tool for urban and regional planning: Concepts, implementation and testing. *Environmental Modelling & Software*, *26*(12), 1675–1684.

Zhang, P., Fan, J., Zhang, P., Zhang, Z., Chen, Z., & Han, L. (2021). Comparative Study on the Effect of Shape Complexity on the Efficiency of Different Overlay Analysis Algorithms. *IEEE Access*, *9*, 144179–144194. Retrieved from https://ieeexplore.ieee.org/abstract/document/9583235

Zlatanova, S., Liu, L., Sithole, G. & Zhao, J. (2014). Space subdivision for indoor applications. *GISt Report* 66. Doi. 10.13140/2.1.2914. 2081

Author's Information

Name	:	Amrit Karmacharya
Academic Qualification	:	Master of Science in Geospatial Technologies
Organization	:	Survey Department
Current Designation	:	Survey Officer
Work Experience	:	10 yrs.
No. Published paper/article	:	3

Nepal Surveyor's Association (NESA)

NESA CEC
Secretariate

Mr. Ambadatta Bhatta
President

Mr. Tanka Prasad Dahal
Vice President

Mr. Saroj Chalise
General Secretary

Mr. Prakash Dulal
Secretary

Mr. Durga Phuyal
Secretary

Mr. Sahadev Ghimire
Treasurer

Mr. Dili Prasad Dahal
Member

Ram Kumar Sah
Member

Mr. Murari Tripathi
Member

Mr. Sundar Devkotta
Member

Mr. Durga Pd. Uppadhaya
Member

Mr. Uttam Khadaka
Member

Mr. Rajiv Kumar Sah
Member

Co-Coordinator
For Office Operation and Management
Mr. Ram Kumar Sah

Background

Professional organization provides common Platform to the professional for fostering Knowledge and ideas, so By Utilizing the opportunity opened for establishing social and professional organizations in the country with the restoration of democracy in Nepal as a result of peoples movement in 1990, Survey Professionals working in different sectors decided to launch a common platform named Nepal Surveyor's Association (NESA) in 1991, as the first government registered Surveyor's Organization in Nepal.

Objectives

The foremost objective of the association is to institutionalize itself as a full-fledged operational common platform of the survey professional in Nepal and the rest go as follows.

- To make the people and the government aware of handling the survey profession with better care and to protect adverse effects from it's mishandling.
- To upgrading the quality of service to the people suggesting the government line agencies to use modern technical tools developed in the field of surveying.
- To upgrading the quality of survey professionals by informing and providing them the opportunity of participation in different trainings, seminars, workshops and interaction with expert in the field of surveying and mapping within and outside the country.
- To upgrade the quality of life of survey professionals seeking proper job opportunities and the job security in governmental and nongovernmental organizations.
- To work for protecting the professional rights of surveyors in order to give and get equal opportunity to all professionals without discrimination so that one could promote his /her knowledge skill and quality of services.
- To advocate for the betterment of the quality of education and trainings in the field of surveying and mapping via seminars, interaction, workshop etc.
- To wipe out the misconceptions and illimage of survey profession and to uplift the professional prestige in society by conducting awareness programs among the professionals and stakeholders.
- To persuade the professional practitioners to obey professional ethics and code of conducts and to maintain high moral and integrity.
- To advocate for better satisfaction of survey Council Act and Integrated Land Act for the better regulation of the profession and surveying and mapping activities in the country.

Organizational Structure

Central Structure of 13 Member only.

Memberships Criteria

Any Survey professional obeying professional ethics and code of conduct, with at least one year survey trainings can be the member of the Association. There are four types of members namely life Member, General Member Founder Member and Honorary Member. At present there are 2031 members in total.

Nepal Geomatics Engineering Society (NGES)

contactgeomatics@gmail.com

About NGES

The Nepal Geomatics Engineering Society (NGES) is a non-profit organization representing approximately 700 Geomatics Engineers across Nepal. As the leading professional group in the country, NGES unites professionals serving in various capacities, including Survey Officers, Survey Engineers, Geomatics Engineers, GIS Consultants, Research Fellows, and Lecturers. Dedicated to advancing the field of Geomatics Engineering, NGES provides a platform for networking, knowledge sharing, and career development within the community.

Through its activities and initiatives, NGES promotes the interests of its members, fosters innovation, and advocates for the rights and recognition of Geomatics Engineers in Nepal. By serving as a collective voice for the profession and contributing to its overall development, NGES plays a vital role in nurturing a dynamic and thriving geospatial sector in the country.

In order to explore and enhance the role of Geomatics engineering in nation building through cooperation among the geomatics graduates and professional practice, the geomatics pioneers of Nepal recognized the importance of a society and hence formed Nepal Geomatics Engineering Society in August 26, 2015.

GIS Day Celebration 2022: In collaboration with Kathmandu Living Lab, NGES organized a map design competition, slogan competition and several other talk programs on OpenStreetMap datasets and GIS technologies to celebrate World GIS Day 2022

International Day for Disaster Risk Reduction: NGES commemorated International Day for DRR by hosting talk program on the utility of geospatial technologies for DRR. National and International experts presented insights and guided the audience through the geospatial perspective

GeoSeries: GeoSeries" is a renowned virtual program for sharing knowledge and experiences in the field of geo-information technology. It has successfully aired 12 episodes, featuring both national and international leaders in the geospatial world.

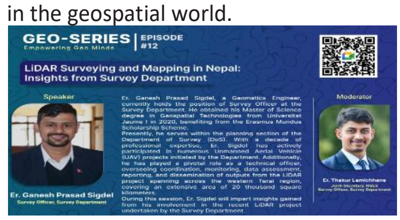

Geomatics Engineering License Syllabus Preparation: NGES in consultation with universities and educationalists lead to develop a comprehensive syllabus for the geomatics engineering license examination to maintain high professional standards within the field and ensure relevance of the examination to contemporary industry requirements.

Addressing System in Nepal: NGES, in collaboration with RUPSON and supported by Asia Foundation's Data for Development Program, organized a groundbreaking event on Addressing System in Nepal

COVID-19 Mapathon: COVID-19 Mapathon, organized by NGES in 2020

Executive Committee: NGES current (4th) Executive committee with previous committee

Briefing on activities of Survey Department, its scope and the progress to the Hon. Minister Balram Adhikary from Director General of the department.

Inspection of CORS station established at the Survey Department premises by Hon' Minister Balram Adhikary.

Event on Global Surveyor's Day March 21, 2024 jointly organized by Nepal Institution of Chartered Surveyors and Survey Department

Students from University of Southern Queensland, Australia visited and interacted with Director General, Deputy Director General and personnel's of Survey Department

Interaction program on annual workplan of survey offices in presence of Director General, Deputy Director General, office chief of survey office and other staff of survey department.

Chief Survey Offer Mr. Narayan Regmi participated in Asia Pacific Forum in Sustainable Developmenit in Bangkok, Thailand held on 20-23 February, 2024

Chief Survey Officer Mr. Mani Prasad Regmi and Dr. Bikash Kumar Karna participated in workshop on "Effective Land Administration in Nepal" held on 27-29 February, 2024 at Dhulikhel

Survey Officer Mr. Gobind Ghimire participated in awareness program on Land Use Implementation at Banepa Municipality

Survey Officer Mr. Girija Pokharel providing technical support for updating land use map at Manthali Municipality

Chief Survey Officer of survey office Makawanpur Mr. Khim Rana attended the program on “Planning and Management of National Surveying and Mapping” from September 18 to December 16, 2023 in Japan.

Making Sense of Geo-spatial data for total solution in National and Local Development Activities

Available Maps and Data

- ❖ Geodetic Control Data
- ❖ CORS Station Data
- ❖ Geoid Data
- ❖ Aerial Photographs
- ❖ Topographic Base Maps
  - ❖ Terai and middle mountain at the scale of 1:25,000
  - ❖ High hills and Himalayas at the scale of 1:50,000
- ❖ Land Use Maps
- ❖ LiDAR Data
- ❖ Political and Administrative Map of Nepal
- ❖ Digital Topographic Data at scales 1:25,000 & 1:50,000
- ❖ Cadastral Plans
- ❖ Orthophoto Maps
- ❖ Image Data
- ❖ SOTER Data
- ❖ Topographic Digital Data at scales 1:100,000 1:250,000 1:500,000 1:1,000,000

Available Services

- ❖ Establishment of control points for various purposes of Surveying and Mapping
- ❖ Cadastral Surveying
- ❖ Surveying and mapping for development activities
- ❖ Topographic and large scale mapping
- ❖ Digital geo-spatial database support
- ❖ GIS Development

Price of some of the publications of Survey Department

- List of Geographical Names, Volume I to V – NRs 600/- per volume.
- The Population and Socio - Economic Atlas of Nepal, 2011 (HardCopy) NRs.2,500.00 (In Nepal), €200.00 (Outside Nepal)
- The Population and Socio - Economic Atlas of Nepal, 2011 (CDVersion) NRs.250/-

Contact Address:

SURVEY DEPARTMENT

Min Bhawan, Kathmandu, Nepal
Phone: +977-1 -4106508, Fax: +977-1 -4106757
E-mail: info@dos.gov.np
website: www.dos.gov.np

ISSN 2717-5022
9 772717 502009